NOTICE

The quality of this microform is heavily dependent upon the quality of the original thesis submitted for microfilming. Every effort has been made to ensure the highest quality of reproduction possible.

If pages are missing, contact the university which granted the degree.

Some pages may have indistinct print especially if the original pages were typed with a poor typewriter ribbon or if the university sent us an inferior photocopy.

Reproduction in full or in part of this microform is governed by the Canadian Copyright Act, R.S.C. 1970, c. C-30, and subsequent amendments.

AVIS

La qualité de cette microforme dépend grandement de la qualité de la thèse soumise au microfilmage. Nous avons tout fait pour assurer une qualité supérieure de reproduction.

S'il manque des pages, veuillez communiquer avec l'université qui a conféré le grade.

La qualité d'impression de certaines pages peut laisser à désirer, surtout si les pages originales ont été dactylographiées à l'aide d'un ruban usé ou si l'université nous a fait parvenir une photocopie de qualité inférieure.

La reproduction, même partielle, de cette microforme est soumise à la Loi canadienne sur le droit d'auteur, SRC 1970, c. C-30, et ses amendements subséquents.

THE SILVER-LEAD-ZINC VEINS OF THE KOKANEE RANGE, BRITISH COLUMBIA

by

Georges Beaudoin
(Ottawa-Carleton Geoscience Centre)

A thesis submitted to the School of Graduate Studies
in partial fulfillment of the requirements
for the degree of *Doctor of Philosophy* in Geology

University of Ottawa
Ottawa, Canada

ISBN 0-315-75053-7

Canada

UNIVERSITÉ D'OTTAWA
UNIVERSITY OF OTTAWA

Doctor of Philosophy
(Geology)

UNIVERSITY OF OTTAWA
Ottawa, Ontario

TITLE: The silver-lead-zinc veins of the Kokanee Range, British Columbia

AUTHOR: GEORGES BEAUDOIN B.Sc. (Univeristé Laval)
M.Sc. (Univeristé Laval)

SUPERVISOR: Dr D.F. Sangster

NUMBER OF PAGES: xi, 168

EXAMINING COMMITTEE:
Dr. E.M. Cameron
Dr. K. Hattori
Dr. D.L. Leach
Dr. H.K. Poulsen
Dr. R.P. Taylor

To the explorers, prospectors, and miners,
who developed the mineral wealth
of the Kokanee Range

ABSTRACT

In the Kokanee Range, southeastern British Columbia, more than 370 Ag-Pb-Zn vein and replacement deposits are hosted by the Middle Jurassic Nelson batholith and surrounding Cambrian to Triassic metasedimentary rocks in the hangingwall of the Slocan Lake Fault, an Eocene, east-dipping, low angle normal fault. K-Ar and step heating $^{40}Ar/^{39}Ar$ analyses on hydrothermal vein and alteration muscovite indicate that hydrothermal fluids were forming vein and replacement deposits 58-59 Ma ago. A 100 Ma time interval is therefore documented between batholith emplacement and spatially associated mineralisation, ruling out any genetic link between the two.

The Pb isotope compositions of galena permit the deposits to be divided into four groups that result from mixing Pb leached from three reservoirs located in the local, upper crustal country rocks, the lower crust, and the upper mantle. Sulfur was derived from local country rocks, and carbon was derived from mantle CO_2 degassing. The $\delta^{34}S_{sulphide}$, $\delta^{18}O_{quartz}$, $\delta^{18}O_{siderite}$, and galena Pb isotopic ratios from veins display regional zonations revealing fluid flow paths of a large, fossil hydrothermal system. Regional isotopic zonations are controlled by deep fracture zones, such as the Slocan Lake Fault, which channelled lower crustal and mantle Pb, and mantle CO_2 to higher crustal levels where mixing occurred with upper crustal fluids which had leached local sulfur and upper crustal Pb. Three contrasting fluids are identified: i) a high salinity, deep-seated and isotopically crust-equilibrated fluid; ii) a low salinity upper crustal fluid of evolved meteoric origin; iii) a late stage meteoric fluid.

Silver-lead-zinc veins form a distinct type of vein deposit characterised by their mineralogy, form, and metal content. Silver-lead-zinc veins are late orogenic features of metamorphosed sedimentary basins within Pb-Zn metallogenic provinces and commonly occur near large crustal faults.

RÉSUMÉ

Le chaînon de Kokanee, au sud-est de la Colombie Britannique, contient plus de 370 gisements filoniens et de remplacement à Ag-Pb-Zn qui sont encaissés par le batholite de Nelson, d'âge jurassique moyen, et par des roches métasédimentaires d'âge cambrien à triassique dans le toit de la faille Slocan Lake, une faille normale de faible pendange d'âge éocène. La datation de muscovites filoniennes et d'altération hydrothermale par les méthodes K-Ar et $^{40}Ar/^{39}Ar$ indique que la la minéralisation fût formée il y a 58-59 Ma. Un intermède de plus de 100 Ma est donc démontré entre la mise en place du batholite et de la minéralisation, rendant impossible tout lien génétique entre les deux.

La composition isotopique du Pb de la galène permet de diviser les gisements en quatre groupes, formés par le mélange de Pb lessivé de trois reservoirs situés dans les roches supracrustales locales, la croûte inférieure, et le manteau supérieur. Le soufre est dérivé des roches supracrustales locales alors que le carbone dérive d'un réservoir profond, probablement par dégazage de CO_2 du manteau supérieur. Les rapports isotopiques du Pb, et $\delta^{34}S_{sulphure}$, $\delta^{18}O_{quartz}$, et $\delta^{18}O_{siderite}$ pour les minéraux filoniens délimitent des zonalités régionales qui tracent le passage des fluides d'un grand système hydrothermal fossilisé. Les zonalités isotopiques régionales sont contrôlées par la présence de zones de fractures profondes, tel que la zone faillée de Slocan Lake, qui ont chenalisé le Pb originant de la croûte inférieure et du manteau supérieur, ainsi que le CO_2 mantellique, vers des niveaux supérieurs de la croûte où ils furent mélangés avec des fluides supracrustaux ayant lessivé du S et du Pb des roches encaissantes locales. Trois fluides différents sont identifiés: i) une saumure d'origine profonde en équilibre isotopique avec la croûte; ii) un fluide supracrustal de faible salinité, d'origine ultimement météorique mais isotopiquement évolué; iii) un fluide tardif d'origine météorique.

Les filons d'argent-plomb-zinc forment un type de gisement caractérisé par une minéralogie, une forme, et un assemblage métallique distinct. Les filons d'argent-plomb-zinc sont un attribut tardi-orogénique de bassins sédimentaires métamorphisés situés à l'intérieur de provinces métallogéniques à Pb-Zn, communément à proximité des grandes failles crustales.

ACKNOWLEDGEMENTS

This project was initiated by D.F. Sangster and I have greatly benefited from his scientific supervision and the numerous and lengthy discussions on the geology of mineral deposits; he has generously shared his knowledge on ore deposits with me. He has encouraged me to follow my own hypotheses while making sure I kept a logical and scientific approach in demonstrating them; his careful reviewing of my writings greatly improved my style and grammar. B.E. Taylor supervised my evolution in the field of stable isotope geochemistry. His scientific method in solving analytical and geologic problems was the source of challenging hypotheses.

K. Bell, A. Bjørlykke, E.M. Cameron, C.I. Godwin, K. Hattori, A.E. Lalonde, R.R. Parrish, J.C. Roddick, and, in particular, R.I. Thorpe reviewed parts of the thesis: their comments and suggestions are greatly appreciated and helped to improve the thesis significantly. J.C. Roddick and C.I. Godwin provided important geochronologic and Pb isotopic data, respectively, and their cooperation is deeply appreciated. I want to thank W.J. McMillan for his support and interest throughout this project. D.A. Brown and J. Logan introduced me to the Kokanee Range. D.A. Brown also provided me with unpublished age data, and numerous country rock samples, whereas H. Ohmoto collected the samples used to date the Bluebell deposit, and R.I. Thorpe provided a hard-to-get sample from the Florence deposit. K. Hattori and G. Skippen kindly allowed the use of their fluid inclusion heating/freezing stage. J.E. Gabites, M. McLaren, A. Pickering, F.B. Quigg, G.St-Jean, R.J.G. Séguin, and J. Sekerka provided some of the data or gave valuable assistance in the laboratory.

Of my colleagues during those years, I wish to thank Frank Brunton, Guy Levesque, Mark Shore, Pierre and Robert Thériault, and Don Watanabe for enjoyable times and squash games.

This study was funded by the Geological Survey of Canada, the British Columbia Ministry of Energy, Mines and Petroleum Resources (Geoscience Research Grants RG89-04 and RG89-37), and NSERC (OGP 0038460). I was supported by NSERC, Fonds FCAR, and University of Ottawa scholarships. Needless to say, their financial assistance is greatly appreciated. B.C. Parks kindly allowed me to use their radio frequency during my journeys alone in the high country.

I would like to thank the mining companies that have given me access to their properties and files: Dickenson Mines, Treminco Resources, Cominco, Dragoon Resources, and Cove Energy Corporation. In particular, I would like to express my gratitude to Steve Phillips, mine manager at Silvana, and his staff, D. Makepeace, M Debriske, and G. Mason-Apps, who authorised me to work underground as I wished and allowed access to Silvana collection of maps and files. The miners at Silvana were kind enough to let me roam around their stopes, steal hoses and wet the muck: they made my underground work an unforgettable experience. Ted Muraro sheared his expertise on the area and provided property data. Pete Leontowitz's enthusiasm was a source of encouragement and his knowledge of the area saved me much time.

Finalement, je désire exprimer ma profonde gratitude à mon épouse, Ann Hackett, qui a su m'encourager tout au long de mes travaux de doctorat. Son support et son enthousiasme m'ont permis de garder le sourire durant ces trois années. Son aide lors de l'assemblage final de cette thèse est grandement appréciée.

TABLE OF CONTENTS

CHAPTER 1
Introduction

CHAPTER 2
Eocene Age for Mineralisation

CHAPTER 3
Isotopic Evidence for Complex Pb Sources

CHAPTER 4
Silver-Lead-Zinc Veins and Crustal Hydrology during Extension

CHAPTER 5
A Descriptive Model for Silver-Lead-Zinc Veins

LIST OF TABLES

LIST OF FIGURES

CHAPTER 1

Introduction

Prologue

The early history of mining development in the Kokanee Range reads like a western tale. In the early 1870's, a prospector named Henry Doan brought samples from the Bluebell deposit to San Francisco. Speculators invested in the prospect and sent a "mining expert", George Hearst, whose son William Randolph was to become a newspaper mogul, and an assayer to investigate. While in Fort Colville, Washington, Doan apparently salted the ore samples. Suspicious, Hearst himself sampled the Bluebell but on site assays showed much lower silver values. Confronted by Hearst, Doan confessed his action. Legend says that Doan was left alone, without provision, a boat, or a rifle, by Hearst and his party, but somehow managed to return to Fort Colville. In 1882, R.E. Sproule located the Bluebell claims but could not record them because the law required him to vacate them for no more than 72 hours and the journey to the gold commisioner's office was longer. In 1883, Thomas Hammill, a "mining scout" who worked for the Ainsworth family, brought the gold commissioner with him and recorded the Bluebell claims under the nose of Sproule. A long lawsuit followed and was eventually settled in favour of Hammill; Sproule then took the law in his own hands and shot and killed Hammill. Sproule was captured by an R.C.M.P. officer near the Idaho border and subsequently hanged. During the following years, many claims were staked near Ainsworth Hot Springs. One hundred years ago, on September 9, 1891, J.L. Seaton and Eli Carpenter found the Payne vein near Sandon. After returning to Ainsworth, Carpenter deceived Seaton by showing him assays from another property

with low silver values. Carpenter and another man went back to the Payne by an indirect route not to attract attention, but were overheard by the hotel manager. Then another party, led by Seaton and called the Noble Five, took the direct route to the Payne, arrived first, and staked many claims in the area of Sandon. A mining boom followed which led to the development of the Slocan, Slocan City, and Ainsworth mining camps which collectively became one of the prominent mining areas of Canada at the turn of the 19th century. At present, only the Silvana mine of Teminco Resources Ltd., in Sandon, is producing.

Present Study

Cairnes (1934; 1935) made, still, the most comprehensive description of the deposits, mainly in the Slocan camp. Hedley (1945; 1952) and Little (1960) mapped sectors of the Kokanee Range and provided information on the mineral deposits. Fyles (1967) mapped the Ainsworth area and his report also provided descriptions of many of the deposits in that area. Brown and Logan (1989) mapped the Kokanee Glacier Park and adjoining area and described the deposits therein. Finally, several theses have focussed on individual or small group of properties (Brame, 1979; Cox, 1979; Logan, 1986; Ohmoto, 1968; Orr, 1971; Roscoe, 1948; Sinclair, 1964).

This project was initiated at the suggestion of Dr D.F. Sangster (Geological Survey of Canada) who considered that silver-lead-zinc veins were an under researched deposit type. The Kokanee Range was selected for study because it was one of the two large Canadian examples of this type of deposit. The other one, the Keno Hill district in the Yukon Territory, has been the subject of a similar study by Lynch (1989a).

At an early stage of this project it became obvious that deposits from the Slocan, Slocan City, and Ainsworth camps shared many features (Beaudoin et al., 1991a) and the decision was

made to study them as an entity. This had never been done before and the available geological database therefore comprised data gathered at different times by geologists with different backgrounds and interests. At the outset of the project, a single geology map of the Kokanee Range was not even available.

Field work

More than 370 veins in the Kokanee Range have each produced more than one tonne of ore, and of these, over 70 were visited during three field seasons, including all 39 deposits from which more than 10 000 t of ore had been produced. Other smaller deposits were also visited, either to obtain a good geographic coverage of the area, or because they were the site of some exploration activity. For each of the deposits, a series of geologic observations were made and representative samples, based on descriptions of the deposit available from geological reports or literature, were collected. The samples were mostly taken from old dumps but, whenever possible, directly from old workings. Detailed mapping and sampling of stopes was carried during more than six weeks of underground work at the Silvana dposit. The observations made underground were essential to correlate the textures observed in dump material from other deposits. Overall over 500 samples comprising about 350 mineralised specimens and 150 country rock samples were collected for various geochemical studies. Fifty-three mineralised samples were taken at the Silvana whereas up to 12 samples were collected in each of the other deposits.

Thesis format

This thesis was originally prepared as a series of four papers; to these a general abstract, an introduction and a conclusion, all unique to the thesis, have been added. Each of the four papers makes one chapter of the thesis. To avoid repetition, the original papers have been slightly

modified: abstracts, repetitive sections of their introduction and regional geology, and references have been combined, and figures and tables have been renumbered. The papers have been submitted to various journals but the versions included in the thesis bear uniform referencing and spelling rules.

A geological compilation map of the Kokanee Range has been published (in pocket; Beaudoin, 1990) and simplified versions of it are used throughout the thesis. Early in this project, it was recognised that dating mineralisation was of paramount importance to understand the genesis of the deposits. Dating was accomplished using K-Ar and $^{40}Ar/^{39}Ar$ step heating analysis of vein and hydrothermal alteration muscovite and K-Ar dating of a suite of coeval lamprophyre dykes. Dr J.C. Roddick, Geological Survey of Canada, provided the K-Ar data and supervised my work in $^{40}Ar/^{39}Ar$ mass spectrometry. These data are in Chapter 2 which was submitted to the Canadian Journal of Earth Sciences (Beaudoin et al., 1992a). Chapter 3 is a Pb isotope study of galenas from a representative selection of Kokanee Range deposits. Following an initial compilation of previous Pb isotope data, it was realised that galena from some of the large deposits had not been analysed for Pb isotopes and that Pb isotope data were not available for some large areas of the Kokanee Range. A proposal to enhance the previous Pb isotope database was presented to Dr C.I. Godwin, The University of British Columbia, who subsequently provided 46 new Pb isotope analyses from galenas I had collected. Chapter 3 is from a paper that was submitted to the Canadian Journal of Earth Sciences (Beaudoin et al., 1992b).

Most of my analytical work is included in Chapter 4. Most of the fluid inclusion microthermometry was performed on a heating and freezing stage that I installed and calibrated for Dr K. Hattori at the University of Ottawa. I did all the stable isotope analytical work with

the exception of the H analyses in muscovite, which were done by J. Sekerka at Stable Isotope Laboratory of the Geological Survey of Canada, and the C-O analyses in carbonates and total sulphur in rocks, which were done by G. St-Jean and M. McLaren at the Stable Isotope Laboratory of the Ottawa-Carleton Geoscience Centre. Dr B.E. Taylor, Geological Survey of Canada, closely supervised most of this work. Chapter 4 is from a paper submitted to Geochimica et Cosmochimica Acta (Beaudoin et al., 1992c). Finally, Chapter 5 is a descriptive model for silver-lead-zinc veins from a paper submitted to Economic Geology (Beaudoin and Sangster, 1992d).

Geological Setting

The Kokanee Range (Fig. 1-1) is located west of the collision boundary between the Ancestral North America terrane and the pericratonic Kootenay terrane, the accreted marginal oceanic basin terrane of Slide Mountain, and the island arc terrane of Quesnellia (Gabrielse and Yorath, 1989). Ancestral North America comprises a 2.1-1.85 Ga crystalline basement overlain by the Middle Proterozoic Purcell Supergroup, a thick passive margin assemblage, possibly deposited in aulacogens, of turbidite deposits grading upward into shallow water sediments (Gabrielse and Yorath, 1989). During the Late Proterozoic, a new rifting event is recorded by deposition of Windermere Supergroup mafic lavas, feldspathic sandstones, and pebble conglomerates. An Upper Proterozoic to Lower Cambrian passive margin consisting of thick mature sandstones (Hamill Group) and platformal limestones (Badshot and Mohican formations) overlies Windermere Supergroup.

The pericratonic Kootenay terrane comprises the Cambro-Ordovician Lardeau and the Carboniferous Milford groups (Klepacki, 1985). The Kootenay terrane represents an off-shelf

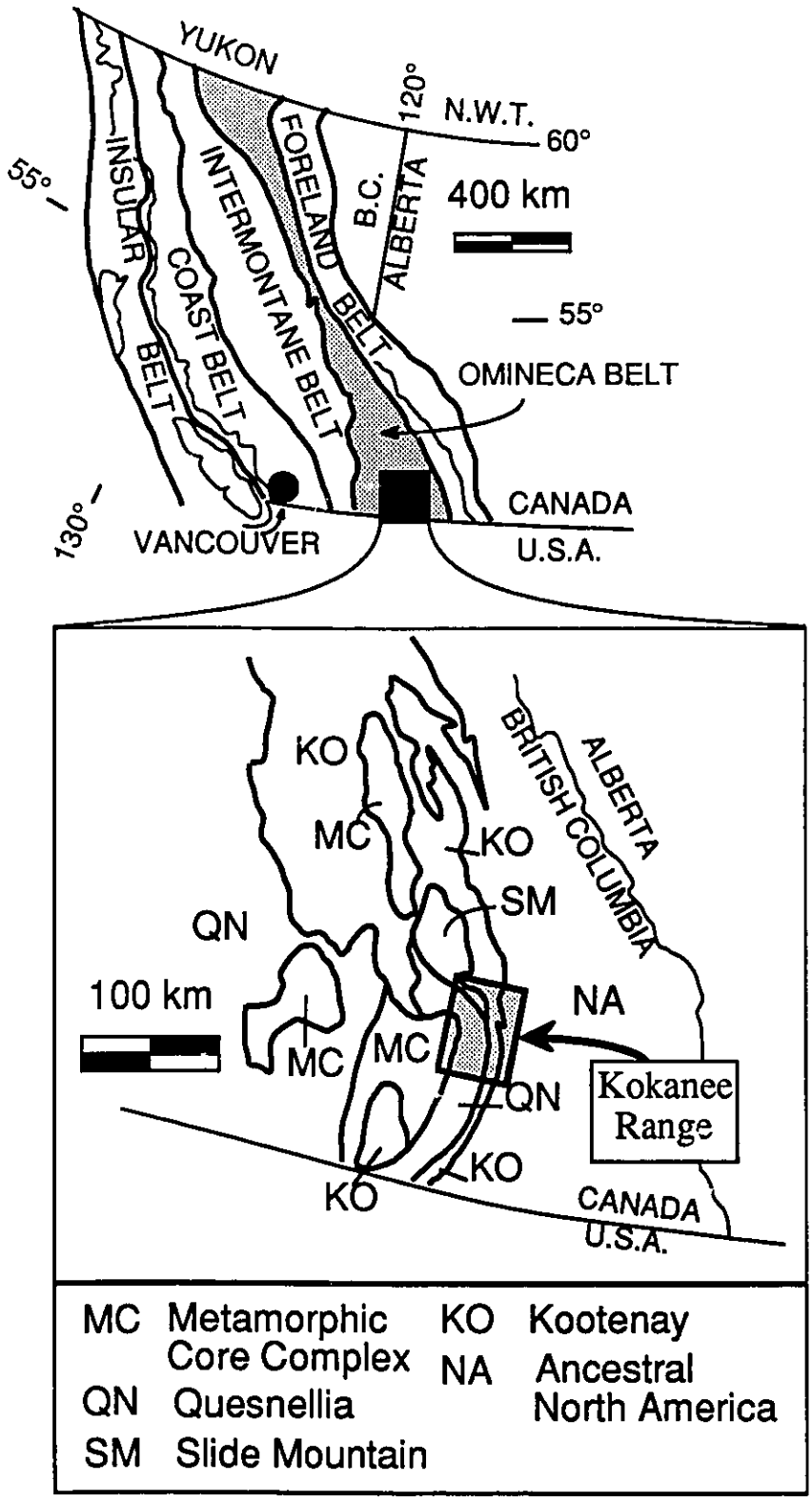

Figure 1-1. Location map of the study area in the Omineca belt of the Canadian Cordillera. The Kokanee Range is west of the collision boundary between Ancestral North America and the pericratonic Kootenay and accreted Slide Mountain and Quesnellia terranes (modified from Gabrielse and Yorath, 1989).

margin facies between Ancestral North America and Slide Mountain and Quesnellia terranes. Sedimentary and volcanic rocks of Kootenay terrane were deposited in an active tectonic environment undergoing episodic rifting and compression (Klepacki, 1985). Slide Mountain terrane, represented by Lower Permian Kaslo Group tholeiitic basalts, formed an oceanic marginal basin to Ancestral North America (Klepacki, 1985). Slide Mountain terrane was bounded to the west by Quesnellia island arc. Upper Triassic Slocan Group argillites and sandstones were deposited in a back arc basin and unconformably overly Kaslo Group (Klepacki, 1985).

By Early Jurassic the pericratonic and accreted terranes had combined to form the Intermontane Superterrane which collided with Ancestral North America during the Middle Jurassic (Gabrielse and Yorath, 1989). Eastward subduction of the oceanic basin of Cache Creek terrane underneath Quesnellia produced large, granodioritic, Middle Jurassic intrusions, such as the Nelson batholith (Gabrielse and Yorath, 1989). Collision resulted in burial of Upper Proterozoic rocks to a depth of over 20 km in less than 10 Ma (Archibald et al., 1983), followed by slow uplift and cooling until latest Cretaceous and rapid uplift and cooling during the Early Tertiary (Archibald et al., 1984). The Kokanee Range is bounded to the west by the Valhalla metamorphic core complex, unroofed from the middle crust as a result of Early-Middle Eocene normal displacement along the low angle, east dipping, Slocan Lake Fault (Carr et al., 1987). Slocan Lake Fault separates the Valhalla metamorphic core complex from Nelson batholith and Slocan Group in the hangingwall. A suite of alkaline intrusions, comprising numerous lamprophyre dykes (minette and kersantite), and the Coryell syenite plutons, intruded during the Eocene and cut the extensional structures (Parrish et al., 1988; Beaudoin et al., 1991a). The veins

and lamprophyre dykes have mutual crosscutting relations, suggesting that both are broadly coeval (Beaudoin et al., 1992a).

Silver-Lead-Zinc Vein and Replacement Deposits

More than 370 Ag-Pb-Zn vein and replacement deposits of Kokanee Range have recorded production of $2.6x10^3$ t Ag, $0.53x10^6$ t Pb, $0.51x10^6$ t Zn, and 0.96 t Au. The deposits are in all intrusive and sedimentary rocks outcropping in the area except those of the Valhalla metamorphic core complex, and consist of veins in fault zones and massive sulphide replacement bodies in limestone adjacent to fractures. Veins are commonly dislocated and brecciated by later fault movements and the breccia fragments are cemented by quartz or carbonates. Narrow phyllic hydrothermal alteration surrounds veins hosted in the Nelson batholith but rarely are observed around veins in sedimentary rocks. Vein mineralogy is dominanted by galena and sphalerite with accessory pyrite, pyrrhotite, chalcopyrite, and a diverse suite of silver minerals and sulphosalts in a gangue of siderite, dolomite, calcite or quartz.

Deposit types

Cairnes (1934) recognized five types of deposits: 1) barren quartz veins with or without pyrite or pyrrhotite; 2) auriferous quartz veins containing disseminated sulphides and gold; 3) veins of massive galena-sphalerite with siderite, quartz, or calcite, the so-called "wet ore"; 4) veins of quartz with galena, sphalerite, and tetrahedrite, characterised by high silver values and where the quartz gangue greatly exceed the abundance of sulphides, the so-called "silver dry ore"; 5) Ag-Au quartz veins with disseminated silver minerals and minor sulphides. Cairnes (1934) considered that all five types where deposited from solutions related in origin but of various compositions. The different types of deposits were envisaged as a unidirectional gradation, mainly

controlled by temperature, between deeper level, barren quartz veins and higher level, Ag-Au quartz veins.

It is obvious that Cairnes (1934) classification was deeply influenced by the prevailing classifications of deposits proposed, with minor differences, by Spurr (1912) and Emmons (1924). My observations, although more limited in the number of deposits investigated and by the accessible workings, indicate that: i) the barren and auriferous quartz vein types are probably unrelated to the silver-lead-zinc veins; and ii) vertical temperature gradients are not a dominant control of mineral deposition and there is no vertical gradation between the deposit types as proposed by Cairnes (1934).

Cairnes (1934) recognised that the barren quartz veins are cut by the silver-lead-zinc veins. Barren quartz veins are common throughout the area and it is here suggested that they were formed as a result of Middle Jurassic folding and greenschist metamorphism of Slocan Group. This is supported by a minimum $^{40}Ar/^{39}Ar$ age of 160 Ma for muscovite in a barren quartz vein near the McAllister deposit (Beaudoin et al., 1991a).

The auriferous quartz veins were believed by Cairnes (1934) to pass at depth to barren quartz and to have formed at lower temperatures than the latter. Only three examples of auriferous quartz veins were described by Cairnes (1934). One of them, the Rockland (now known as the Willa), is hosted by a roof pendant in the Nelson batholith, of Early Jurassic Rossland Group volcanic and related intrusive rocks. The deposit, described as a Cu-Au porphyry-type, consists of disseminated mineralisation hosted by feldspar and quartz latite porphyries, and heterolithic breccias (Brown and Logan, 1989).

Cairnes (1934) noted that pyrite was much more conspicuous in the lower than in the

upper workings of deposit types three and four, therefore suggesting a gradation between auriferous quartz veins and massive galena-sphalerite veins. In the eastern part of the Silvana deposit, however, no gradational mineralogical variation between the lowermost and uppermost workings was noted. Actually, abundant pyrrhotite was identified in massive sphalerite-galena-siderite lenses from the upper workings after it was realised that the ore was magnetic. Coarse grained, hexagonal pyrrhotite crystals were found in small vugs as well as disseminated in siderite. In summary, there is no evidence of a gradation between auriferous quartz veins and silver-lead-zinc veins. Furthermore, some of the auriferous mineralisation is older (e.g. the Willa deposit) than the silver-lead-zinc veins.

Cairnes (1934) argument was that each deposit type grades upward into the successive one and was based mainly on the mineralogical evidence "*that successive stages of mineralization, in addition to possessing certain distinctive mineral characters, have tended to reproduce, at depth and on a relatively small scale, the mineralogic features of preceding stages*" (p. 117). Although Cairnes (1934) related these vertical mineralogical changes to a temperature gradient, he recognised that "*it is unlikely that marked differences of temperature would exist at any one time at the site of nearby deposits, or that compositions of mineralizing solutions entering neighbouring fractures at the same time would be unlike, the presumption is that nearby deposits of unlike types formed at different stages during the period of mineralization as the general temperature fell*" (p. 117). Therefore, the proposed vertical mineralogical zoning and gradation between deposit types did not result from a vertical temperature gradient. Vertical zoning has not yet been described in any detail. To the contrary, Roscoe (1948), Hedley (1952), and observations made during the course of this study suggest that the inferred vertical

mineralogical zoning is due to the availability of open fractures during the different stages of mineralisation. Thus, the third, fourth, and fifth types suggested by Cairnes (1934) are considered here to be sub-types of the silver-lead-zinc veins of the Kokanee Range. The first and second types are considered older and unrelated to the hydrothermal system that formed the silver-lead-zinc veins.

Structural control

The structural control of the veins was not studied in detail. Observations were made wherever possible but most of them were done during detailed study of the Main Lode at the Silvana deposit (Beaudoin and Sangster, 1990). In general, mineralisation is contained in dilation structures in fault zones or, less commonly, in tension fractures. Tension fractures generally strike northeast and dip steeply to the southeast. Cairnes (1934) considered that these fractures were controlled by an older fabric made of a regional set of joints. Hedley (1952) also recognised this set and noted that its strike is commonly perpendicular to that of the strata. Most of the mineralisation is contained in dilation structures in fault zones. Hedley (1952) recognised two types of faults in Sandon area: tangential faults, which roughly follow the commonly southeastern bedding and are seldom mineralised, and crosscutting faults which strike mostly to the northeast, dip steeply to the southeast, and are commonly mineralised. Hedley (1952) also recognised that small mineralised faults had a dominant 030-070 strike with a steep southeastern dip whereas large mineralised faults had a dominant 045-090 strike with a shallow south to southeast dip averaging 45º. Hedley (1952) determined oblique, normal and sinistral displacements, up to several hundred feet, for all the faults studied.

In Ainsworth area, Fyles (1967) found that most of the mineralisation was hosted by

structures displaying minor normal faulting. Fyles (1967) found three dominant orientations for the structures containing large or small deposits: i) 000-020/45, named bedded veins and which are parallel to the regional foliation; ii) SE/60; and iii) 070-090/55.

My observations on the few accessible veins confirmed previous descriptions. The attitude of the structures containing mineralisation was studied using average strike and dip values reported in the literature or measured in this study for the 39 deposits of the Kokanee Range with recorded production of more than 10 000 t of ore. This set of deposits, although representing only 10% of all deposits with production data, produced most of the ore in the Kokanee Range. It was judged that the use of a smaller data set comprising only the larger deposits would enable an analysis focussed on those structural features most important for mineralisation. The attitude and geographic distribution of the structures containing the 39 larger deposits is displayed on Figure 1-2 and their attitudes are compiled on a rose diagram (Fig. 1-3). Three domains can be readily identified. The first domain comprises deposits hosted by the Nelson batholith and have northeast or northwest strikes (Fig. 1-2). These two orientations correspond with two dominant sets of joints in the Nelson batholith (Cairnes, 1934). The second domain comprises deposits hosted by Cambrian to Triassic metasedimentary rocks near Ainsworth where the three attitudes defined by Fyles (1967) are displayed (Fig. 1-2). The third domain comprises deposits hosted by Slocan Group sedimentary rocks north of the Nelson batholith which occur within a broad, roughly s-shaped area (Fig. 1-2). Deposits in the third domain have two dominant strikes, northeast and east, which are well displayed in a rose diagram (Fig. 1-3) and correspond to Hedley's (1952) classification of, respectively, small and large structures. Most of these structures are faults that display fabrics consistent with oblique, normal and sinistral displacement with the exception of

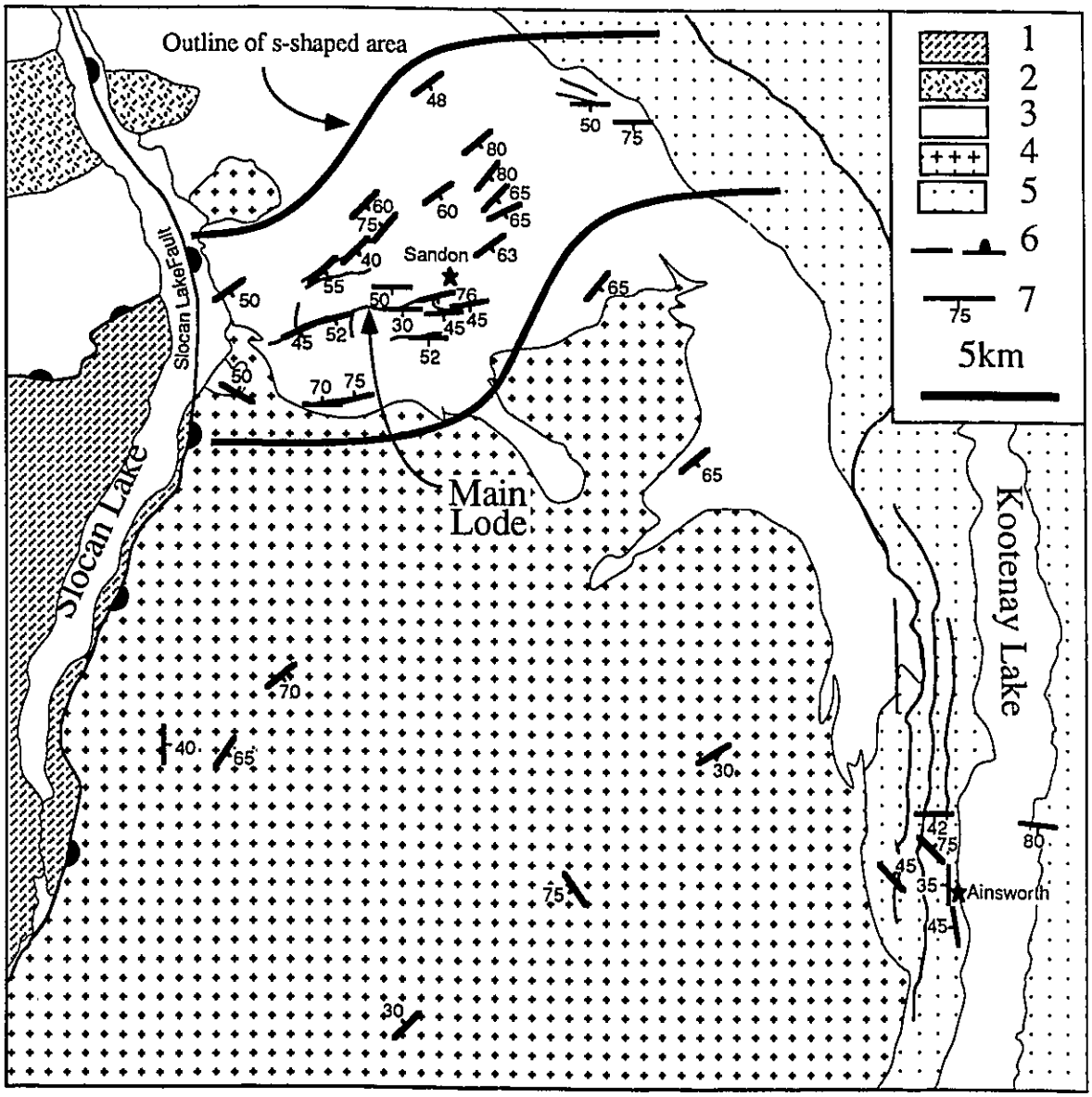

Figure 1-2. Simplified geology map of the Kokanee Range showing the location and average strike and dip of the structures containing mineralisation in the larger deposits. 1- Rocks of the Valhalla metamorphic core complex; 2- Granitic pluton of probable Cretaceous age; 3- Upper Triassic Slocan Group; 4- Middle Jurassic Nelson batholith; 5- Paleozoic sedimentary and metamorphic rocks; 6- Fault, normal; 7- Average stike and dip of the structures containing mineralisation.

the Van Roi and Hewitt deposits. These two deposits occur along an east-west fault zone with anomalous dips to the north (Fig. 1-2) and comprised of multiple narrow shear zones with fabrics indicating up-dip, reverse displacement.

The Main Lode is the local name of an east-west fault zone containing six of the 39 larger deposits of the Kokanee Range, including the Silvana where detailed observations were made (Fig. 1-2). In the eastern end of the Silvana deposit, the Main Lode is narrow, up to 2 m, and penetrative deformation does not extend into the wallrock (Beaudoin and Sangster, 1990). This is different from many other areas where the Main Lode consists of up to 50 m of sheared and brecciated rocks (Cairnes, 1935; Hedley, 1952). These observations were confirmed by visits to old workings in the western part of Silvana and in the Silversmith deposits. In the eastern part of Silvana, in contrast, pre-mineralisation fabrics consist of shear zones present, and probably only preserved, at the margins of the Main Lode, which invariably indicate oblique normal and sinistral displacement. These early shear zones are invaded by mineralisation and cut by later structures. Massive siderite-sphalerite-galena form lenses commonly less than 2 m thick with down-dip and strike lengths of up to tens of metres. These lenses are dissected by a complex network of narrow shear zones commonly marked by a seam of graphitic schist. Deformation within the sulphide lenses is variable. Siderite and sphalerite lenses commonly display only brittle fractures or discrete shear zones. Massive galena, however, is commonly intensely foliated and contains coherent fragments of apparently undeformed massive siderite-sphalerite. Uglow (1917) gave many examples of foliated galena from the Kokanee Range. Where foliated galena is coarser grained, and flattened galena grains define s-shaped foliation planes indicating late stage oblique, normal and sinistral, displacement similar to earlier deformation. Another common late

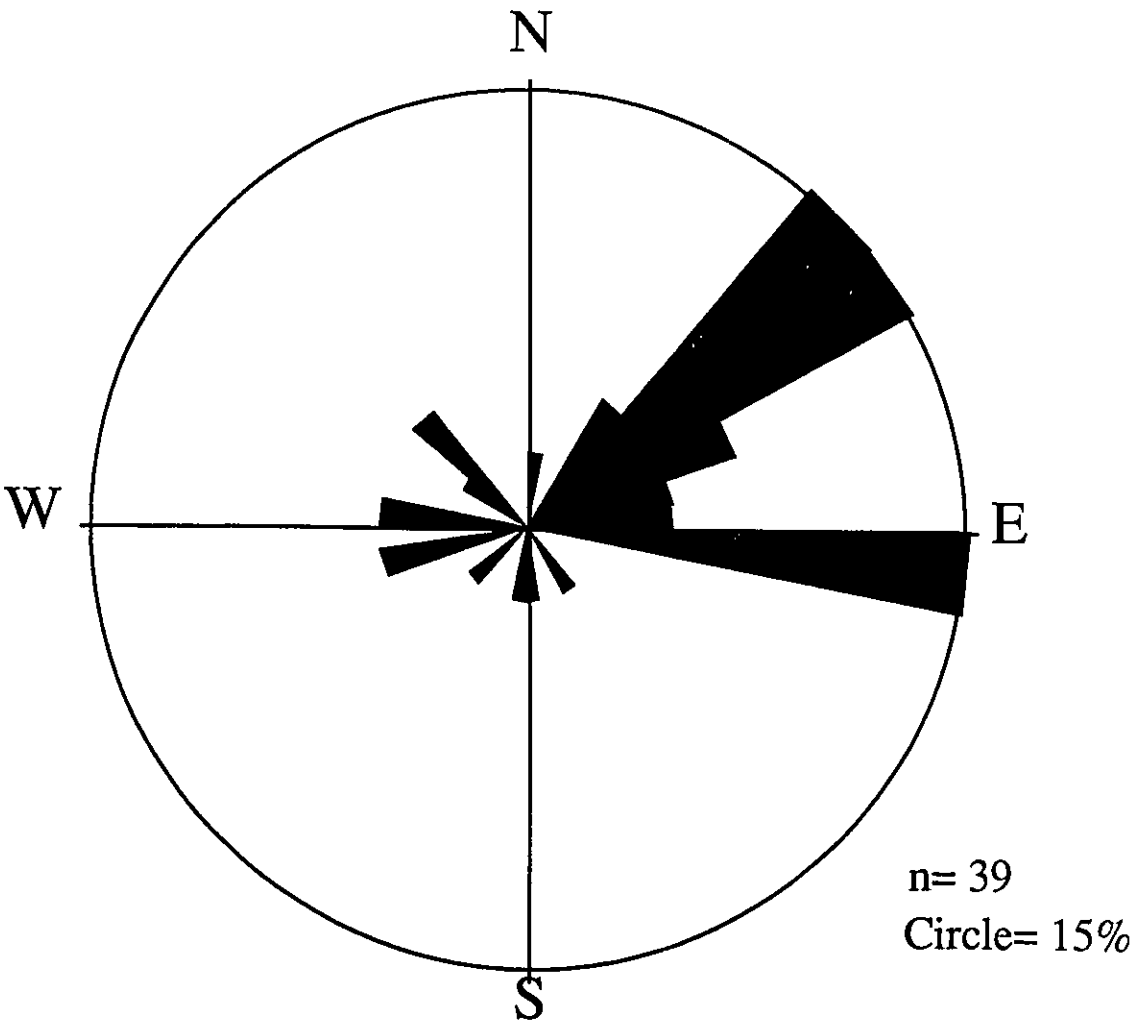

Figure 1-3. Rose diagram of the average stike of the structures containing mineralisation in the larger deposits. The two dominant east and northeast orientations are well displayed.

stage deformation consist of breccias of siderite-sphalerite-galena cemented by quartz, dolomite, or calcite. Late brecciation is a common feature noted in nearly all the deposits visited in the Kokanee Range.

The broad, s-shaped area defined by the larger deposits of the third domain is similar to branching patterns for many of the veins at the scale of the deposit. Many examples of veins branching in an "s" pattern have been described by Cairnes (1934; 1935) and Hedley (1952), and have been observed at Silvana. The "s" pattern is therefore observed at both the scale of the district and that of the deposit. The northeast and east-west orientations of the pattern both have oblique, normal and sinistral movement, therefore indicating that they are not a set of conjugate fractures. The preferred hypothesis is that the "s" pattern represents a set of en échelon east-west, oblique normal and sinistral, strike-slip faults linked by northeast-southwest faults. It is likely that the northeast-southwest link faults are, in many instances, older structural elements such as a dominant joint set (Cairnes, 1934; Hedley, 1952) favorably oriented to extensional reactivation. A genetic association with the Slocan Lake Fault cannot be documented at present but it is likely that, as suggested by dating of mineralisation (Beaudoin et al., 1991a), the faults containing mineralisation were formed or activated as a result of Eocene extension.

CHAPTER 2

Eocene Age for Mineralisation

New geochronological data constraining the age of Kokanee Range Ag-Pb-Zn vein and replacement deposits are presented in this chapter. Previously, these deposits were widely considered to be Middle Jurassic in age although conflicting geological relationships have been known for some time, and Fyles (1967), Ohmoto and Rye (1970), LeCouteur (1973), and Brown and Logan (1989) suggested that some of the deposits could have been formed in the Tertiary.

Previous Interpretations of Age of Mineralisation

Since the early days of mining, mineralisation has been linked genetically to the intrusion of the granodioritic Nelson batholith. This interpretation was based on the spatial association of vein and replacement deposits with the Nelson batholith in the Kokanee Range and elsewhere in southeastern British Columbia (Bateman, 1925; Cairnes, 1934). Cairnes (1934, p. 69) recognized that mineralisation "*took place after a period of shearing and fracturing of an upper consolidated part of the granite*", and Bateman (1925, p. 565) concluded that mineralisation resulted from the "*expulsion from the unconsolidated interior of the batholith of the metallizing solutions that gave rise to the ore deposits*". From information available at that time, Cairnes (1934) deduced that the age of the Nelson batholith was Cretaceous and that the structures containing mineralisation formed in Late Cretaceous to Early Tertiary times and could be related to the "Rocky Mountain" (Laramide) orogeny.

Detailed mapping in the Ainsworth area by Fyles (1967) revealed that the veins cut the dominant foliation. From an extensive study of lead-zinc mineralisation in the Kootenay Arc,

Fyles (1967, p. 70) concluded that "*early workers regarded the Nelson plutonic rocks as a source of lead-zinc mineralization, but careful studies have found no evidence that any ore deposit or group of deposits is related to any one pluton*". Irvine (1957) and Ohmoto and Rye (1970) suggested that mineralisation at the Bluebell deposit was most likely Tertiary on the basis of crosscutting relationships with pre-ore lamprophyre dykes, widely regarded as Tertiary, and inclusion fluids with low δD similar to present meteoric waters in the area. Inclusion fluids from euhedral, vug filling quartz crystals from the Bluebell deposit yielded a Rb/Sr isochron with an age of 19.2 ± 5.9 Ma (Changkakoti et al., 1988).

Reynolds and Sinclair (1971) inferred a genetic relationship between the Nelson batholith and mineralisation, based on rock and galena lead isotope studies. LeCouteur (1973), however, concluded that the deposits could not be considered directly related to the Nelson batholith because it was too old and some of its rock lead was more radiogenic than that of the ore deposits. LeCouteur preferred to interpret galena Pb of the Slocan City and Slocan camps to have been a mixture drived from normal upper crustal sources during the Eocene (50 Ma). Andrew et al. (1984) proposed that Ainsworth camp lead was originally syngenetic Cambrian mineralisation that was subsequently remobilized in vein and replacement deposits during the Mesozoic or Tertiary. Slocan City and Slocan camps Pb isotopic compositions were interpreted to plot on a "mixing line isochron" of 160 Ma, thus supporting a genetic relationship between mineralisation and the Nelson batholith. Similarly, Brown and Logan (1989) concluded, from a study of deposits hosted in the Nelson batholith, that galena lead was derived by mixing three lead reservoirs in the batholith during the Middle Jurassic.

Field Evidence

Constraints on the age of mineralisation can be deduced from relations with rock units and structural elements of known ages. Mineralisation cuts all rock units outcropping in the area with the exception of some of the lamprophyre dykes and the rocks of the Valhalla metamorphic core complex. The Valhalla complex is separated from hangingwall Nelson batholith and Slocan Group by Slocan Lake Fault, a large, east-dipping, low-angle normal fault active during the Eocene (47 to ~57 Ma; Parrish et al., 1988). There are no Ag-Pb-Zn deposits west of Slocan Lake Fault which indicates that mineralisation is older than, or coeval with, late stages of Eocene extensional faulting.

Mineralisation is contained in structures with ductile to brittle fabrics and is surrounded by phyllic hydrothermal alteration halos within the Nelson batholith, the youngest country rock hosting mineralisation. Various geochronological methods yield an age of 170-165 Ma for the Nelson batholith (Nguyen et al., 1968; Archibald et al., 1983; Ghosh, 1986; Carr et al., 1987), which corresponds to the Middle Jurassic epoch. Accordingly, mineralisation is younger than Middle Jurassic. In Ainsworth area, vein and replacement deposits cut a Middle Jurassic foliation (Archibald et al., 1983) and, consequently, the deposits are interpreted to be younger than Middle Jurassic in this area.

Lamprophyre dykes are widespread in the Kokanee Range although few geochronologic data are available. The dykes were emplaced in all sedimentary and plutonic rocks of the Kokanee Range and are undeformed. Most of the lamprophyres are kersantites but a few minettes have been described (Cairnes, 1934; Fyles, 1967; Klepacki, 1985; this work). The dykes commonly tend "*to be followed by fissures and shear zones*" (Cairnes, 1934, p. 73). This is

particularly obvious west of Ainsworth where some veins and dykes are nearly parallel to the foliation (Fyles, 1967). Hedley (1945) described a "magnetic ore" from the lower workings of the Whitewater deposit, consisting of galena and sphalerite in a gangue of pyrite, pyrrhotite, and silicates. Hedley reported that this "magnetic ore" replaced a highly altered lamprophyre dyke along gradational or sharp contacts, suggesting the dyke to be pre-ore. Cairnes (1934), however, also reported that lamprophyre dykes cut veins in three different deposits. At the Enterprise deposit, most lamprophyres are pre-ore, but two of them cut the vein and are thus post-ore (Little, 1960). A visit to the only level accessible (#8) in 1989 failed to reveal any lamprophyre dykes. At the Alpine deposit a swarm of vertical kersantite dykes cuts a shallow dipping quartz vein at nearly right angles. Mineralisation is broadly coeval with lamprophyre magma intrusion.

Analytical Methods

K-Ar and $^{40}Ar/^{39}Ar$ analyses were performed at the Geochronology Laboratory of the Geological Survey of Canada, with the exception of those of D.A. Brown which were performed at The University of British Columbia (J. Harakal, analyst). Decay constants recommended by Steiger and Jäger (1977) have been used. Thirteen analyses were carried out in 1972 for D.F. Sangster using techniques described in Wanless et al. (1973), and seven more were prepared and analyzed in 1989-1990 using techniques described in Hunt and Roddick (1988). The purity of the mica separates was >99.5%. Potassium contents of >7.0% for most micas indicate that they have not been significantly altered, whereas three with 5.6 to 6.5 %K may have some chlorite present (Tables 2-1, 2-2). Four micas analyzed for $^{40}Ar/^{39}Ar$ were prepared in a similar manner and handpicked to 100% purity. Their K concentrations, determined from the $^{40}Ar/^{39}Ar$ analyses, range from 8.3 to 9.1% whereas one sample (148-5) proved to be a fine intergrowth of

muscovite, siderite and quartz and has only 4.5% K.

The micas for $^{40}Ar/^{39}Ar$ dating were weighed (21 to 58 mg) and wrapped in aluminium foil packets for neutron irradiation. The packets were loaded in an aluminium can 40 mm long by 19 mm in diameter along with packets of the MMHb-1 hornblende $^{40}Ar/^{39}Ar$ flux monitor with an assumed age of 518.9 Ma (Roddick, 1983). The can was irradiated for 1.25 days in position 5C of the enriched uranium research reactor at McMaster University, Hamilton, Ontario. It received an approximate fast neutron fluence of 1.1×10^{18} neutrons/cm^2, which results in a mean J factor of 6.9×10^{-3}. Flux variation over the irradiation can had a range of 2.0% and is mainly along the axis of the can. This results in an uncertainly of J for individual samples of about 0.5% (1σ). The errors quoted on the integrated ages take account of this J uncertainty, though the individual step ages in the data table and spectra diagrams do not. Complete procedures for $^{40}Ar/^{39}Ar$ analyses are detailed in Roddick (1990).

K-Ar Dating of Lamprophyre and Gabbro Dykes Intrusion

From the previous discussion, it is clear that establishing the age of intrusion of the broadly coeval lamprophyre and gabbro dykes would help constrain the age of mineralisation. Some geochronologic data are available on the age of lamprophyre and gabbro dykes in southern British Columbia and northern Washington (Nguyen et al., 1968; Yates and Engels, 1968; Fyles et al., 1973; Jones et al., 1973; Macdonald, 1974; Hunt and Roddick, 1988; Mortimer et al., 1990). With the exception of Fyles et al. (1973) who dated nine lamprophyre dykes to constrain the age of Cu-Au-Mo mineralisation in Rossland, none of the other previous studies reported more than two lamprophyre K-Ar ages. These previous dates are compiled in Figure 2-2 and discussed individually below. Seven representative dykes, located on Figure 2-1, have been dated

using the K-Ar method on biotite (Table 2-1). These data are supplemented by seven whole rock K-Ar ages and one hornblende K-Ar age from lamprophyre and gabbroic dykes analysed in 1972, and one biotite K-Ar age from a lamprophyre dyke, provided by D.A. Brown (Fig. 2-1, Table 2-1). These new and previous dates are compiled in Figure 2-2.

The lamprophyre dykes dated in this study (Fig. 2-1) are kersantites consisting of biotite and pyroxene phenocrysts in a matrix of plagioclase laths. Biotite is commonly greenish, with occasionally corroded grain margins and compositional zoning. Clinopyroxene is slightly to completely altered to amphibole and carbonate. Some rounded phenocrysts with typical networks of serpentine and sulphide veinlets and carbonatized cores could be alteration products after olivine in some dykes.

Lamprophyre dyke biotite and hornblende K-Ar ages define two alkaline magmatic events: an Eocene event ranging from 40 to 52 Ma, and an Early Cretaceous event ranging from 129 to 141 Ma (Fig. 2-2). The Eocene event is constrained by ten ages from previous work (Yates and Engels, 1968; Fyles et al., 1973; Macdonald, 1974) and nine ages from this study (Table 2-1), all ages having a mode at 47.5 Ma (Fig. 2-2). This tight grouping of ages supports a well constrained and short lived alkaline magmatic event in the southern Omineca Belt in British Columbia and northern Washington (Armstrong, 1988). This alkaline magmatism is coeval with Middle Eocene crustal extension in southern British Columbia (Parrish et al., 1988), and could be a product of mantle upwelling as a result of crustal thinning rather than the distal product of subduction magmatism, as suggested by Armstrong (1988).

The Early Cretaceous event is defined by three dykes having biotite K-Ar ages ranging from 129 Ma to 141 Ma (Fig. 2-2). A lamprophyre and a vogesite from farther west in

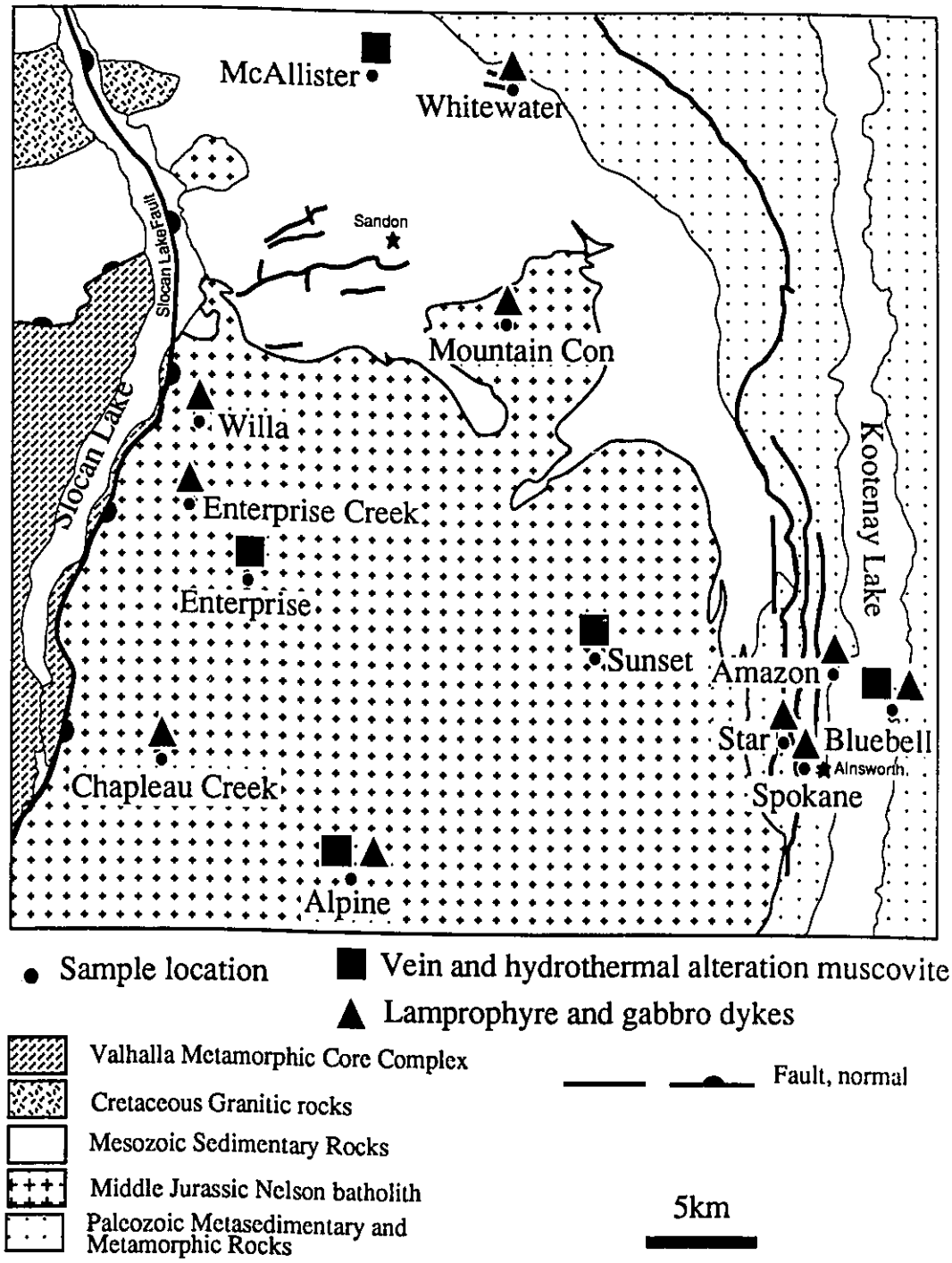

Figure 2-1. Simplified geology map of the Kokanee Range displaying the location of deposits sampled for vein and hydrothermal alteration muscovite, and of lamprophyre and gabbro dykes.

Table 2-1. K-Ar data for lamprophyre and gabbro dykes

Location	Lithology	Sample	Ore[1]	M.[2]	K (wt %)	^{40}Ar ($10^{-7}cm^3/g$)	^{40}Ar (%)	Age (Ma)	+/-(2σ)
Alpine#	Kersantite	127-6	Post	BI	7.56	151.2	94.9	50.7	0.8
	Kersantite	127-7	Post	BI	7.61	150.7	94.5	50.2	0.8
Enterprise Creek	Kersantite	ENT-2		BI	7.51	117.7	88.7	39.9	0.7
Mountain Con#	Metagabbro	81-3	Pre	BI	7.11	405.4	97.6	141.1	2.6
Spokane#	Kersantite	28-8	Pre	BI	6.16	108.0	86.0	44.5	0.8
Whitewater#	Kersantite	33-9	Pre	BI	7.32	142.5	86.0	49.4	1.0
Chapleau Creek	Kersantite	131-1		BI	7.67	147.3	62.0	48.8	1.0
Jersey#[3]	Lamprophyre	SP-1724		WR	3.01	71.9	82	*60	3
Amazon#	Lamprophyre	SP-1726	Pre	WR	1.38	83.8	77	*150	7
Star#	Lamprophyre	F-70-42	Pre	HN	0.92	16.4	63	*45	3
Bluebell#	Gabbro	67-0-147	Pre	WR	1.96	22.7	55	*30	3
	Gabbro	67-0-143	Pre	WR	1.98	20.3	60	*26	5
	Gabbro	67-0-143	Pre	WR	1.98	21.6	74	*28	3
	Gabbro	67-0-144	Pre	WR	2.03	22.2	63	*28	2
	Gabbro	67-0-145	Pre	WR	3.18	36.9	84	*30	2
Willa#[4]	Lamprophyre	DB87-145		BI	7.94	163.1	76.2	52.1	1.8[4]

#. Deposit name. *. Sample analysed in 1972, otherwise in 1989-1990. Model ages computed using decay constants from Steiger and Jäger (1977). 1. Timing relative to mineralisation. 2. Material analysed: BI, biotite; HN, hornblende; WR, whole rock. 3. Stratiform Pb-Zn massive sulphides in Cambrian limestones. 4. D.A. Brown (personal communication, 1990), error quoted at 1σ.

Quesnellia terrane have biotite K-Ar ages of, respectively, 129 ± 5 Ma and 135 ± 3 Ma (Jones et al., 1973; Mortimer et al., 1990). The Mountain Con dyke (141.1 ± 2.6 Ma) is a metamorphosed mafic rock originally composed of phenocrysts of pyroxene in a matrix of pyroxene and plagioclase. Pyroxene is replaced by epidote with a rim of tangential flakes of biotite. Biotite also occurs as disseminations in the matrix. At the contact with a mineralised vein, the metagabbro is replaced by chlorite, carbonate, and sericite, possibly during hydrothermal alteration. The vein consists of drusy quartz prisms growing inward from the contact. Along the contact, altered pyroxene phenocrysts are cut by the vein, thus proving the dyke to be older. The K-Ar age of biotite in the Mountain Con dyke could be that of intrusion or an older age reset

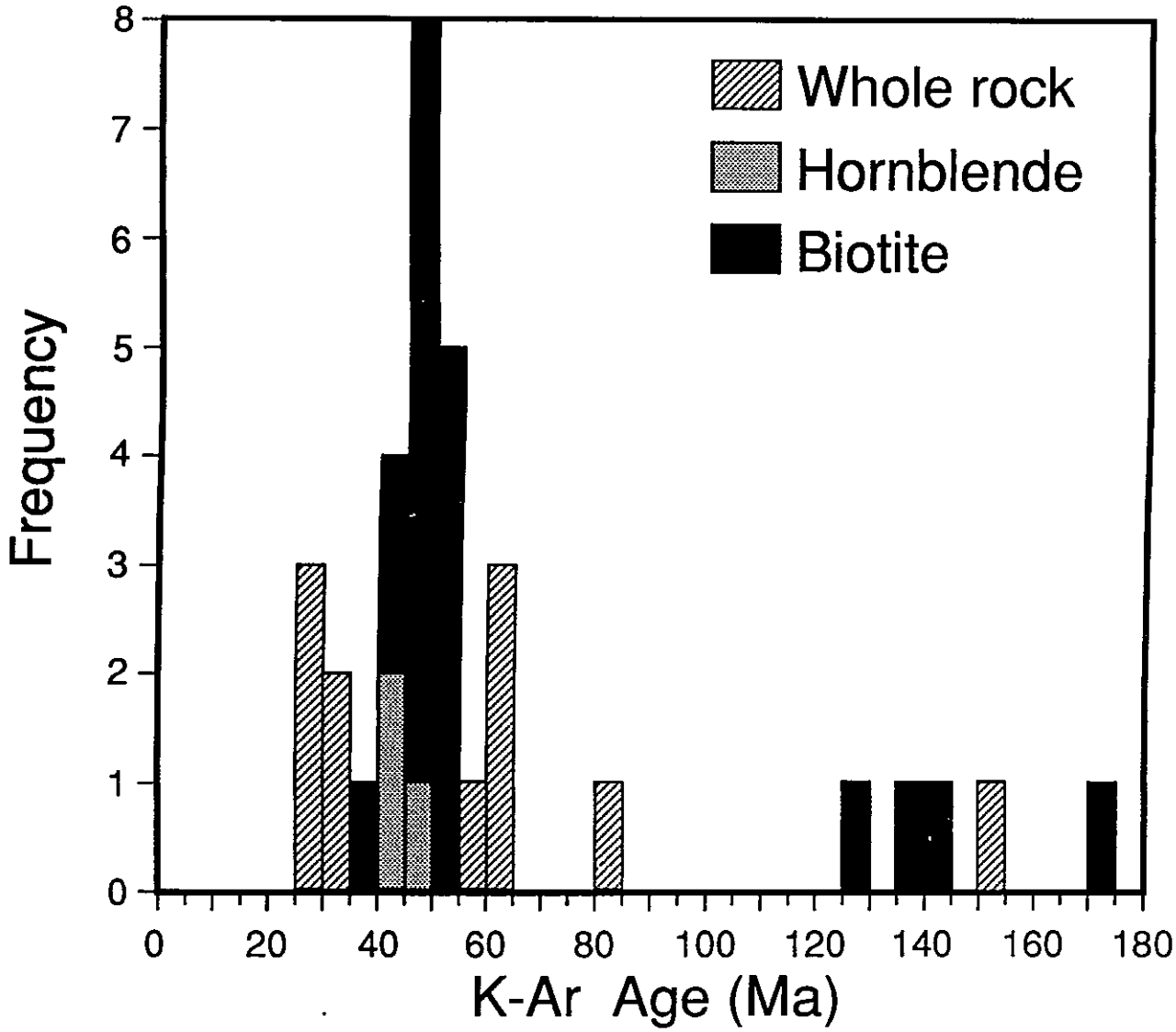

Figure 2-2. Histogram of lamprophyre and gabbro dykes biotite, hornblende, and whole rock K-Ar ages in the southern Omineca belt, British Columbia and Washington. Data from this study, Nguyen et al. (1968), Yates and Engels (1968), Fyles et al. (1973), Jones et al. (1973), Macdonald (1974), Hunt and Roddick (1988), and Mortimer et al. (1990). All ages calculated using constants from Steiger and Jager (1977).

during metamorphism. An early Cretaceous alkaline magmatic event in Quesnellia is possible but yet incompletely documented. Mortimer et al. (1990) interpreted these Early Cretaceous dykes as an alkaline back-arc east fringe to the Coast Plutonic Complex. Another lamprophyre dyke, with a biotite K-Ar age of 172 ± 6 Ma (Nguyen et al., 1968), intruded the Nelson batholith which has a slightly younger, but not significantly different zircon U-Pb age (169 ± 3 Ma; Carr et al., 1987), thus suggesting that biotite incorporated some extraneous radiogenic argon, and is not representative of the Early Cretaceous magmatic event.

Lamprophyre and gabbro dyke whole rock K-Ar ages display a wide range from 26 to 147 Ma compared to biotite and hornblende ages (Fig. 2-2). In the Rossland area, older ages for the Conglomerate dyke (58.1 ± 2.0 and 60.5 ± 2.0 Ma) compared to the other dykes, were interpreted by Fyles et al. (1973) to result from incorporation of radiogenic argon through partial melting of ubiquitous country rock inclusions in the dyke. Incorporation of extraneous argon appears likely for some of the other whole rock ages. A mafic dyke (62 ± 3 Ma) and a diabase (84 ± 3 Ma) dyke (Hunt and Roddick, 1988) are reported to cut rocks which are younger than the K-Ar ages of the dykes. A lamprophyre dyke (150 ± 7 Ma; Table 1) from the Amazon deposit intruded Paleozoic metasedimentary rocks reset to Eocene ages (Mathews, 1983). Macdonald (1974) reported a biotite K-Ar age of 49.5 ± 1.5 Ma for a post-ore lamprophyre dyke near the stratiform Jersey Pb-Zn deposit, hosted in Cambrian carbonates. The older 60 ± 3 Ma whole rock K-Ar age reported in this study (Table 2-1) for a similar dyke thus likely results from incorporation of extraneous radiogenic Ar.

Gabbroic dykes sampled at the Bluebell deposit, originally described as lamprophyres (H. Ohmoto, pers. com. to D.F. Sangster, 1971), likely represent the pre-ore dykes referred to by

Irvine (1957). The dykes commonly consist of partly altered phenocrysts of zoned plagioclase in a matrix of randomly oriented plagioclase laths partly to completely altered to a fine grained assemblage of muscovite, carbonate, and opaques. Where preserved, the texture is intergranular. Calcite amygdules are occasionally found. Bluebell gabbro dykes yield whole rock K-Ar ages ranging from 26 to 30 Ma (Table 2-1, Fig. 2-2). The dykes are cut by sulphide veins and are thus older than mineralisation. It is suggested that these Oligocene ages date the alteration of the dykes rather than their intrusive age. The narrow range of ages for the dykes indicates almost complete resetting of the K-Ar system by crystallisation of alteration muscovite. According to a Rb-Sr isochron from inclusion waters, Changkakoti et al. (1988) concluded that hydrothermal fluids were precipitating late stage, vug filling, quartz prisms 19.2 ± 5.9 Ma ago in the Bluebell deposit. The Bluebell-Ainsworth area is also well-known for its present geothermal activity. For example, mining at the Bluebell deposit was difficult because large amounts of hot water flooded the underground workings. Furthermore, past and present hot springs at Ainsworth, on the opposite shore of Kootenay Lake, and elsewhere in the area (Klepacki, 1985) attest to strong geothermal activity which may have caused gabbro dyke alteration.

Dating of Mineralisation

Dating of mineralisation was performed on vein and hydrothermal alteration muscovite from four deposits using K-Ar and step heating $^{40}Ar/^{39}Ar$ methods.

Enterprise deposit

A muscovite separate (148-5) from the Enterprise deposit (Fig. 2-1) is from a narrow hydrothermal phyllic alteration halo surrounding a drusy quartz-siderite-galena-sphalerite vein hosted by the Nelson batholith. Flakes of muscovite finely intergrown with quartz and siderite

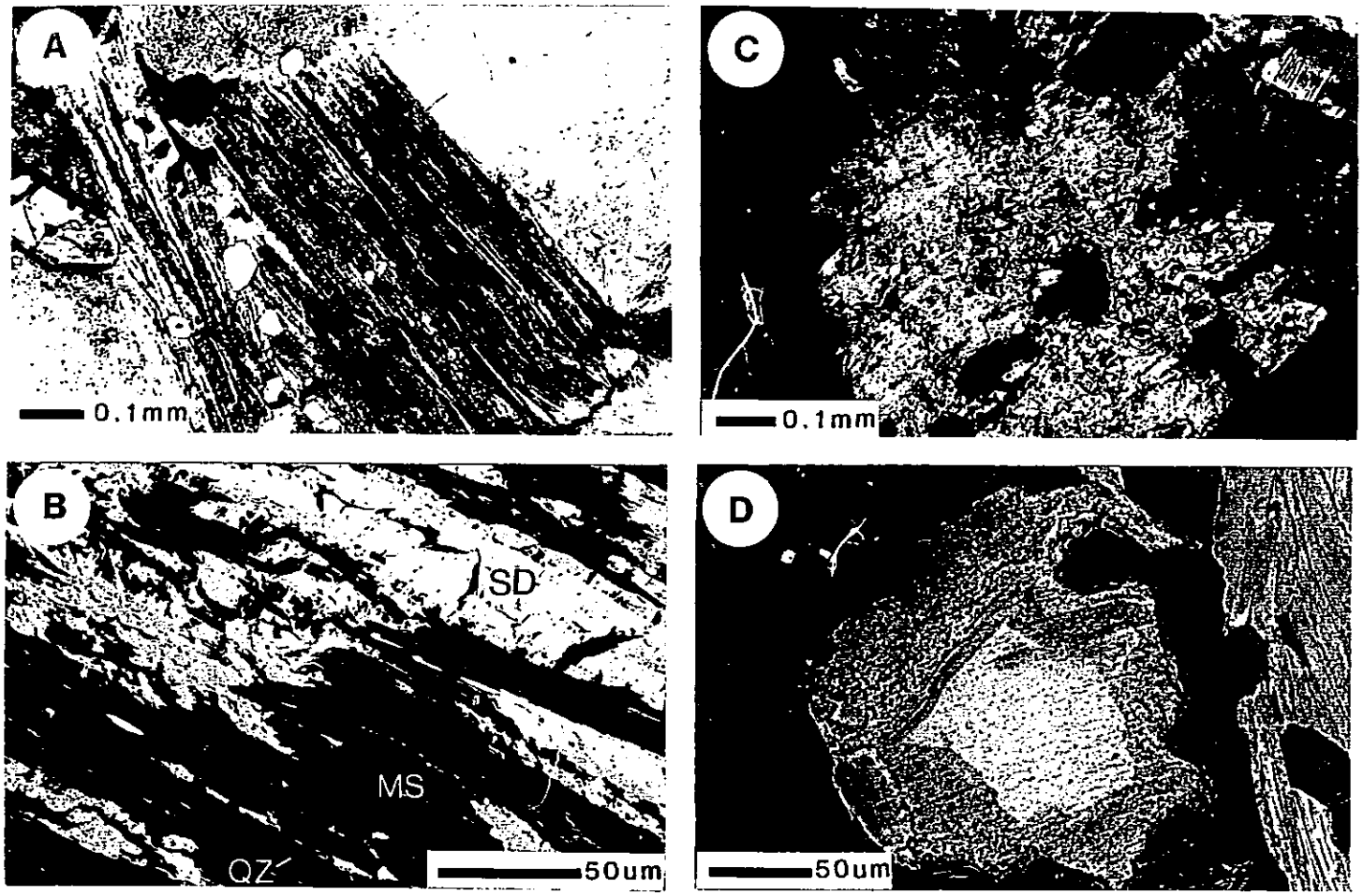

Figure 2-3. A) Hydrothermal alteration flake of muscovite intergrown with quartz and siderite, Enterprise deposit. Muscovite overgrows the granitic texture of clear anhedral quartz and sub-euhedral, sericitised potassium feldspar. B) SEM backscattered electron image displaying a muscovite (medium grey) flake intergrown with quartz (dark grey) and siderite (light grey). C) Typical hydrothermal alteration muscovite replacing feldspar from Nelson granodiorite near the Alpine deposit vein. Remnants of feldspar are surrounded by a coarse and irregular grain of muscovite overgrowing finer grained flakes of muscovite. D) SEM backscattered electron image displaying two intergrown muscovite from the vein near the McAllister deposit. An older, light grey muscovite is overgrown by a younger, darker muscovite.

overgrow the granitic texture (Figs. 2-3A, B). Muscovite was not completely separated from quartz and siderite and the resulting concentrate contained only 4.5% K instead of about 9% expected in pure muscovite. The presence of siderite in the concentrate is reflected by 1.1% Ca in the analysis. Figure 2-4A presents the step heating $^{40}Ar/^{39}Ar$ age spectra and the Ca/K ratio associated with each gas fraction. Whereas there is some variation among the step ages, they range only from 56 to 60 Ma with a total integrated age of 59.5 ± 0.7 Ma (Table 2-2). Four steps from 40 to 80% of cumulative ^{39}Ar represent gas release from muscovite, as they have the lowest Ca/K ratios and are essentially free of any effects of gas release from siderite. These four steps have an age of 58.2 ± 0.7 Ma in good agreement with the total integrated age and provide the best estimate of the age of hydrothermal alteration associated with vein mineralisation.

Bluebell deposit

At the Bluebell deposit (Fig. 2-1), three samples of hangingwall Cambrian mica schists and pre-folding dyke have K-Ar ages ranging from 50 to 55 Ma (Table 2-3). They have been reset by a Middle Eocene thermal event which is documented along the shores of Kootenay Lake (Mathews, 1983) or have resulted from slow cooling following the Middle Cretaceous plutonic event (Archibald et al., 1984). Phlogopite from a mica layer in Cambrian Badshot Formation marble has an age of 76 ± 4 Ma (Table 2-3), significantly older than the other ages for the country rocks. This is likely the result of incomplete resetting of older phlogopite during the Eocene thermal event, of incorporation of extraneous radiogenic argon during metamorphic crystallisation of phlogopite, or from a higher closure temperature of phlogopite relative to biotite. Muscovite from a quartz-sulphide vein cutting a gabbro dyke yields an age of 59 ± 3 Ma (Table 2-3), identical to step heating $^{40}Ar/^{39}Ar$ age spectra of hydrothermal alteration muscovite

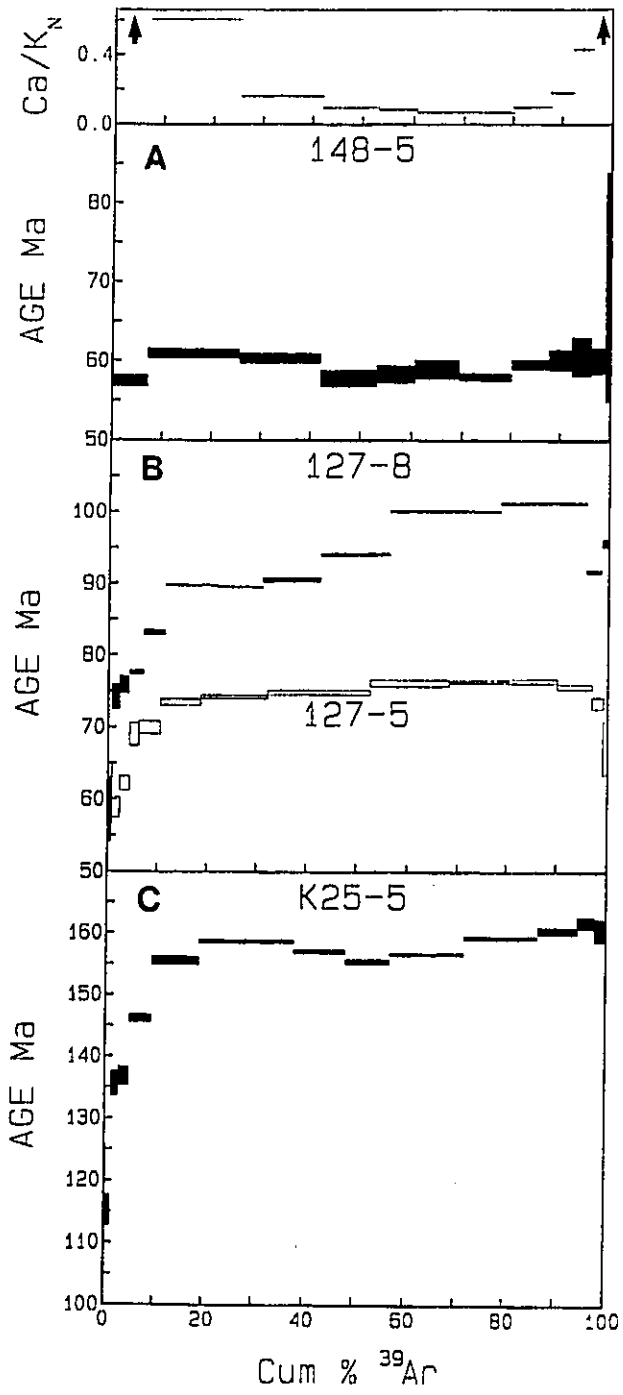

Figure 2-4. Step heating $^{40}Ar/^{39}Ar$ age spectra for hydrothermal alteration muscovite from data in Table 2-2. A) Flat age spectrum from Enterprise deposit overlain by the Ca/K_N ratio for each gas fraction. Arrows are for Ca/K_N ratios around 2 (out of scale). The gas fractions with lowest Ca/K_N ratios, between 40 and 80% ^{39}Ar cumulative gas release, are more reliable and have an age of 58.2 ± 0.7 Ma. B) Hump shaped spectra from the Alpine deposit, both characterized by low temperature release of gas fractions with ca. 60 Ma ages followed, after a steep rise, by a flat (127-5) or a complicated (127-8) central portion and younger ages in the final gas fractions released. C) Complicated spectrum from a small vein near McAllister deposit displaying an initial steep rise of age followed by a shallow u-shaped pattern.

at the Enterprise deposit. This age contrasts with whole rock ages (26-30 Ma, Table 2-1) from these altered gabbro dykes cut by the vein, and we suggest that muscovite in the vein as well as other hostrock micas in the Bluebell deposit remained closed to Ar diffusion during dyke alteration. Distinction between mineralisation and the Eocene thermal event is difficult, likely because the two are coeval.

Alpine deposit

Two hydrothermal alteration muscovites from a quartz-sulphide vein at the Alpine deposit (Fig. 2-1) have been analysed by $^{40}Ar/^{39}Ar$ step heating. Sample 127-5 is a muscovite from a narrow (10 cm) hydrothermal phyllic alteration halo, developed at the contact with the vein in the host granodiorite, in which muscovite completely replaces biotite and minor clinopyroxene, and partly replaces K-feldspar and plagioclase along grain boundaries and fractures. Figure 2-3C displays a large and irregular muscovite overgrowing a finer grained muscovite, both replacing feldspar. Remnants of corroded feldspar are interstitial to muscovite flakes (Fig. 2-3C). The age spectrum for this sample (Fig. 2-4B; Table 2-2) is hump-shaped with a steep increase of ages from 58 Ma to 73 Ma in the first 15% of ^{39}Ar cumulative gas release to a near-flat spectrum for a significant proportion of the spectrum, reflecting ages between 73 and 75 Ma. Three steps between 53 and 90% of cumulative ^{39}Ar gas release have concordant ages of 76.3 ± 0.7 Ma, only slightly older than the total integrated age of 74.2 ± 0.7 Ma. There is, however a significant decrease in ages for the last 10% of cumulative ^{39}Ar gas release, down to 67 Ma.

The other muscovite analysed by $^{40}Ar/^{39}Ar$ (127-8) is from rounded to angular quartz-muscovite aggregates less than 1 cm in diameter, considered to be fragments of strongly altered country rock incorporated in the quartz vein. Two grain size populations of muscovite are found.

Table 2-2. Step heating $^{40}Ar/^{39}Ar$ data for vein and hydrothermal alteration muscovite.

Temperature (°C)	^{36}Ar	^{37}Ar	^{38}Ar	^{39}Ar	^{40}Ar	% Atmos. ^{40}Ar	Apparent Age +/- 2σ		^{39}Ar (%)
		($x10^{-9}$ cm³)							
Enterprise deposit									
148-5									
600	0.038	0.851	0.057	3.330	26.55	41.9	57.5	0.7	7.1
700	0.011	0.639	0.022	8.610	45.74	7.4	60.9	0.6	18.4
750	0.011	0.155	0.011	7.738	40.82	7.6	60.3	0.6	16.6
800	0.011	0.062	0.013	5.219	27.45	11.3	57.8	1.0	11.2
850	0.008	0.035	0.010	3.423	18.47	12.8	58.3	1.1	7.3
900	0.006	0.037	0.007	4.129	21.44	8.4	58.9	1.2	8.8
935	0.008	0.043	0.010	4.993	25.77	9.3	58.0	0.5	10.7
970	0.004	0.044	0.006	3.543	18.31	6.9	59.6	0.6	7.6
1000	0.004	0.048	0.006	2.151	11.57	9.7	60.2	1.3	4.6
1050	0.002	0.093	0.006	1.752	9.25	7.2	60.6	2.4	3.7
1100	0.003	0.303	0.006	1.291	7.12	12.0	60.1	1.6	2.8
1250	0.012	2.361	0.025	0.417	5.79	59.5	69.4	14.5	0.9
1450	0.012	1.076	0.017	0.124	4.26	81.8	77.1	76.8	0.3
Total	0.13	0.20	5.75	46.72	262.5	14.5	59.5	0.7	
10^{-9} cm³/g	6.1	272.37	9.28	2214.13	12442.6				
Alpine deposit									
127-5									
600	0.026	0.008	0.035	0.772	11.61	67.1	60.8	4.3	0.8
700	0.008	0.006	0.006	1.584	9.84	23.1	58.9	1.4	1.6
750	0.010	0.008	0.008	1.959	12.82	22.7	62.2	1.0	2.0
800	0.005	0.005	0.006	1.780	11.36	12.0	69.0	1.6	1.8
850	0.011	0.007	0.009	4.318	27.89	11.7	70.0	0.9	4.3
900	0.014	0.008	0.015	8.078	52.38	7.6	73.5	0.4	8.1
935	0.016	0.006	0.023	13.341	85.50	5.5	74.3	0.2	13.4
970	0.017	0.000	0.037	20.535	130.26	3.8	74.9	0.3	20.7
1000	0.010	0.001	0.026	15.295	97.92	2.9	76.2	0.4	15.4
1050	0.009	0.007	0.021	12.059	77.67	3.2	76.4	0.1	12.1
1100	0.006	0.005	0.018	9.678	61.99	2.7	76.4	0.3	9.7
1150	0.002	0.005	0.012	6.856	42.86	1.3	75.7	0.3	6.9
1250	0.001	0.005	0.003	2.170	13.33	2.6	73.4	0.8	2.2
1450	0.002	0.010	0.003	0.884	5.28	8.4	67.2	3.7	0.9
Total	0.13	0.22	0.08	99.31	640.7	6.2	74.2	0.7	
10^{-9} cm³/g	6.0	3.60	9.87	4457.31	28757.0				
127-8									
600	0.093	0.014	0.050	1.806	35.94	76.2	58.6	4.5	0.7
700	0.019	0.029	0.010	3.806	28.51	19.5	74.2	1.7	1.5
750	0.016	0.016	0.015	5.186	36.88	13.2	75.9	1.2	2.0
800	0.027	0.006	0.021	7.382	54.58	14.5	77.6	0.3	2.9
850	0.031	0.025	0.029	10.798	82.34	11.1	83.2	0.4	4.2
900	0.042	0.018	0.070	26.804	208.85	5.9	89.8	0.1	10.5
930	0.019	0.003	0.058	23.384	176.72	3.2	89.5	0.1	9.1
970	0.020	0.013	0.079	30.027	228.10	2.6	90.6	0.3	11.7

Table 2-2. Step heating $^{40}Ar/^{39}Ar$ data for vein and hydrothermal alteration muscovite (cont.).

Temperature (°C)	^{36}Ar	^{37}Ar	^{38}Ar	^{39}Ar	^{40}Ar	% Atmos. ^{40}Ar	Apparent Age +/- 2σ		^{39}Ar (%)
		($\times 10^{-9}$ cm^3)							
Alpine deposit (cont.)									
1000	0.021	0.011	0.099	34.582	272.47	2.3	94.1	0.2	13.5
1050	0.027	0.015	0.171	56.769	473.79	1.7	100.2	0.2	22.2
1100	0.015	0.041	0.131	44.035	369.74	1.2	101.3	0.1	17.2
1150	0.004	0.038	0.020	7.476	57.20	2.0	91.7	0.2	2.9
1250	0.003	0.097	0.007	2.880	23.44	3.7	95.7	0.6	1.1
1450	0.002	0.087	0.008	0.724	7.41	7.2	115.4	5.3	.3
Total	0.34	0.77	0.41	255.66	2056.0	4.9	93.6	0.9	
10^{-9} cm^3/g	5.8	7.11	13.25	4399.55	35380.4				
Small vein near McAllister deposit									
K25-5									
600	0.065	0.018	0.058	0.295	22.01	87.8	110.2	15.5	0.4
700	0.013	0.242	0.007	0.802	11.44	33.4	115.2	2.5	1.0
750	0.008	0.743	0.005	1.115	15.00	16.3	135.6	2.0	1.3
800	0.012	0.441	0.011	1.927	25.55	14.4	136.8	1.5	2.3
850	0.029	0.046	0.018	3.694	53.63	16.2	146.2	0.6	4.4
900	0.021	0.010	0.017	8.030	110.45	5.7	155.6	0.6	9.6
950	0.019	0.010	0.026	15.914	216.54	2.6	158.7	0.3	19.0
975	0.009	0.004	0.014	8.666	116.35	2.4	157.1	0.3	10.3
1000	0.010	0.005	0.014	7.388	98.76	3.0	155.5	0.4	8.8
1050	0.016	0.009	0.020	12.327	165.96	2.9	156.7	0.2	14.7
1100	0.011	0.007	0.025	12.412	168.38	1.9	159.4	0.2	14.8
1150	0.005	0.004	0.010	6.653	90.67	1.7	160.4	0.6	7.9
1200	0.001	0.006	0.007	2.781	37.95	0.9	161.8	0.9	3.3
1450	0.002	0.011	0.001	1.953	26.76	2.1	160.6	1.8	2.3
Total	0.22	0.23	1.56	83.96	1159.4	5.7	156.1	1.5	
10^{-9} cm^3/g	10.8	74.81	11.12	4034.45	55715.9				

Coarse grained muscovite (0.01 to 0.5 mm) overgrows fine grained muscovite (<0.01 mm) that is interstitial to quartz grains. The age spectrum for this sample (Fig. 2-4B; Table 2-2) is more complex than that of 127-5, with a similar steep rise from 58 to 88 Ma in the first 15% of cumulative ^{39}Ar gas release and a near-flat region at 89 Ma to 42 % of cumulative ^{39}Ar gas release. The next three steps rise to 100 Ma with a decrease of age in the final 5% gas to about 91-95 Ma. The total integrated age is 93.6 ± 0.9 Ma.

Hump-shaped patterns such as these are similar to age spectra, described by Wijbrans and

McDougall (1986) and Scaillet et al. (1990), for mixtures of two structurally different micas grown at different times. Wijbrans and McDougall (1986) suggested that different gas release properties of the micas resulted in the younger mica dominating the high temperature portion of the age spectra, thus producing a spectra with young final ages. Wijbrans and McDougall (1986) concluded that the actual shapes of the spectra were a function of the mixture ratio, and the chemical and physical properties of the two micas, with intermediate plateau ages between the true ages of the two micas.

In the two hydrothermal alteration assemblages analysed from the Alpine deposit, a coarse grained muscovite overgrows a fine grained muscovite. Textural evidence is inconclusive to determine if the two muscovites of Figure 2-3C represent two different hydrothermal events. This possibility is considered unlikely, however, because of the close spatial association and limited extent (10 cm) of hydrothermal alteration. Rather, it is suggested that the two muscovites represent two stages of progressive hydrothermal alteration, in which the early, fine grained muscovite crystallised before complete degassing of old, radiogenic argon from the Nelson batholith, possibly because of low fluid/rock ratio. During prograde hydrothermal alteration, recrystallisation of early, fine grained muscovite to coarse grained muscovite resulted in complete argon degassing, possibly in conjunction with a higher integrated fluid/rock ratio. Both Alpine samples are probably different mixtures of variably degassed early muscovite and more completely degassed late muscovite. A similar process has been reported by Bonhomme et al. (1987). In that case, mixtures of hydrothermal alteration clays crystallised after partial to complete degassing of radiogenic argon derived from hostrocks. A K-Ar age of 82 ± 3 Ma (Table 2-3) for another Alpine hydrothermal alteration muscovite separate also indicates incomplete

Table 2-3. K-Ar data for mineralisation, hydrothermal alteration, and hostrocks

Deposit	Lithology	Sample	M[1]	K (wt %)	$^{40}Ar^*$ ($10^{-7}cm^3/g$)	(%)	Age +/-(2σ) (Ma)	
Mineralisation								
Bluebell	Mica layers with sulphides in marble	67-0-35	PH	7.09	212.8	87	*76	4
	Post-lamprophyre quartz-sulphides vein	67-0-44	MS	7.01	162.6	74	*59	3
Hostrocks								
Bluebell	Mica schist, 30 cm from ore	67-0-103	MS	5.56	121.3	78	*55	3
	Mica schist, 15 m from ore	66-0-40B	BI	7.63	150.9	81	*50	3
	Pre-folding dacite dyke	F-70-29	BI	6.45	127.6	48	*50	3
Alteration								
Alpine[2]	Vein alteration of Nelson granite	JL87-397	MS	9.20	301.0	82.3	82.3	2.9
Sunset[2]	Vein alteration of Nelson granite	SUNSET	MS	8.41	321.2	90.0	95.7	3.3

Model ages computed using constants from Steiger and Jäger (1977). 1. Material analysed: BI, biotite; PH, phlogopite; MS, muscovite. 2. D.A. Brown (personal communication, 1990), errors quoted at 1σ. *. Analysed in 1972.

chemical resetting of the argon system. Hydrothermal alteration muscovite from the Sunset deposit (Fig. 2-1), with an age of 96 ± 3 Ma (Table 2-3), could also represent a mixed age between the time of emplacement of the Nelson batholith and the age of hydrothermal alteration.

One marked feature of both Alpine age spectra is the steep increase from initial ages of about 58 Ma. The first gas release should represent a maximum time of closure of the argon system to diffusion during crystallisation of hydrothermal alteration muscovite. The agreement of these initial ages in both samples suggests that a significant event has been dated. In addition,

it is the same age as recorded at the Enterprise and Bluebell deposits, further supporting the validity of this age as the time of a widespread hydrothermal event that resulted in alteration and mineralisation.

Small vein near McAllister deposit

Interstitial seams of muscovite occur in a quartz veinlet cutting Slocan Group pelites and minor dolostones near the McAllister deposit (Fig. 2-1). This vein was sampled because it contained muscovite, which is not found in the ore of the McAllister deposit; sulphides were suspected but SEM analyses demonstrated these were Fe oxydes. The muscovite (K25-5) comprises two finely intergrown generations. SEM back-scattered electron imagery shows an older, light grey muscovite rimmed by a younger, darker muscovite (Fig. 2-3D). The step heating $^{40}Ar/^{39}Ar$ age spectrum rises steeply from an initial gas release age of 110 Ma to 157 Ma by 20% of cumulative ^{39}Ar gas release (Fig. 2-4C; Table 2-2). The remaining heating steps have a shallow u-shaped pattern with ages ranging from 154 to 160 Ma. The integrated age is 156.8 ± 1.5 Ma. The spectrum is consistent with a minor loss of radiogenic Ar during an event at or younger than 110 Ma. This could be the event responsible for the darker rimming muscovite, although the irregular u-shaped pattern suggests a more complex history, possibly with both the older and younger phases degassing over most of the gas release. In this case the coarser muscovite is at least 160 Ma old, the oldest age in the highest temperature gas release. In contrast to the Alpine samples, no high temperature age decrease is present.

The relation of the vein containing K25-5 muscovite to the McAllister deposit is not certain, although the vein is close to the deposit. Primary fluid inclusions from ore stage quartz at the McAllister deposit are commonly CO_2-rich and display evidence of boiling, a feature not

observed in quartz from sample K25-5. Stable and Pb isotope studies indicate that the McAllister was formed at the same time and from the same hydrothermal system as the Enterprise deposit (Beaudoin et al., 1992b; 1992c). It is suggested that the small vein sampled close to the McAllister is older than, and unrelated to, the McAllister ore stage event. The older age for the muscovite suggests that the vein was formed as a result of Early-Midlle Jurassic deformation and greenschist metamorphism, or intrusion of the Nelson batholith. Cairnes (1934) considered that barren quartz veins were older than the Ag-Pb-Zn veins. Resetting of the Ar system could be a result of McAllister ore stage hydrothermal fluid flow.

Age of Mineralisation

The spatial association of Ag-Pb-Zn veins with granitic batholiths has been interpreted by other workers to reflect a genetic link. The nature of the genetic link has evolved with time from extremely differentiated "ore magma" (Spurr, 1912) to a point source of heat driving convection of non-magmatic hydrothermal fluids (Sinclair et al., 1980). When veins occurred within the batholith, some unknown "magma below" was invoked as the source of the metals (Emmons, 1924).

Vein muscovite at the Bluebell deposit has a K-Ar age of 59 ± 3 Ma. Hydrothermal alteration muscovite at the Enterprise deposit has a 58.2 ± 0.7 Ma $^{40}Ar/^{39}Ar$ age. A hydrothermal event circa 60 Ma is also recorded in hydrothermal alteration muscovites at the Alpine deposit. Therefore, hydrothermal fluids precipitated Ag-Pb-Zn vein and replacement mineralisation about 58 Ma ago. At the Alpine deposit, the circa 60 Ma vein is cut by a swarm of 50.5 Ma kersantite dykes indicating a hydrothermal event of less than 10 Ma duration. In Ainsworth area, the 44.5 ± 0.8 Ma Spokane deposit dyke (Table 2-1) is cut by mineralisation. If the 59 Ma vein from the

Bluebell deposit is taken as an older limit for mineralisation, this younger age constrains the duration of the hydrothermal event in the Kokanee Range to about 15 Ma (Fig. 2-5) although individual deposits were likely emplaced over a shorter period of time.

Geochronologic data (Fig. 2-5) are consistent with field evidence which indicate that mineralisation is younger than Middle Jurassic Nelson batholith and foliation in Ainsworth area, but coeval or older than Early and Middle Eocene unroofing of the Valhalla metamorphic core complex and movement of the Slocan Lake Fault (Fig. 2-5). Middle Eocene lamprophyre and gabbro dykes are broadly coeval with mineralisation (Fig. 2-5). During extension, the Valhalla metamorphic core complex was rapidly unroofed from mid-crustal levels (Parrish et al., 1988). Displacement along the Slocan Lake Fault represents the last event of brittle failure along a transcrustal shear zone which possibly cuts the Moho (Cook et al., 1988; Parrish et al., 1988). Beneath Kokanee Range, the Moho is at a depth of about 35 km, in contrast to nearly 45 km east of Kootenay Lake (Cook et al., 1988). This is interpreted to indicate mantle upwelling as a result of crustal thinning. It is suggested that mantle upwelling, in turn, resulted in adiabatic partial melting and intrusion of a suite of lamprophyre and gabbro dykes in southern British Columbia. Furthermore, crustal thinning and mantle upwelling likely resulted in the high regional heat flow for which southeastern British Columbia is noted. The area is also underlain by a lower crust with high electrical conductivity, interpreted to be due to an interstitial fluid phase (Gough, 1986; Jones et al., 1988). It is proposed that the combination of a high heat flow regime and a hydrous lower crust, developed in an extensional setting, led to fluid flow controlled by fracture porosity and subsequent formation of the Ag-Pb-Zn vein and replacement deposits of the Kokanee Range. Thus, mineralisation and dyke intrusion are both considered to be coeval products of Eocene

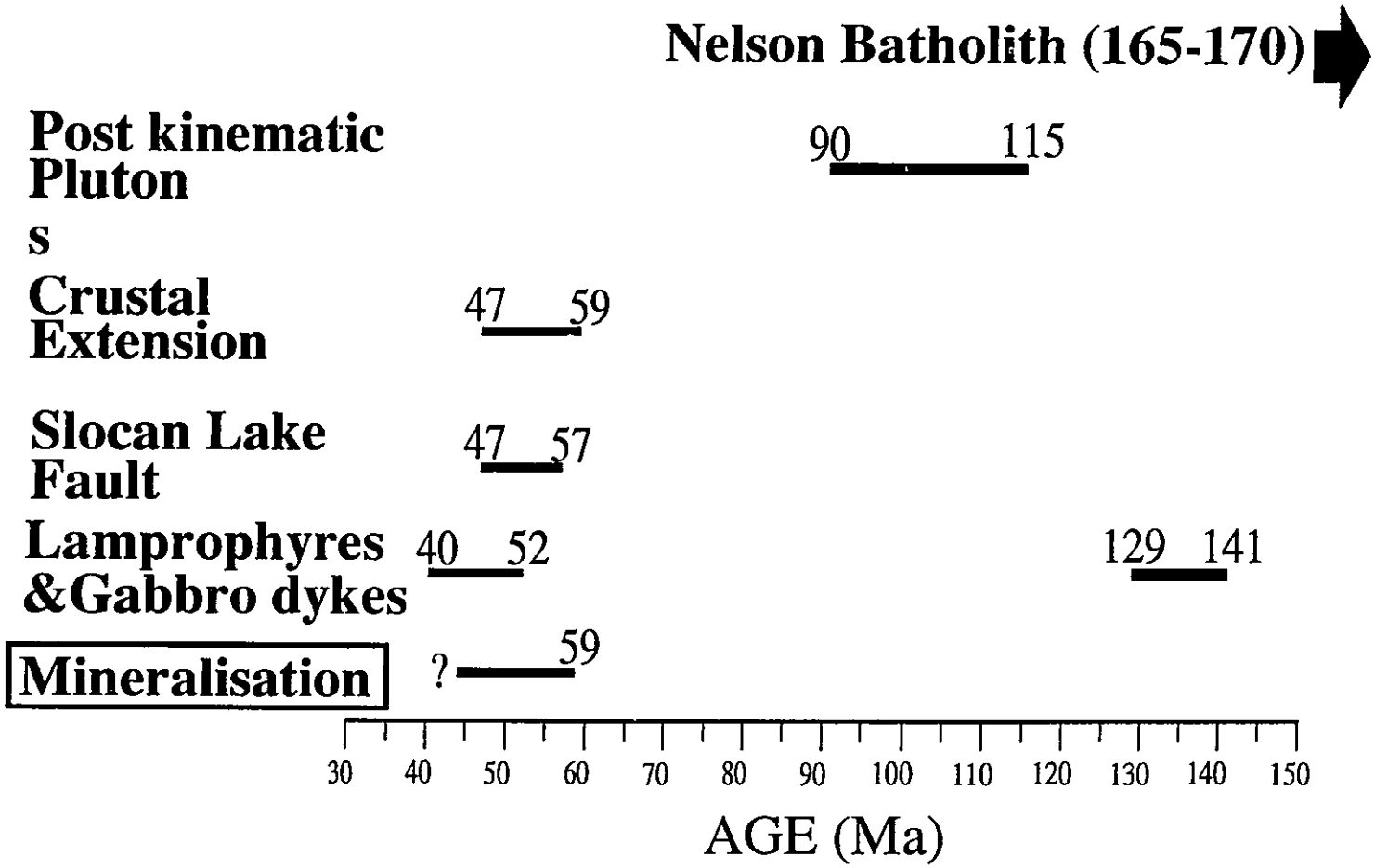

Figure 2-5. Summary diagram displaying the large time interval between intrusion of the Nelson batholith and mineralisation. Mineralisation is Eocene and coeval with crustal extension, displacement along the Slocan Lake Fault, and lamprophyre dyke intrusion.

crustal extension.

A 100 Ma age interval between hydrothermal mineralisation and intrusion of the Nelson batholith is documented which makes any genetic link between the two unlikely. In recent years, geochronologic dating of Ag-Pb-Zn vein mineralisation has become available for a few other districts. In the Harz Mountains of Germany, concentric mineral zoning around the Brocken pluton was used to argue that there is a genetic link between mineralisation and plutonism (Dahlgrün, 1950). Mertz et al. (1989), however, demonstrated that the youngest age for the main mineralisation stage is 170 Ma younger than that of the Brocken granite. Fryklund (1964) argued that the Ag-Pb-Zn veins of the Coeur d'Alène district, U.S.A., were genetically linked with the Cretaceous Gem stocks, but Leach et al. (1988) demonstrated that post ore-stage vein sericite has K-Ar ages ranging from 876 to 77 Ma. This indicates at least a Late Proterozoic age for mineralisation, in accord with galena lead isotope data (Zartman and Stacey, 1971). Adequate geochronological data on mineralisation is therefore essential to infer a genetic link between intrusive rocks and spatially associated mineralisation. A striking example is provided by Farrar et al. (1990) who demonstrated that the Palca 11 W-Sn-Cu vein in Choquene district, Peru, was older than the felsic stocks with which it had been previously associated.

Conclusions

Step heating $^{40}Ar/^{39}Ar$ spectra and K-Ar analyses indicate an age of crystallisation of vein and hydrothermal alteration muscovite of 59 Ma in the Kokanee Range. Coeval lamprophyre dykes indicate that hydrothermal mineralisation had ceased at the Alpine deposit by 50.5 Ma but was continuing in Ainsworth area at 44 Ma (Fig. 2-5). The hydrothermal system in the Kokanee Range was active for at least 15 Ma, but likely for a shorter period of time in each deposit.

Lamprophyre and gabbro dyke biotite and hornblende K-Ar ages define two alkaline magmatic events (Fig. 2-5). The Early Cretaceous event (129-141 Ma) is poorly constrained. The Eocene event (40-52 Ma) is well documented in southern British Columbia and northern Washington. It probably represent alkaline magmatism resulting from mantle upwelling during Eocene crustal extension.

Mineralisation is coeval with Middle Eocene crustal extension during which the Valhalla metamorphic core complex was rapidly uplifted in the footwall of the transcrustal Slocan Lake Fault (Fig. 2-5). Crustal thinning and mantle upwelling produced elevated heat flow and a hydrous lower crust in the Kokanee Range. High heat flow and extensional structures were probably responsible for hydrothermal fluid movement and flow paths.

The Ag-Pb-Zn vein and replacement deposits of the Kokanee Range have long been thought to be genetically related to the intrusion of the large, granodioritic Nelson batholith. We have documented an age interval between batholi... ...placement and mineralisation of at least 100 Ma which makes any genetic link between the two unlikely. Large age difference between granitic intrusion and Ag-Pb-Zn vein mineralisation in two other "granite-related" vein orefields have also been recently documented in the Harz Mountains, F.R.G., and the Coeur d'Alène district, Idaho. We conclude that a genetic relationship between an intrusion and mineralisation based on spatial association without adequate geochronological data, is unwarranted for Ag-Pb-Zn vein districts.

CHAPTER 3

Isotopic Evidence for Complex Pb Sources

Introduction

The Ag-Pb-Zn vein and replacement deposits of the Kokanee Range have been the focus of several Pb isotope studies since the first data were published by Russell and Farquhar (1960). Sinclair (1964), Reynolds and Sinclair (1971), and Cox (1979) used galena and rock Pb isotope ratios to support a direct genetic link between the Middle Jurassic Nelson batholith and spatially associated mineralisation. LeCouteur (1973) reached a contrary conclusion from these studies and, based on field relations and galena Pb isotopic compositions, suggested that the deposits were more likely Eocene in age. Although the previous authors agreed on an upper crustal source for most of the Pb, they had to suggest an exotic lower crustal reservoir, in order to explain the peculiar Pb isotopic signature for deposits near Ainsworth, including the Bluebell deposit.

Andrew et al. (1984) proposed a new framework for interpretation of Pb isotope compositions in the Cordillera using the "Bluebell" and "Shale" Pb evolution curves. They suggested that Pb isotopic compositions of galenas from the Kokanee Range plotted on two "mixing line isochrons" joining the Bluebell and Shale curves at 580 Ma and 160 Ma. This interpretation was based on the assumption that the Bluebell deposit was syngenetic with its Lower Cambrian host rock. Logan et al. (1988) divided the deposits hosted by the Nelson batholith into three groups, based on their Pb isotopic compositions, and suggested that each group represents mixtures of Pb from three different sources mixed during the Jurassic to Tertiary.

Radiometric dating indicates that the Ag-Pb-Zn deposits of Kokanee Range are Eocene in age (Beaudoin et al., 1992a). Mapping and geochronological studies of the Slocan Lake Fault (Parrish, 1984) and the Valhalla complex (Carr et al., 1987) showed that the Valhalla is a Paleocene-Eocene metamorphic core complex exposed during crustal extension in southeastern British Columbia (Parrish et al., 1988). The Pb isotopic compositions of sedimentary and igneous country rocks in the region (Ghosh, 1986; Bevier, 1987) place new constraints on the location and age of the possible Pb reservoirs for the Kokanee Range deposits. In the light of these constraints, a lead isotopic study of the Ag-Pb-Zn deposits was undertaken incorporating all previous, as well as new, data to reinterprete the sources of Pb for these deposits.

Lead Isotopes

New and published galena lead isotope analyses for the Kokanee Range vein and replacement deposits are compiled in Table 3-1, which contains 147 isotope compositions, including 46 new determinations, from 74 deposits located in Figure 3-1. Analytical techniques used for the new determinations of Pb isotopic ratios are reported in Godwin at al. (1988). All Pb isotope ratios are normalized to the Broken Hill standard values of Richards et al. (1981), with the exception of four galena Pb isotope ratios from the Bluebell deposit reported by Ohmoto (1968) for which the original normalisation standard was not reported. In this paper, average galena Pb isotope ratios for each deposit, rather than individual analyses, are plotted in order to give each deposit equal weight.

Geographic distribution

The deposits can be divided into four groups using average galena Pb isotope ratios (Fig. 3-2). Deposits of the Kokanee group are hosted by the Nelson batholith, with the exception of

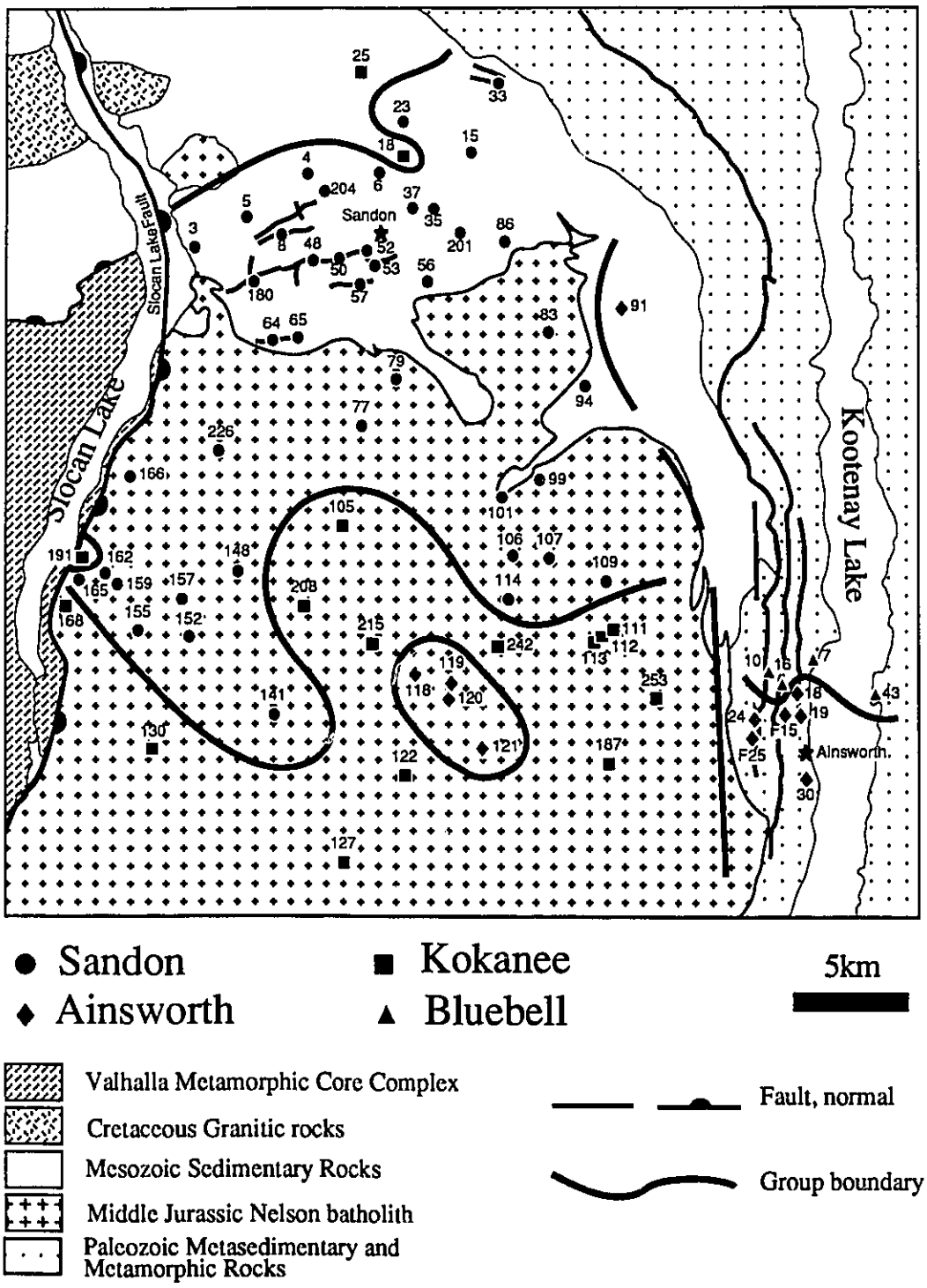

Figure 3-1. Simplified geology map showing the location of the Ag-Pb-Zn vein and replacement deposits for which Pb isotope data are available. Also displayed is the distinct geographic distribution of the four groups of deposits. The number beside each deposit is indexed in Table 3-1.

Table 3-1. Compilation of galena Pb isotope ratios

Number[a]	Deposit	$^{206}Pb/^{204}Pb$	$^{207}Pb/^{204}Pb$	$^{208}Pb/^{204}Pb$	Reference[b]
Sandon group					
082FNW 86	Utica	18.786	15.633	38.984	6
		[c]18.986	15.565	38.553	8
		18.752	15.603	38.904	12
082FNW 8	Alamo	18.685	15.633	39.102	12
082FNW 65	Hewitt	18.681	15.578	38.883	8
		18.694	15.610	38.997	9
		18.702	15.608	39.020	7
082FNW 155	Ottawa	18.841	15.656	39.093	8
		18.874	15.635	39.046	6
		18.888	15.627	39.033	12
082FNW 152	Arlington	18.847	15.640	39.020	6
		18.853	15.629	39.091	10
082KSW 23	Lucky Jim	18.774	15.626	39.006	6
082KSW 33	Whitewater	18.796	15.649	38.818	6
082FNW 3	Bosun	18.737	15.626	39.013	6
082FNW 5	California	18.619	15.611	39.029	6
082FNW 94	Cork-Province	18.790	15.628	39.015	6
082FNW 162	Coronation	18.965	15.650	38.939	6
082FNW 148	Enterprise	18.717	15.628	38.944	6
		18.755	15.631	39.098	12
082FNW 79	Fisher Maiden	18.739	15.627	38.948	6
082FNW 101	Index	18.758	15.642	38.933	6
082FNW 57	Ivanhoe	18.743	15.637	38.995	6
082FNW 166	Kalispell	18.701	15.625	38.945	6
082FNW 157	Little Tim	18.811	15.634	39.129	6
		18.847	15.628	39.031	12
		19.088	15.679	38.921	12
		18.980	15.643	38.978	12
		18.843	15.623	38.946	12
082FNW 37	Noble Five	18.894	15.657	39.019	6
		18.745	15.616	39.022	12
082KSW 6	Payne	18.740	15.626	39.024	6
082FNW 35	Reco	18.85	15.76	39.27	1
082FNW 52	Ruth-Hope	18.699	15.624	38.992	6
082FNW 180	Standard	18.664	15.628	39.000	6
082FNW 204	Victor	18.715	15.617	38.969	6
		18.670	15.603	38.923	3
		18.671	15.603	38.913	5
		18.763	15.627	39.044	12
		18.905	15.704	38.940	12
082FNW 226	Silver Leaf	18.626	15.607	38.906	6
082FNW 201	Vulture	18.704	15.621	39.006	6
083FNW 53	Silversmith	18.721	15.642	39.045	6
082FNW 64	Van Roi	18.708	15.640	39.027	6

Table 3-1. Compilation of galena Pb isotope ratios (continued)

Number[a]	Deposit	$^{206}Pb/^{204}Pb$	$^{207}Pb/^{204}Pb$	$^{208}Pb/^{204}Pb$	Reference[b]
082FNW 50	Silvana	18.713	15.622	38.985	6
		18.767	15.610	38.970	8
		18.773	15.613	38.983	12
		18.725	15.619	39.006	12
		18.708	15.602	38.964	12
		18.714	15.606	38.974	12
		18.728	15.622	39.026	12
082FNW 106	Revenu	18.968	15.657	39.158	10
082FNW 99	BNA	18.873	15.647	39.033	10
082FNW 109	Baltimore	18.981	15.655	39.177	10
		18.978	15.650	39.172	12
082FNW 141	Marmion	18.859	15.631	39.026	10
082FNW 114	Silver Cup	19.031	15.668	39.111	10
082FNW 77	Comstock	18.693	15.618	38.961	10
		18.704	15.628	38.998	10
082KSW 15	Northern Belle	18.748	15.632	39.006	6
082FNW 48	Carnation	18.790	15.632	39.024	9
082FNW 165	White Hope	18.878	15.639	39.042	9
082FNW 83	Flint	18.725	15.642	38.975	7
082FNW 56	Noonday	18.692	15.631	39.117	7
082KSW 4	Monitor	18.819	15.631	38.944	12
Kokanee group					
082FNW 187	Olsen	19.110	15.670	39.144	12
		19.108	15.660	39.130	12
		19.109	15.665	39.137	12
		19.109	15.669	39.149	12
		19.113	15.666	39.146	12
		19.287	15.673	39.201	12
		19.308	15.693	39.275	12
082KSW 25	McAllister	19.072	15.653	38.913	12
082KSW 18	Rambler	19.254	15.674	39.071	12
082FNW 112	Scranton	18.989	15.634	38.890	8
		19.308	15.620	38.769	3
		18.868	15.643	38.638	5
		18.997	15.685	38.889	7
		18.885	15.654	38.689	6
		19.000	15.669	38.851	12
		18.994	15.662	38.835	12
082KSW 2	Molly Hughes	18.919	15.657	38.721	6
082FNW 130	Chapleau	19.137	15.672	38.901	6
082FNW 127	Alpine	19.171	15.666	38.937	10
082FNW 111	Pontiac	18.974	15.655	38.770	10
082FNW 113	Sunrise	18.881	15.653	38.702	10
		18.959	15.644	38.739	10

Table 3-1. Compilation of galena Pb isotope ratios (continued)

Number[a]	Deposit	$^{206}Pb/^{204}Pb$	$^{207}Pb/^{204}Pb$	$^{208}Pb/^{204}Pb$	Reference[b]
082FNW 122	Oro Fino	19.144	15.667	39.047	10
		19.137	15.661	39.047	12
		19.130	15.654	38.446	12
082FNW 105	Para	19.007	15.653	38.789	10
		19.011	15.647	38.768	10
082FNW 215	Silver Ranch	19.044	15.654	38.822	10
082FNW 253	Al	18.980	15.644	38.762	10
082FNW 242	King Solomon	19.185	15.674	38.995	10
082FNW 208	Jumbo	19.069	15.650	38.810	10
		*18.697	15.620	39.025	12
082FNW 191	Hamilton	19.100	15.667	38.863	12
Ainsworth group					
082FNE (F)15	Highland	17.531	15.491	38.227	6
082FNE 24	Silver Hoard	17.790	15.515	38.272	6
082FNE (F)25	Number One	17.765	15.523	38.318	6
082FNE 30	Highlander	17.553	15.504	38.222	6
082FNE 18	Lakeshore	17.536	15.449	38.133	3
		17.559	15.496	38.184	5
082FNE 91	Montezuma	17.580	15.500	38.218	6
082FNE 19	Nicolet	17.567	15.495	38.179	6
082FNW 120	Smuggler	17.590	15.492	38.187	10
082FNW 119	Slocan Chief	17.783	15.522	38.354	10
082FNW 118	Blackburn	17.719	15.520	38.317	10
082FNW 121	Molly Gibson	17.587	15.489	38.177	10
		17.599	15.494	38.191	10
Bluebell group					
082FNE 16	Florence	*18.807	15.627	39.062	11
		17.460	15.481	37.944	6
		17.454	15.463	37.851	12
		17.571	15.469	38.206	12
082FNE 43	Bluebell	17.478	15.481	37.936	6
		17.506	15.482	38.037	12
		17.508	15.488	38.052	12
		17.443	15.458	37.744	12
		17.444	15.463	37.862	12
		17.436	15.472	37.849	12
		17.427	15.464	37.819	12
		17.440	15.456	37.837	12
	Kootenay	17.499	15.482	38.036	2
	Chief zone	17.468	15.469	37.975	2
		17.477	15.450	37.829	3

Table 3-1. Compilation of galena Pb isotope ratios (continued)

Number[a]	Deposit	$^{206}Pb/^{204}Pb$	$^{207}Pb/^{204}Pb$	$^{208}Pb/^{204}Pb$	Reference[b]
082FNE 43	Bluebell	17.01	15.02	36.92	1
	(continued)	17.01	15.04	36.89	1
		17.35	15.31	37.63	1
		17.61	15.41	37.84	1
		17.61	15.34	37.59	1
		17.65	15.71	38.18	1
		17.54	15.57	38.17	1
		17.57	15.59	38.18	1
		17.713	15.726	38.896	4
		17.642	15.700	38.740	4
	Comfort	17.447	15.458	37.943	2
	zone	17.607	15.608	38.494	4
		17.664	15.710	38.788	4
		17.425	15.440	37.866	2
		17.400	15.353	37.818	2
082FNE 10	Triumph	17.534	15.499	38.198	6
		17.486	15.479	37.969	6
082FNE 7	Amazon	17.528	15.641	38.188	5

a. British Columbia mineral deposit MINFILE database number for each deposit, only the last digits are reported on Figure 2. b. Key to references: 1-Russell and Farquhar (1960), 2-Kanasewich (1962), 3-Sinclair (1964), 4-Ohmoto (1968), 5-Reynolds and Sinclair (1971), 6-LeCouteur (1973), 7-Cox (1979), 8-Andrew et al. (1984), 9-Logan (1988), 10-Logan et al. (1988), 11-Godwin et al. (1988), 12-This study. c. *: analysis not included in average Pb isotope ratios of the deposit.

one deposit hosted by the granitic Mount Carpenter stock, a probable satellite of the Nelson batholith, and two deposits hosted by the Slocan Group (Fig. 3-1). Deposits of the Sandon group are hosted by either the Nelson batholith or the Slocan Group (Fig. 3-1). Deposits of the Ainsworth group are found in a N-S zone along the shores of Kootenay Lake, hosted by the Milford, Kaslo, and Slocan groups, but four deposits are in the Nelson batholith, isolated within the area of the Kokanee group (Fig. 3-1). Deposits of the Bluebell group are hosted by the Badshot Formation, and the Lardeau and Milford groups, and form a cluster north of Ainsworth.

Each of the Kokanee, Sandon, Ainsworth, and Bluebell groups has an exclusive

geographic distribution (Fig. 3-1). Deposits of three of the four groups are found in the Nelson batholith as well as in surrounding sedimentary rocks. The geographic boundaries of each of the groups crosscut geological contacts, suggesting deposition of galena after the presently exposed geological framework was established. In many areas, the boundaries between the groups are sharp and well defined but elsewhere, such as northwest of Ainsworth, accurate location of the boundaries is hampered by the scarcity of deposits.

Interpretation

Mixing systematics

Comparison of Figures 3-2 and 3-3 demonstrates that the $^{208}Pb/^{206}Pb$ versus $^{207}Pb/^{206}Pb$ plot (Fig. 3-2) permits a better separation of the four groups of deposits. Each group, in $^{208}Pb/^{206}Pb$ versus $^{207}Pb/^{206}Pb$ space, forms a linear array with a statistically significant regression coefficient (Table 3-2). Therefore, the more scattered linear arrays displayed by the groups on $^{207}Pb/^{204}Pb$ and $^{208}Pb/^{204}Pb$ versus $^{206}Pb/^{204}Pb$ plots (Fig. 3-3) are real, although the regression coefficients are less significant (Table 3-2) because of analytical ^{204}Pb error.

Because the linear arrays of each group are distinct and do not overlap in $^{208}Pb/^{206}Pb$ versus $^{207}Pb/^{206}Pb$ space (Fig. 3-2), each array can be interpreted to define a mixing line independant of the others. Accordingly, the four groups could represent mixtures of Pb derived from as many as eight different reservoirs. Although this hypothesis cannot be rejected, it is not favoured because deposits from all groups are Eocene (Beaudoin et al., 1992a) and each group is geographically distinct with boundaries that cut geological contacts (Fig. 3-1). These observations would require that all Pb reservoirs coexisted in or beneath the Kokanee Range without relation to surface geology. Furthermore, this hypothesis does not take into account the

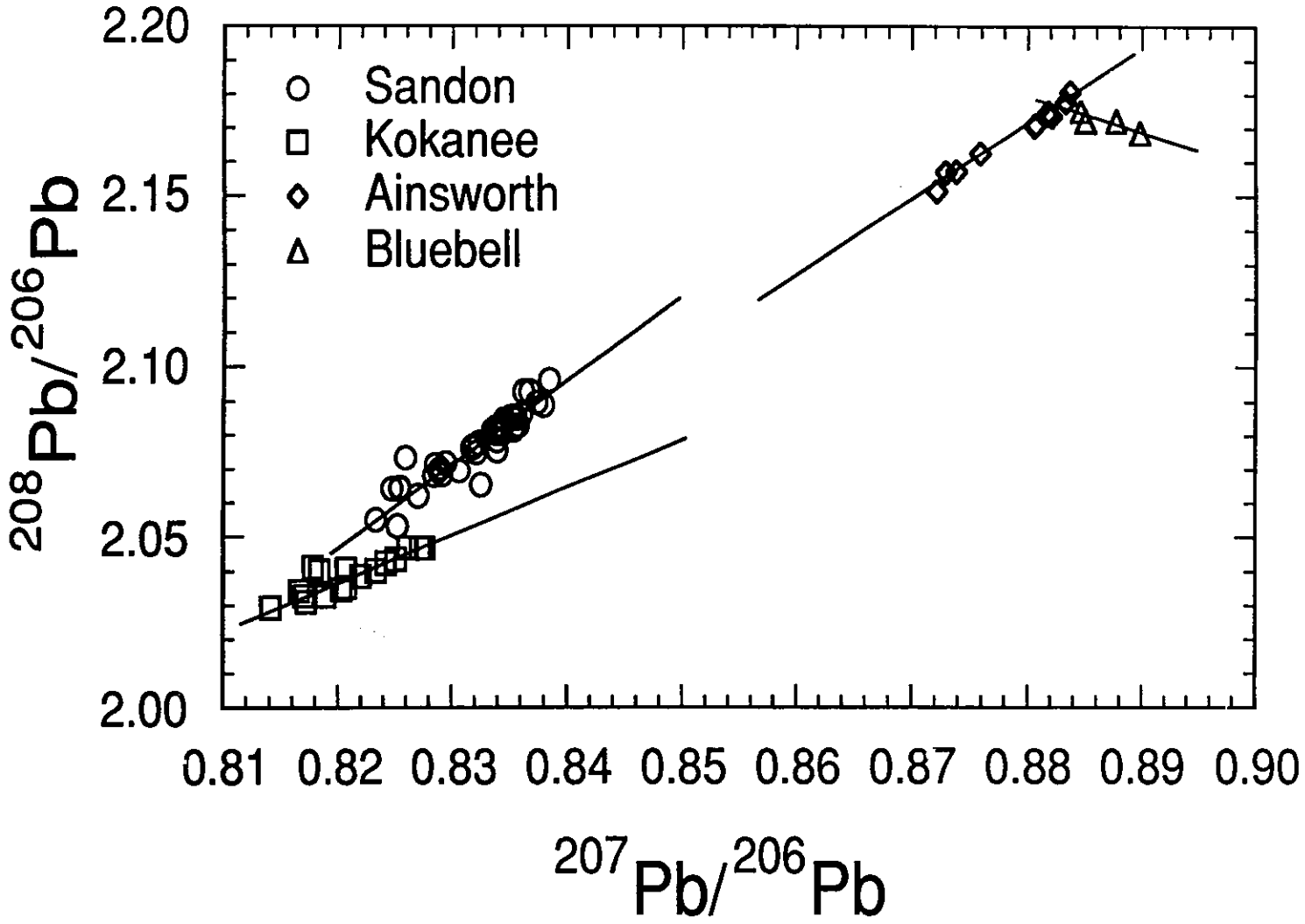

Figure 3-2. $^{208}Pb/^{206}Pb$ versus $^{207}Pb/^{206}Pb$ diagram of the average Pb isotope ratios for each deposit. The data form four linear arrays with significant regression coefficients (Table 3-2). The lines drawn through the arrays represent the least squares reduced major axes slopes of the regressions (Table 3-2). No graphical representation of analytical error is displayed because many points represent average Pb isotopic composition for a deposit, and analytical error varies with the source of the data (see Table 3-1).

Pb isotopic relationships between the four groups indicated by statistically equivalent slopes at the 2α=0.01 level of confidence for the Sandon and Ainsworth groups (Table 3-2) and the intersection between the Sandon and Kokanee, and between the Ainsworth and Bluebell linear arrays (Fig. 3-2).

In $^{207}Pb/^{204}Pb$ versus $^{206}Pb/^{204}Pb$ space (Fig. 3-3A), the slopes of the four groups are statistically equivalent at the level of significance of 2α=0.01, based on a test of Davis (1986). Similar slopes and intercepts for the four groups suggest they lie on the same line (Table 3-2) as proposed by Sinclair (1964), Reynolds and Sinclair (1971) and LeCouteur (1973). These authors calculated slopes similar to those of Table 3-2 for subsets of the present database and interpreted them as secondary isochrons. The regression line could also be interpreted as a mixing line between two Pb reservoirs with different values of $\mu=^{238}U/^{204}Pb$. The secondary isochron and single two-component mixing line hypotheses, however, do not explain the lack of collinearity among the four groups in $^{208}Pb/^{206}Pb$ versus $^{207}Pb/^{206}Pb$ (Fig. 3-2) and $^{208}Pb/^{204}Pb$ versus $^{206}Pb/^{204}Pb$ spaces (Fig. 3-3B).

In $^{208}Pb/^{204}Pb$ versus $^{206}Pb/^{204}Pb$ space (Fig. 3-3B), the Ainsworth and Sandon groups form linear arrays with statistically equivalent slopes at the level of significance of 2α=0.01 (Table 3-2). A regression of both groups also yields a slope statistically equivalent to thAT for each individual array (Table 3-2). Therefore, the Ainsworth and Sandon groups are interpreted to lie on a tridimensional Pb isotope mixing line between a lower crustal Pb reservoir and the upper crustal Pb reservoir. The gap between the Ainsworth and Sandon groups likely results from two different families of mixing ratios between the two Pb reservoirs. The linear array for the Kokanee group is also a mixing line, but it has a statistically different slope than those for the

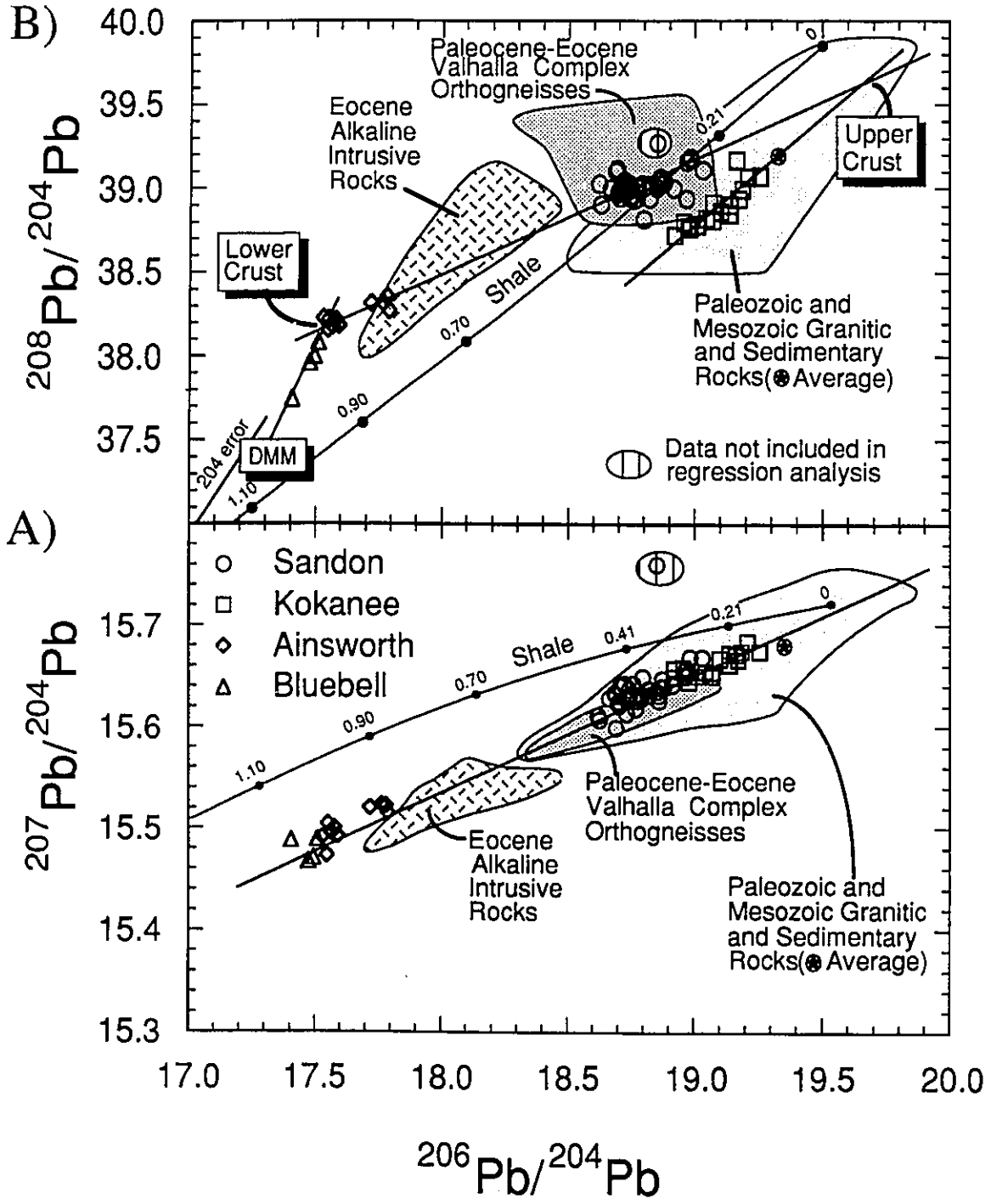

Figure 3-3. Average Pb isotope compositions for each deposit: A) $^{207}Pb/^{204}Pb$ versus $^{206}Pb/^{204}Pb$; B) $^{208}Pb/^{204}Pb$ versus $^{206}Pb/^{204}Pb$. The straight line drawn through the four groups in A) represents the least squares reduced major axes slopes of the combined regression of all four groups (Table 3-2). In B), the regression line through the Ainsworth and Sandon arrays intercepts the regression lines for the Bluebell and Kokanee groups. Fields are outlined for whole rock Pb isotope data recalculated to 60 Ma for Paleozoic and Mesozoic granitic and sedimentary rocks and for Eocene alkaline intrusions (Ghosh, 1986; Bevier, 1987), and feldspar Pb isotope compositions for Paleocene-Eocene orthogneisses of the Valhalla metamorphic core complex (Bevier, 1987). The Shale curve is from Godwin and Sinclair (1982) and DMM is from Hart (1988). No graphical representation of analytical error is displayed because many points represent average Pb isotopic compositions for the deposits and analytical error varies with the source of data (see Table 3-1). Some old data were not included in the regression analysis because they plot outside of the linear arrays and probably reflect analytical errors.

Table 3-2. Slopes and regression coefficients for the linear arrays

Group		$^{207}Pb/^{204}Pb$ v. $^{206}Pb/^{204}Pb$	$^{208}Pb/^{204}Pb$ v. $^{206}Pb/^{204}Pb$	$^{208}Pb/^{206}Pb$ v. $^{207}Pb/^{206}Pb$
Ainsworth[1]	m	0.15 ± 0.02	0.64 ± 0.07	2.20 ± 0.06
	b	12.8 ± 0.3	27.0 ± 1.3	0.24 ± 0.06
	r^2	0.738	0.742	0.981
	n	11	11	11
Bluebell	m	0.25 ± 0.11	3.1 ± 0.1	-1.1 ± 0.2
	b	11.1 ± 1.8	-16.6 ± 2.1	3.1 ± 0.2
	r^2	0.078	0.988	0.780
	n	4	4	4
Kokanee	m	0.11 ± 0.02	1.3 ± 0.2	1.4 ± 0.2
	b	13.6 ± 0.3	14.8 ± 2.8	0.9 ± 0.1
	r^2	0.665	0.764	0.774
	n	17	17	17
Sandon	m	0.14 ± 0.01	0.7 ± 0.1	2.5 ± 0.2
	b	13.0 ± 0.3	25.9 ± 1.8	0.03 ± 0.12
	r^2	0.601	0.205	0.856
	n	41	41	42
Sandon + Ainsworth	m		0.67 ± 0.019	
	b		26.3 ± 0.4	
	r^2		0.959	
	n		52	
Sandon+ Ainsworth+ Kokanee	m	0.114 ± 0.002		
	b	13.5 ± 0.3		
	r^2	0.979		
	n	73		

1. m: slope; b: ordinate intercept; r^2: regression coefficient; n: number of observations. Deposits not included in regression analysis are highlighted on Figures 3 and 4. Slopes and ordinate intercepts for the linear arrays were calculated using the least squares reduced major axes (Davis 1986).

Ainsworth and Sandon arrays (Table 3-2). The Kokanee linear array intercepts the Sandon-Ainsworth mixing line at $^{206}Pb/^{204}Pb$= 19.69 (Fig. 3-3), and this intercept could represent a common upper crustal mixing end-member. Similarly, the linear array for the Bluebell group is a mixing line with a statistically different slope than the Sandon-Ainsworth mixing line (Fig. 3-3B, Table 3-2). The Bluebell linear array, although apparently similar to a ^{204}Pb error line, is not

regarded as such because the slope is steeper than that of an error line (Fig. 3-3), and because some of the points are average of many analyses (e.g. Bluebell: n=26). They should thus not define a ^{204}Pb error trend. Furthermore, any trend due to ^{204}Pb error is eliminated in $^{208}Pb/^{206}Pb$ versus $^{207}Pb/^{206}Pb$ space. Because the Bluebell group also forms a linear array in that space (Fig. 3-2), the hypothesis that the Bluebell linear array is due to ^{204}Pb error is rejected. The Bluebell linear array intercepts the Sandon-Ainsworth mixing line at $^{206}Pb/^{204}Pb=17.53$, which could represent a common lower crustal end-member.

Lead reservoirs

The Kokanee group linear array is parallel to, and near the centre of, the field of rock Pb isotope ratios (Ghosh, 1986), recalculated to 60 Ma, for Paleozoic and Mesozoic granitic and sedimentary rocks outcropping in the Kokanee Range (Fig. 3-3). The Kokanee group galena Pb therefore can be regarded as derived from upper crustal Pb from the country rocks that host mineralisation. In $^{208}Pb/^{204}Pb$ versus $^{206}Pb/^{204}Pb$ space (Fig. 3-3B), the most uranogenic compositions of Sandon group lie within the field for the country rocks, suggesting that these rocks form the upper crustal Pb reservoir for the mixing line between Sandon and Ainsworth groups.

Granulite are commonly considered to form the lower crustal, thorogenic Pb reservoir (Zartman and Doe, 1981). Thorogenic Pb evolves within granulite facies segments of the lower crust that are isolated from mixing with the mantle and upper crust during orogenies (Rudnick and Goldstein, 1990). Geophysical modelling indicates that the basement of the Kokanee Range is composed of metasedimentary rocks (Eaton and Cook, 1990), which are likely to contain significant amounts of metamorphosed equivalents of the Middle Proterozoic Purcell and Upper

Proterozoic Windermere supergroups. Lower-Middle Proterozoic granulite xenoliths from the Kilbourne Hole, New Mexico, could be examples of a metapelitic segment of the lower crust that is enriched in ^{208}Pb (Reid et al., 1989). The Middle Aldridge Formation is part of a thick sequence of metapelites near the base of the Purcell Supergroup, and some samples have an isotopic signature enriched in ^{208}Pb (Ghosh, 1986). It is thus reasonable to assume that the basement of the Kokanee Range may contain rocks enriched in ^{208}Pb and which form the lower crustal Pb reservoir.

Galena Pb isotope ratios for the Sandon group are adjacent to and overlapping with (Fig. 3-3A), or contain (Fig. 3-3B), the field for feldspar Pb isotope ratios (Bevier, 1987) from Paleocene Airy quartz monzonitic and Eocene Ladybird granitic orthogneisses of the Valhalla complex. U-Pb systematics within the xenocrystic cores of magmatic zircons from the Valhalla orthogneisses indicate their derivation, in part, from 1.0 to 2.5 Ga rocks (Bevier, 1987; Parrish et al., 1988). The Valhalla orthogneisses could therefore represent a mixture of Pb derived from the Proterozoic metasedimentary basement isolated in the lower crust in addition to the dominant component of Pb derived from the upper crust suggested by Bevier (1987). The orthogneisses are interlayered with three sheets of sillimanite-K-feldspar grade paragneisses (Carr et al., 1987). Since the Valhalla paragneisses have not exceeded the amphibolite grade of metamorphism, it is presumed that their Pb isotopic compositions reflect those of their upper crustal precursors.

The Ainsworth group is positioned at the low $^{206}Pb/^{204}Pb$ end of the Sandon-Ainsworth mixing line, indicating a large contribution of lower crustal Pb relative to upper crustal Pb (Fig. 3-3). The Bluebell linear array is a mixture between the lower crustal Pb reservoir and a reservoir depleted in U and Th (Fig. 3-3B). This depleted reservoir cannot be represented by Pb in Late

Proterozoic galena that was remobilised by hydrothermal fluids during the Eocene because the Shale curve, which represent upper crustal Pb in the Canadian Cordillera (Godwin and Sinclair, 1982), has $^{207}Pb/^{204}Pb$ ratios that are much too high. Country rocks exposed in the area do not have Pb isotopic signatures compatible with the depleted reservoir, and an external, deep-seated Pb reservoir must be considered. The Depleted MORB Mantle (DMM) of Hart (1988) lies on the trajectory of the Bluebell array (Fig. 3-3) and the array could result from mixing between a DMM-like and lower crustal Pb reservoirs. A depleted upper mantle at the western margin of Ancestral North America is supported by extrusion of tholeiitic basalts during repeated Late Proterozoic to Mesozoic rifting events (Klepacki, 1985; Gabrielse and Yorath, 1989).

Eocene alkaline intrusive rocks, comprising lamprophyre and gabbro dykes and Coryell syenite (Bevier, 1987), have initial Pb isotope ratios that plot within an elongate field between the Sandon and Ainsworth arrays, and overlap some of the most radiogenic galena Pb of the Ainsworth group (Fig. 3-3). In $^{208}Pb/^{204}Pb$ versus $^{206}Pb/^{204}Pb$ space (Fig. 3-3B), the field for Eocene alkaline intrusive rocks is not parallel to the Sandon-Ainsworth mixing line but projects towards DMM, suggesting a depleted upper mantle beneath the Kokanee range during the Eocene. The field for Eocene alkaline intrusions also projects towards the field for Eocene orthogneisses within the Valhalla metamorphic core complex, suggesting that the alkaline intrusions were contaminated with Pb from the orthogneisses. The Pb isotopic signature of the Eocene alkaline intrusions could also result from mixing, during melting of their mantle source, of a DMM-like domain with mantle domains enriched through subduction of oceanic crust and its sedimentary cover during Mesozoic accretion of the Cordillera.

Discussion

Lead was leached from three different reservoirs, two of them deep-seated, by hydrothermal fluids to form the Kokanee Range Ag-Pb-Zn deposits (Fig. 3-4). The geological features controlling leaching and mixing of Pb from the different reservoirs are examined below. The deposits sampled in this study account for 91% of the Pb produced in the Kokanee Range. Kokanee group Pb, representing 2.3% of that produced, had a source in the upper crust, whereas Sandon (37.0%) and Ainsworth (6.4%) groups are mixtures of the same upper crustal Pb with a lower crustal Pb. The Bluebell group Pb (45.3%) was derived as a mixture from lower crustal and depleted upper mantle reservoirs (Fig. 3-4).

The interaction between hydrothermal fluids and the lower crustal and depleted upper mantle reservoirs probably depended on the presence of deep fracture zones. Contours of $^{208}Pb/^{206}Pb$ abut against the Slocan Lake Fault (Fig. 3-5), a geometric relationship which could result if the Slocan Lake Fault cut the contour pattern or if this fault were a major conduit connecting the lower crustal Pb reservoir with higher crustal levels (Fig. 3-6). The Eocene ages for mineralisation and deformation along the Slocan Lake Fault (Beaudoin et al., 1992a) argues for a direct link between the Slocan Lake Fault and the pattern of $^{208}Pb/^{206}Pb$ ratio contours. The apparent crosscutting relation may have resulted from the emanation of the hydrothermal fluids exclusively into the hangingwall rocks of the shallow dipping fault zone, or from post-mineralisation displacement along the fault zone. The Main Lode, southwest of Sandon (Fig. 3-1), is an east-west, south-dipping normal fault zone containing, and surrounded by, most of the large deposits of the Kokanee Range (Beaudoin and Sangster, 1991). Lead isotope ratios become more uranogenic in an irregular pattern north, south, and east of the Main Lode (Fig. 3-5), indicating

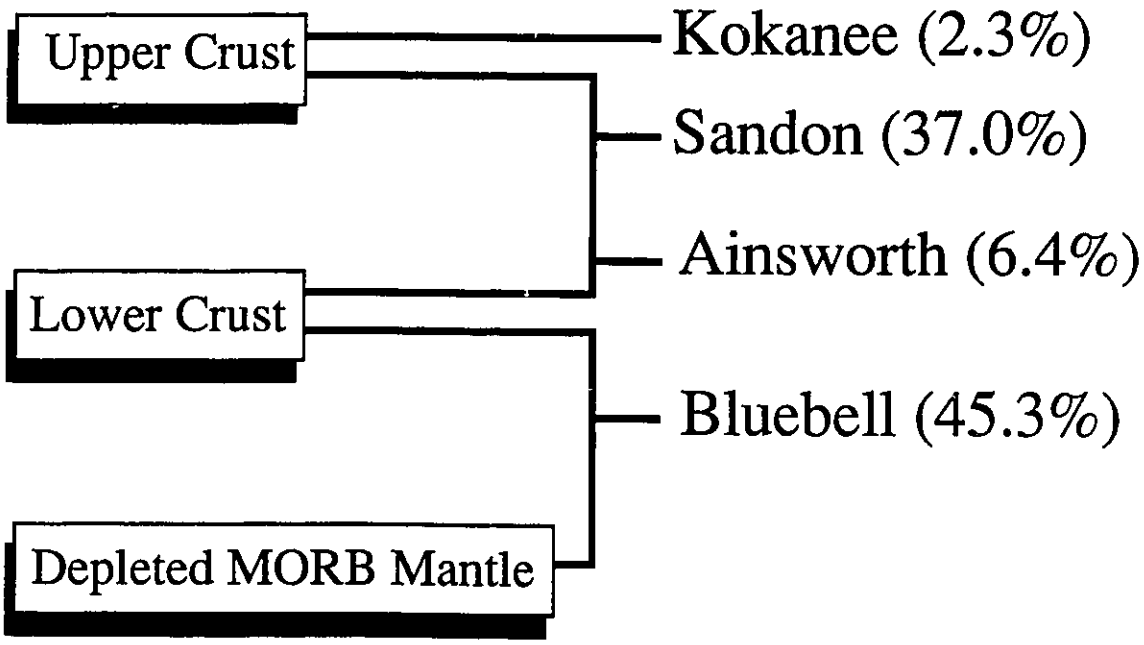

Figure 3-4. Schematic diagram displaying the relationships between the three Pb reservoirs and the four groups of deposits. The number beside each group indicates the proportion of the Pb produced by deposits of that group relative to the total production for the Kokanee Range.

that the proportion of Pb derived from the lower crustal reservoir decreased in a direction away from this zone of hydrothermal fluid flow. This progressive dilution of the lower crustal signature produced a second order Pb isotope zonation suggesting that the Main Lode was a major hydrothermal fluid pathway in the upper crust.

The Pb isotopic signature of the Sandon group of deposits could have resulted from the leaching of metals from the Valhalla orthogneisses, with some contribution from the paragneisses. This is unlikely because the Pb isotope zoning pattern (Fig. 3-5) indicates a contribution of Pb from local country rocks. Two hypotheses can be considered: i) Sandon group Pb could be a mixture dominated by Pb isotope compositions comparable to feldspars from the Valhalla orthogneisses with a minor contribution from the local upper crustal country rocks. The thinness of the orthogneisses in the footwall of the Slocan Lake Fault (400 m; Carr et al., 1987) is an argument against this hypothesis which, furthermore, implies that the statistically identical slopes and ordinate intercepts for the Ainsworth and Sandon groups arrays are coincidental; ii) Sandon group Pb could also be mostly derived from local upper crustal country rocks, but with a significant admixture of Pb leached from rocks of the lower crustal reservoir, which were also a source for the Pb in the magmas that formed the Valhalla orthogneisses. Using the isotopic compositions for the upper and lower crustal reservoirs defined by the intersections of the Sandon-Ainsworth mixing line with the Kokanee and Bluebell arrays, and assuming that similar concentrations of Pb were leached from both reservoirs by the hydrothermal fluids, about 50 to 70% of Sandon group Pb was leached from the upper crustal reservoir. This hypothesis, however, also implies that the similarity in Pb isotopic compositions between the Sandon group and the Valhalla orthogneisses is coincidental. At present we favour the second hypothesis, but there is

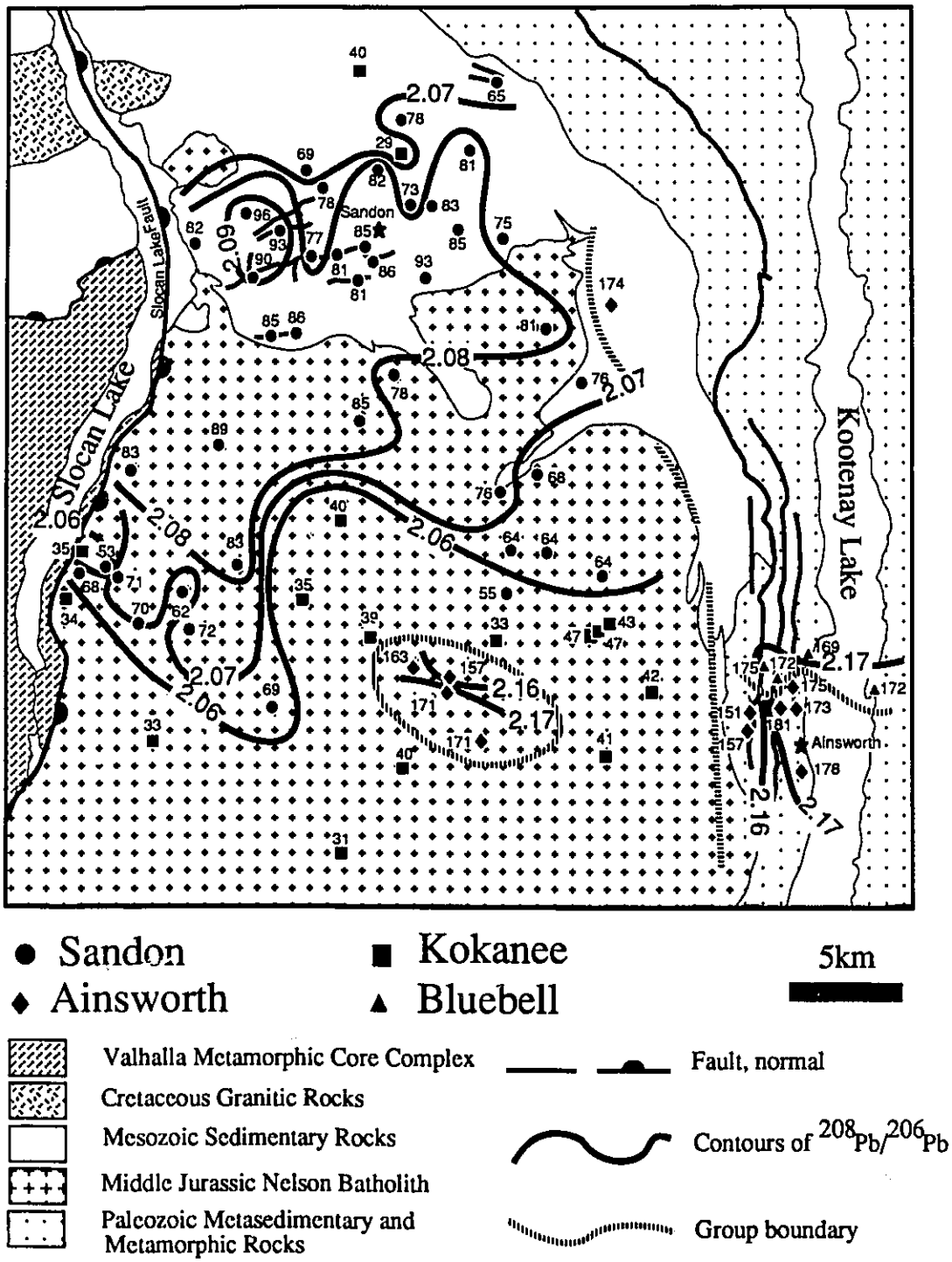

Figure 3-5. Average $^{208}Pb/^{206}Pb$ ratio for each deposit, see Figure 3-1 and Table 3-1. Number besides deposit location are the variable digits of the $^{208}Pb/^{206}Pb$ ratio (ex. 86=2.086; 171=2.171). The lines show the approximate extrapolated position of constant $^{208}Pb/^{206}Pb$ ratios as indicated along each line; contoured for Sandon, Bluebell, and Ainsworth group only.

not yet conclusive evidence in support of either of the hypotheses.

In the Ainsworth area (Fig. 3-5), metasedimentary rocks are sliced by north-south, west-dipping normal faults (Fyles, 1967) which, at depth, probably merge with the Ainsworth Fault (Fig. 3-6), a conjugate of the Slocan Lake Fault (Varsek and Cook, 1991). In that area, $^{208}Pb/^{206}Pb$ ratios are high near Kootenay Lake and decrease westward, away from the faults (Fig. 3-5). The zonation of $^{208}Pb/^{206}Pb$ ratios in the Ainsworth and Sandon groups is interpreted to be due to leaching local upper crustal rocks enriched in ^{206}Pb. The four deposits of the Ainsworth group that lie within the Nelson batholith and are surrounded by deposits with Kokanee group Pb isotopic signature (Fig. 3-1) are along a prominent fracture zone (Brown and Logan, 1989), again suggesting that introduction of Pb from deep-seated sources was structurally controlled.

The structures containing the Bluebell and Florence deposits (Bluebell group) strike east-west. These are the only large deposits of both the Bluebell and Ainsworth groups with this orientation, although some smaller deposits of the Ainsworth group also have east-west strikes. The other large deposits of Ainsworth group strike north-south of northwest-southeast. The east-west strike of the Bluebell and Florence deposits could be the expression of a structural feature which allowed leaching of Pb from a deep-seated reservoirs, and focused hydrothermal flow. It is also noteworthy that large deposits of both the Sandon and Bluebell groups that are contained by east-west structures account for 71% of the Pb produced from the Kokanee Range. Therefore, it is apparent that structures of this orientation are fundamental to the formation of large deposits in the Kokanee Range.

Figure 3-6 is a schematic east-west crustal cross-section through the Kokanee Range at the time of mineralisation. Beneath the Kokanee Range, the lower crust and upper mantle are

characterised by high heat flow, electrical conductivity, and low density upper mantle (Gough, 1986). High electrical conductivity in the lower crust could result from ionic conduction within saline waters in interconnected pores or fractures (Gough, 1986). Magnetotelluric data modelling indicates that the high electrical conductivity results from narrow zones with large gradients in resistivity, such as deformation corridors, rather than from a uniformly resistive lower crust (Jones et al., 1988). Gough (1986) suggested that the lower crustal saline waters were derived from mantle degassing and partial melting. Paleocene-Eocene crustal thinning and mantle upwelling likely resulted in the high heat flow in southeastern British Columbia. Beaudoin et al. (1992a) suggested that a suite of coeval lamprophyre and gabbro dykes resulted from adiabatic partial melting of upwelled mantle. The mantle processes responsible for the generation of these lower crustal fluids and alkaline mantle melts were likely initiated during Paleocene-Eocene crustal extension and were probably maintained until present by an elongate mantle upflow beneath the Canadian Cordillera (Majorowicz and Gough, 1991). Fluids derived from the lower crust and/or mantle CO_2 degassing could have been channelled upwards along extensional structures, such as the Slocan Lake Fault (Fig. 3-6). Indeed, Slocan Lake Fault has been seismically imaged down to the Moho and may even displace it (Cook et al., 1988; Parrish et al., 1988). In this high heat flow regime, evolved meteoric fluids convected in the upper crust through fracture porosity formed or activated by crustal extension (Fig. 3-6). These evolved meteoric fluids leached upper crustal Pb from the country rocks they encountered and mixed with fluids ascending from the lower crust and depleted upper mantle. Alternatively, lower crust and upper mantle segments may have been rapidly uplifted to higher crustal levels as a result of crustal extension during the Paleocene-Eocene. The lower crustal and upper mantle rocks could

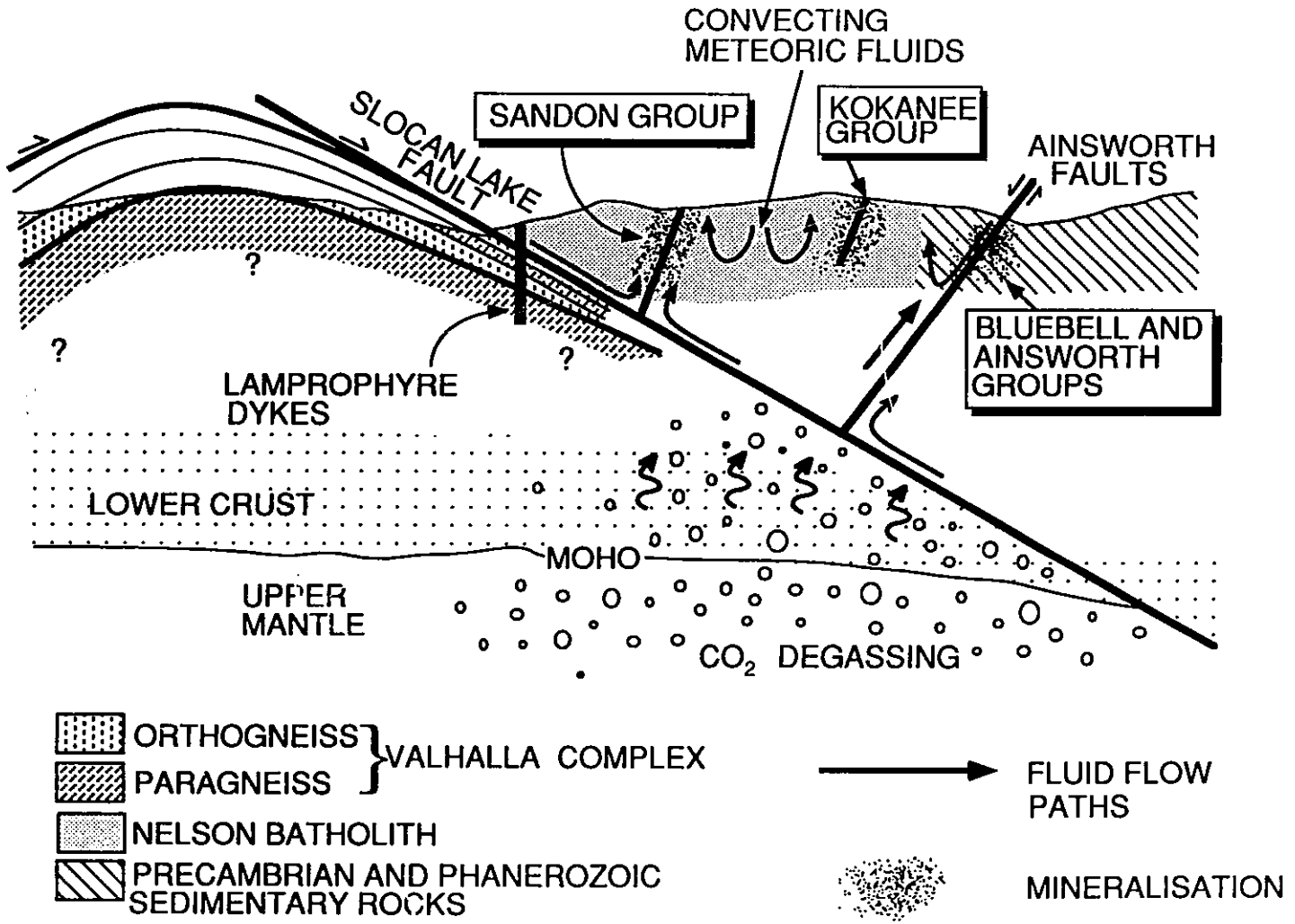

Figure 3-6. Schematic crustal cross-section through the Kokanee Range during the Eocene with overlying rocks removed to the present erosion surface. The four groups of deposits are displayed in relation to the postulated structural elements which allowed leaching of the lower crustal and depleted upper mantle reservoirs. The structural framework, whereby a thinned continental crust overlies an upwelled upper mantle, is adapted from Carr et al. (1987) and Cook et al. (1988).

then have reached levels where they were leached by hydrothermal fluids. In that case, it is possible that the Kokanee group deposits were formed early in the history of the hydrothermal system, before the deep-seated reservoirs were sufficiently uplifted to permit leaching of Pb by hydrothermal fluids. Dating of mineralisation (Beaudoin et al., 1992a) indicates that at least some deposits of the Sandon, Kokanee, and Bluebell groups were formed at essentially the same time, whereas some deposits of the Ainsworth group could have formed later in the same hydrothermal system. The Pb isotopic compositions of rocks are, however, essentially constant for the presently measured duration of hydrothermal activity (14 Ma) in the Kokanee Range (Beaudoin et al., 1992a), and therefore the possible range in mineralisation ages does not affect interpretation of the Pb isotopic compositions.

Conclusions

The Kokanee Range Ag-Pb-Zn vein and replacement deposits can be divided, on the basis of galena Pb isotope ratios, into four groups, named Sandon, Ainsworth, Kokanee, and Bluebell, each of which plot as a distinct linear array in tridimensional Pb isotopic space. Each group also has an exclusive geographic distribution that cuts geological boundaries.

The Sandon and Ainsworth groups represent two families of Pb compositions produced by mixing an upper crustal and a lower crustal Pb reservoirs. Bluebell group Pb are mixtures of lower crustal Pb and a depleted upper mantle Pb reservoirs. Kokanee group Pb are mixtures from upper crustal sources only, identified as the local country rocks. The Proterozoic metasedimentary basement beneath the Kokanee Range probably forms the lower crustal Pb reservoir, whereas evidence for an underlying depleted upper mantle is provided by Pb isotopic data for Eocene alkaline intrusive rocks.

Mixing between the upper crustal, lower crustal, and depleted upper mantle Pb reservoirs was controlled by deep crustal fracture zones. Segments of, or fluids derived from, the lower crust and the upper mantle were leached by, or mixed with evolved meteoric water convecting in the upper crust. Fracture porosity, meteoric water convection, and mineralisation resulted from Paleocene-Eocene crustal extension.

CHAPTER 4

Silver-Lead-Zinc Veins and Crustal Hydrology during Extension

Introduction

Metamorphic core complexes are comprised of high grade metamorphic rocks unroofed from the middle and lower crust during crustal extension induced by the collapse of mountain belts (Dewey, 1988). They are a common feature of the North and South American Cordilleras (Parrish et al. 1988; Dalziel and Brown, 1989; Lister and Davis, 1989), and have been described elsewhere in Europe (Echtler and Malavieille, 1990; Malavieille et al., 1990; Matte et al., 1990; Platt and Vissiers, 1989; Selverstone, 1988), and Papua New Guinea (Davies and Warren, 1988). Metamorphic core complexes are bounded by, and unroofed along, large, low angle normal faults, also known as detachment faults, that can reach the Moho. These fault zones are commonly altered by hydrothermal fluids (Reynolds and Lister, 1987; Kerrich and Rehrig, 1987). Various fluid origins have been proposed including a high temperature, commonly reduced and crust equilibrated fluid, variously interpreted to be metamorphic, magmatic, or evolved meteoric; a low temperature, oxidized, evolved meteoric water or a basinal brine; and late stage meteoric water (Kerrich and Rehrig, 1987; Kerrich, 1988; Roddy et al., 1988; Smith et al., 1991).

Gold mineralisation and low angle normal faults associated with metamorphic core complexes form a popular exploration model in the southwestern U.S. (Sawkins, 1990). Examples of the link between low angle normal faults and mineralisation are the Cu-Fe sulphide and Mn-

Fe-Cu oxide deposits of the Whipple-Buckskin-Rawhide area of southeastern California and western Arizona (Spencer and Welty, 1986); Cu-Au-Ag mineralisation from the Bullard district, Arizona (Roddy et al., 1988); and auriferous quartz veins associated with the South Mountains metamorphic core complex in Arizona (Smith et al., 1991).

This chapter investigates the relationships between the Ag-Pb-Zn vein and replacement deposits of the Kokanee Range and the crustal hydrology of hydrothermal fluids in the Slocan Lake Fault. Formation of the Kokanee Range Ag-Pb-Zn vein and replacement deposits was intimately related to extensional tectonics, involving crustal thinning, mantle upwelling, and extension along the Slocan Lake Fault, a large, low angle, normal fault at the boundary of the Valhalla metamorphic core complex. Fluid inclusion data, and sulphur, carbon, and oxygen isotopic data which characterise the multiple sources of isotopic tracers along the flow paths of several hydrothermal fluids migrating in the crust at the time of mineralisation, are used to examine this relation. Regional zonation of O isotope ratios in rocks has been used to map meteoric-hydrothermal systems around shallow intrusions (Criss and Taylor, 1986). The approach applied in this study was to map $\delta^{18}O$ zonation in both vein minerals and hostrocks. Oxygen and lead (Beaudoin et al., 1992b) isotope zonations are correlated and provide a powerful tool to map hydrothermal fluid flow paths at the time of mineralisation.

Fluid Inclusions

Fluid inclusions in zoned and disseminated sphalerite, as well as in quartz and siderite precipitated immediatly before or after different stages of deposition of sphalerite or galena were studied to characterise processes taking place before or during mineralisation. Most of the fluid inclusions studied had petrographic attributes (Roedder, 1984) that support a primary origin,

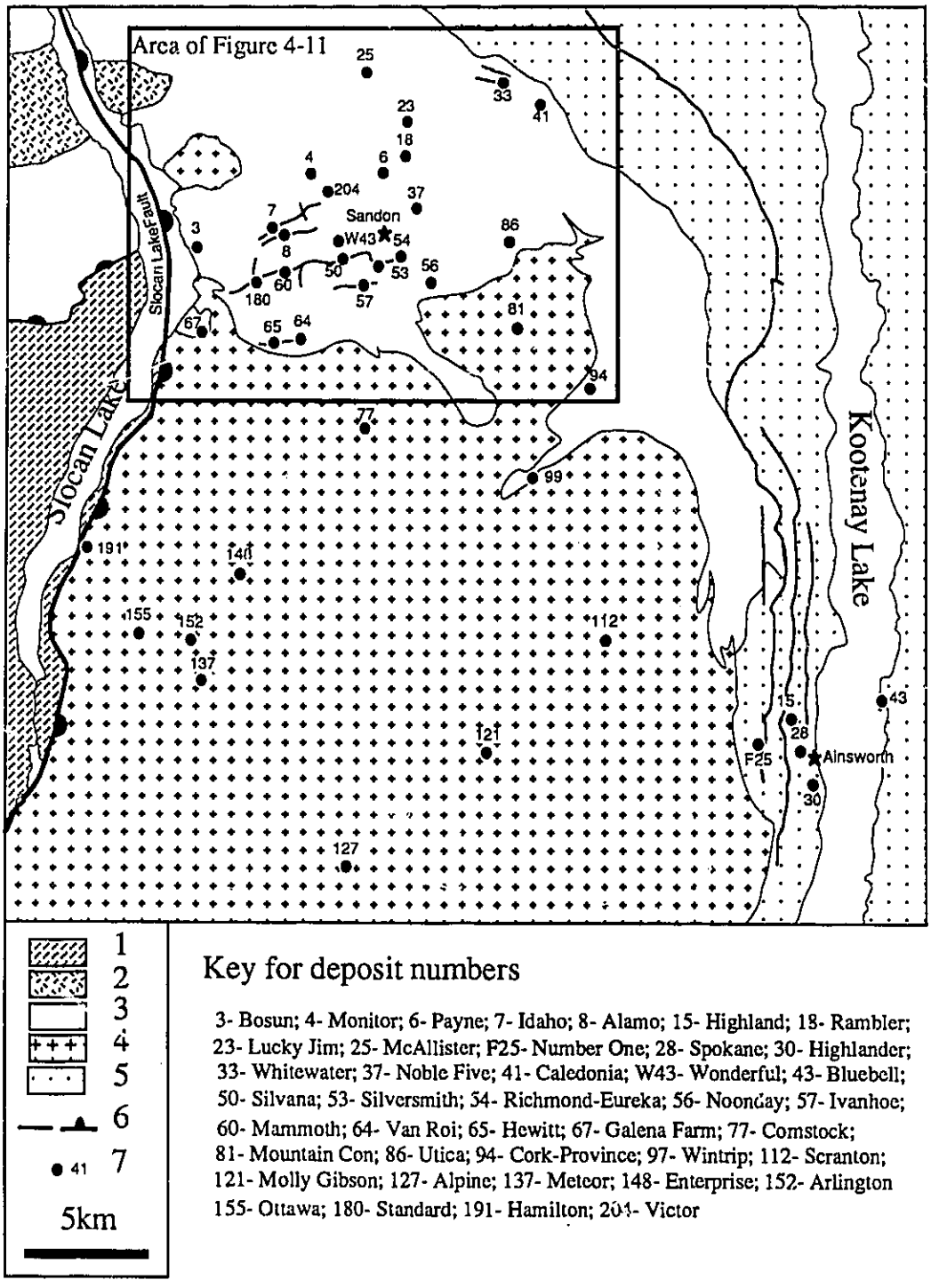

Figure 4-1. Geology map of the Kokanee Range showing the location of the deposits analysed for fluid inclusions and stable isotopes. 1- Rocks of the Valhalla metamorphic core complex; 2- Granitic pluton of probable Cretaceous age; 3- Upper Triassic Slocan Group; 4- Middle Jurassic Nelson batholith; 5- Paleozoic sedimentary and metamorphic rocks; 6- Faults, normal; 7- Deposit location with number.

although in the early stages of this study pseudosecondary and secondary inclusions were also examined. In general, fluid inclusion microthermometric data were acquired in zoned sphalerite, zoned quartz, or clear quartz. The deposits selected for microthermometry are located on Figure 4-1 and are from three (Sandon, Ainsworth, Kokanee) of the four groups of deposits in the Kokanee Range defined by Pb isotopes (Beaudoin et al., 1992b). Fluid inclusions from the Bluebell deposit, which typifies the fourth group of deposits, have been studied in detail by Ohmoto and Rye (1970). The samples selected for microthermometry do not represent a complete record of the P-T-X evolution of the hydrothermal system in one deposit but, rather, are representative of various stages of the P-T-X evolution of the hydrothermal system at the scale of the district.

Analytical technique and classification of inclusions

Microthermometric measurements were performed on 100 µm thick, doubly polished plates, using a Fluid Inc. gas flow heating and freezing stage calibrated at CO_2 melting temperature (-56.6ºC), H_2O melting temperature (±0.0ºC), and the H_2O critical point (374.1ºC) using synthetic inclusions from Synflinc Inc. Calibration was verified regularly but no correction was required. Precision for melting (Tm) and CO_2 homogenisation (Th_{CO2}) temperature is ±0.1ºC and most determinations were made by temperature cycling, whereas precision for the total homogenisation temperature (Th) is ±1ºC. The salinity of the liquid phase was estimated from the melting temperature of ice or clathrate using data from Potter et al. (1978) and Bozzo et al. (1973). Fluid inclusion data are summarised in Table 4-1.

Three types of fluids are present as inclusions. The most common are type 1 aqueous fluid inclusions in sphalerite, quartz, and siderite consisting of H_2O-NaCl liquid and a vapour phase

Table 4-1. Summary of fluid inclusion data

Deposit	Types	Mineral	Temperature (°C)	Salinity wt.%NaCl	$\delta^{18}O_{quartz}$	Comments
Meteoric water dominated fluid						
Highlander	1	Qz	214 ± 11 (L)	3.2 ± 2.2	-3.7	Mixing
Spokane	1	Qz	241 ± 9 (L)	4.4 ± 0.1	-2.9	
Enterprise	1	Sp	190 ± 17 (L)	2.0 ± 1.0	-1.3	Late stage mineralisation
Dilution						
Meteor	1	Qz	284 ± 14 (L) 153 ± 7 (L)	4.3 ± 2.0	11.6	Primary, mixing? Healed fracture
Mountain Con	1	Sp	226 (L) 176 ± 10 (L)	8.4 1.9	15.6	Primary Pseudose condary
Idaho	1	Sp	195 ± 13 (L) 164 ± 14 (L)	9.4 ± 0.4 3.6 ± 0.3	13.6	Primary Pseudosecondary
Ivanhoe	1	Sp	195 ± 11 (L)	9.6 ± 0.2 14.0 ± 1.4	11.9	Late } same crystal of Early } banded sphalerite
Van Roi	1	Qz, Sp	217 ± 15 (L)	11.2 ± 2.1 4.4 ± 1.4	15.6	2 fluids with high and low salinities? Mixing?
Molly Gibson	1	Sd	223 (L)	11.5	7.5	$\delta^{18}O$ suggest meteoric water
Standard	1	Sp	210 ± 4 (L)	13.3 ± 1.2	12.1	
Boiling and dilution						
Rambler	2	Qz	313 ± 17 (L)	10.1 ± 0.8 6.4 ± 0.7	15.7	2 fluids with high and low salinities. Boiling?

Table 4-1. Summary of fluid inclusion data (continued)

Deposit	Types	Mineral	Temperature[1] (°C)	Salinity wt.%NaCl	$\delta^{18}O_{quartz}$ [2]	Comments
Boiling and dilution (continued)						
Silvana	1,3	Sp	275 ± 22 (L)	10.5 ± 1.3	7.1	Primary. $\delta^{18}O_{siderite}$= 14.8
			210 ± 5 (L)	11.4 ± 0.8		Pseudosecondary
			123 ± 13 (L)	2.6 ± 0.3		Secondary
Bosun	1	Sp	238 (L)	12.8	15.6	Minimum temperature
	1	Qz	255 ± 17 (L)			}
	2	Qz	266 (V)	3.0		} Boiling
	1	Qz	317 ± 7 (L,V)	14.0 ± 2.9		Boiling, mixing
Boiling						
Whitewater	2	Qz	270 ± 9 (L,V)	5.1 ± 0.9	18.4	Boiling
McAllister	2	Qz	286 (L,V)	4.2 ± 1.4	16.2	Boiling, mixing?
Noble Five	1	Qz	199 ± 38 (L,V)	4.4 ± 2.7	16.3	Healed fracture } mixing?
	2,3	Qz	292 ± 6 (L,V)	5.8 ± 1.8		Boiling }
Alpine	2,3	Qz	292 ± 12 (L)	4.1 ± 0.4	13.3	Boiling
Scranton	2,3	Qz	307 ± 33 (L,V)	4.4 ± 1.0	15.3	Boiling
	1	Qz	143 (L)	3.6		Secondary

1. (L,V): total homogenisation to liquid (L) and/or vapour (V). 2. Average ore stage $\delta^{18}O$ value (Table 4-2).

occupying 1 to 20% of the inclusion volume at 40ºC. In fifty percent of type 1 inclusions a clathrate crystallised during melting but no type 1 inclusions nucleated $CO_{2(l)}$ upon freezing. Type 1 fluid display a large range of Th (75-330ºC) with a normal distribution (average Th= 214ºC; Fig. 4-2A). Since type 1 fluid was not trapped during boiling, these Th are less than the true trapping temperature. Addition of a pressure correction of 80 to 140ºC, based on data from Potter (1977), a minimum pressure of trapping of 1 to 1.5 kb (see below) assuming that type 1 fluid inclusions were trapped at the same pressure than those of types 2 and 3, and estimated salinities (below), would shift the average Th to at least 300ºC. Most of the low temperature (<180ºC) type 1 fluid inclusions result from healing planes of inclusions. Type 1 fluid inclusions commonly homogenise to liquid but 2 inclusions from 2 different deposits homogenised to vapour. Type 1 fluid displays a large range in salinity, from 0.9 to 17.2 wt. % NaCl eq., with 2 modes at 4.0-4.5 and 10.0-10.5 wt. % NaCl eq. (Fig. 4-2B). Low salinity type 1 fluid inclusions are commonly abundant in quartz, whereas high salinity inclusions are more typical of sphalerite (Table 4-1).

Type 2 inclusions trapped a H_20-NaCl-CO_2 fluid characterised by a high density CO_2 phase (0.502 to 0.901 g/cm^3) that homogenises to liquid between 4.2 and 30.6ºC (Fig. 4-3A). Visual estimates of the volume fraction of carbonic fluid are highly variable, ranging from 0.05 to 1.00. Type 2 inclusions are commonly found in massive or drusy quartz veins and were studied where quartz was in contact with disseminated sulphides, but a few were also observed in zoned sphalerite. Type 2 inclusions typically coexist with types 1 and/or 3 inclusions within a growth zone or a clear crystal. The salinity and Th in type 2 fluid inclusions range from 2.8 to 12.9 wt. % NaCl eq., and 165 to 340ºC, respectively (average Th= 280ºC; Fig. 4-2A). Total homogenisation of type 2 fluid is commonly to liquid but 5 inclusions from 4 deposits

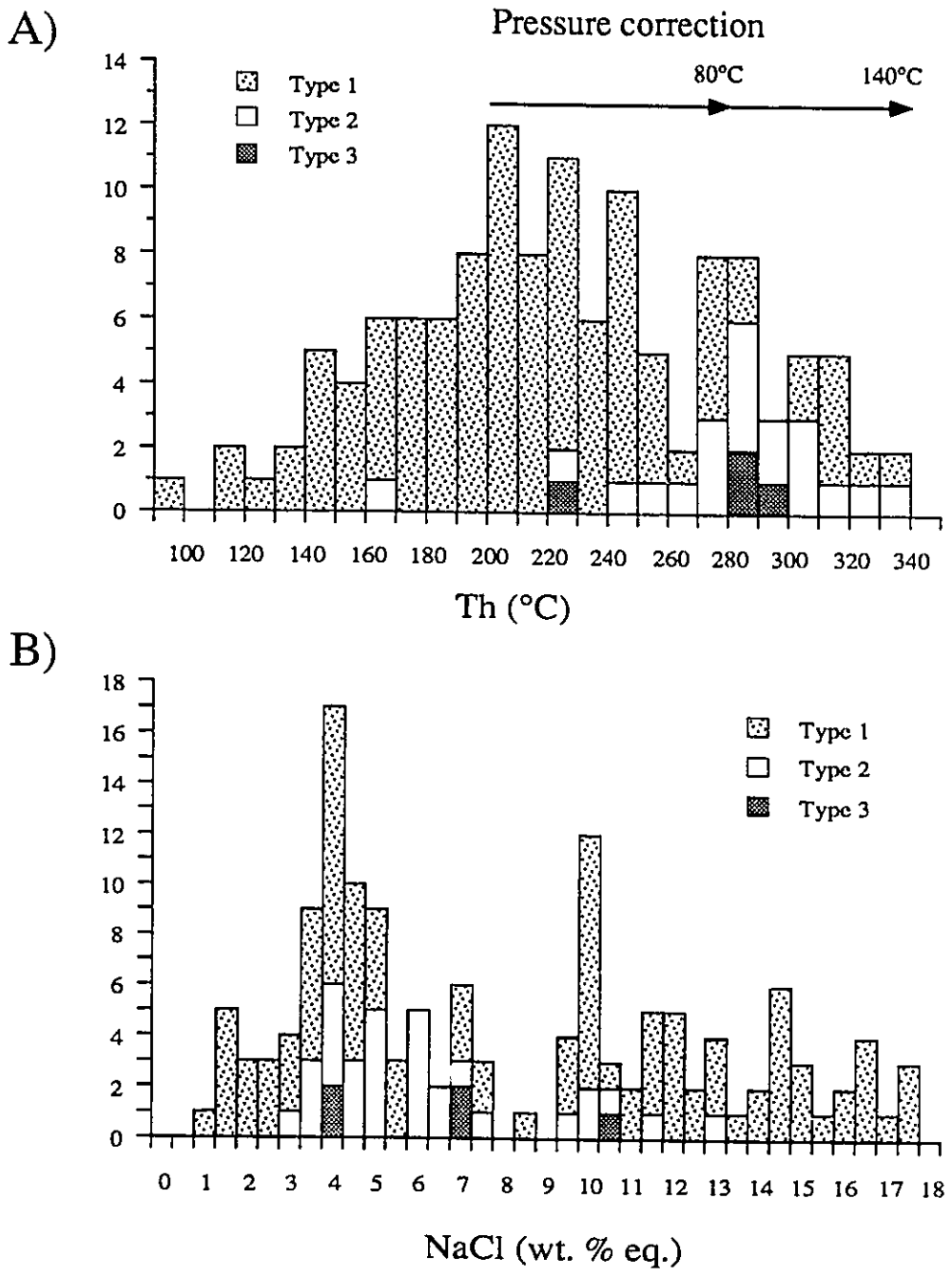

Figure 4-2. Histograms for fluid inclusion data. A) Temperature of total homogenisation, the magnitude of the pressure correction, discussed in the text, is shown. B) Salinity.

homogenised to vapour. Tm_{CO2} have a normal distribution, ranging from -56.7 to -57.7ºC and averaging -57.1ºC (Fig. 4-3B).

Type 3 inclusions trapped a H_2O-NaCl-CO_2 fluid characterised by a low density CO_2 phase (0.200 to 0.332 g/cm^3) that homogenises to vapour between 20.8 and 29.7ºC (Fig. 4-3A). Visual estimates of the volume fraction of carbonic fluid range from 0.15 to 0.30: this small range of volume fractions compared to type 2 inclusions could be apparent because of the small number of data for type 3 inclusions. Type 3 inclusions commonly coexist with type 2 inclusions in quartz or with type 1 inclusions in zoned sphalerite. Total homogenisation is to the liquid phase with one exception to vapour, over a range of Th of 228 to 298ºC (Fig. 4-2A). Salinity of type 3 fluid inclusions in quartz ranges from 3.8 to 7.0 wt. % NaCl eq., whereas one inclusion in sphalerite has a salinity of 10.4 wt. % NaCl eq. (Fig. 4-2B), similar to coexisting type 1 inclusions. Only two Tm_{CO2} were measured: -57.4 and -57.1ºC, and they are similar to values for type 2 fluid (Fig. 4-3B).

Estimation of X_{CH4}, X_{CO2}, and the trapping pressure

CO_2 was present in nearly 60% of the inclusions studied by microthermometry. Assuming only CH_4 is present with CO_2, the range of Tm_{CO2} of -57.7 to -56.7ºC for type 2 and 3 inclusions (Fig. 4-3B), indicates approximately 0 to 7 mole % CH_4 (average ≈ 3 mole %), based on Burruss (1981). Relative to the total inclusion content, X_{CH4} is below 0.01 for most fluid inclusions but reaches 0.04 for an inclusion containing pure carbonic fluid.

Mole fractions of CO_2 (X_{CO2}) and the trapping pressure were estimated using FLINCOR (Brown, 1989), microthermometric, and volumetric data. Pressures calculated using the equation of state of Brown and Lamb (1989) are 15 to 2835 bars higher than those calculated using the

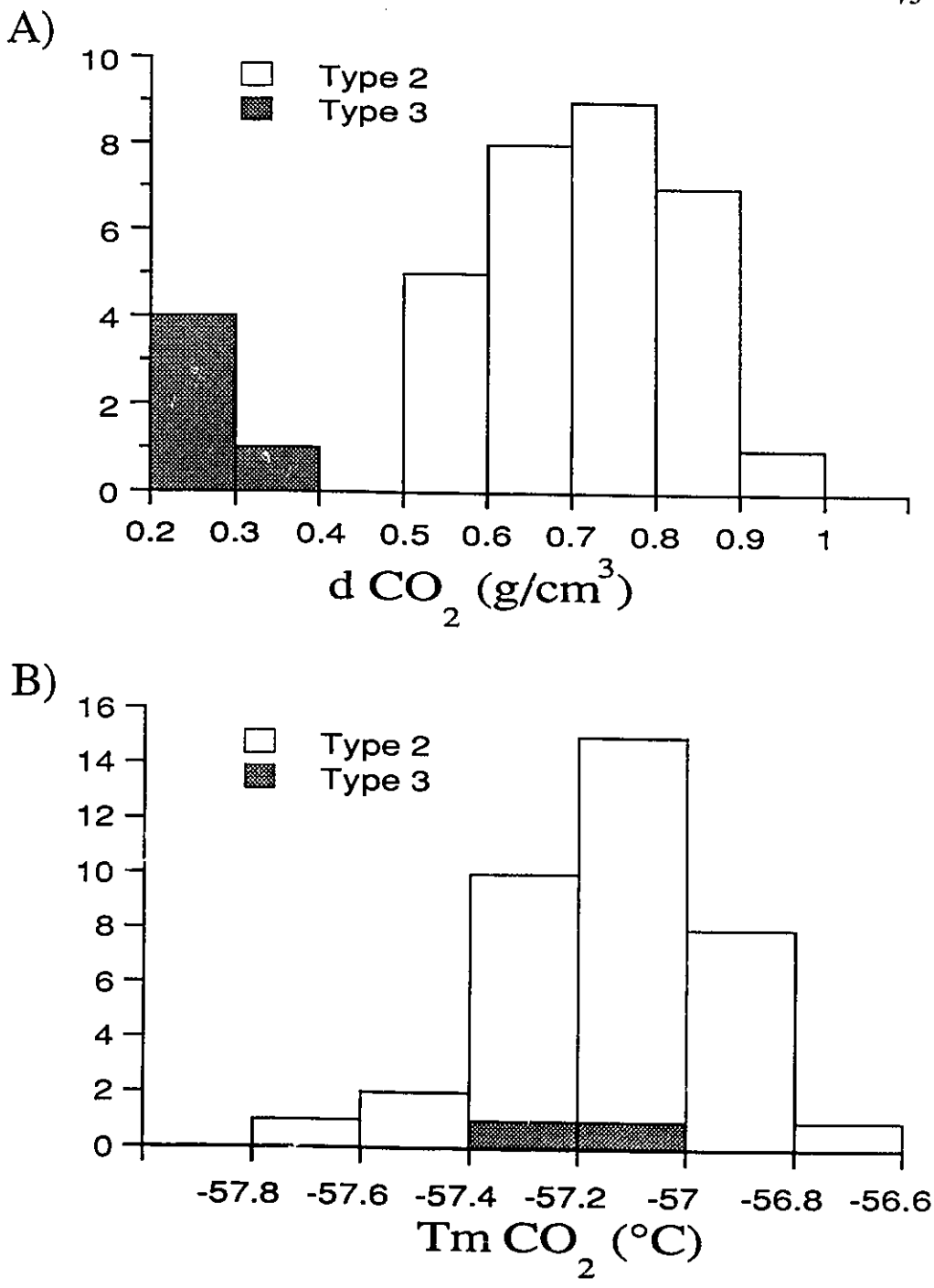

Figure 4-3. A) Histogram of the density of the CO_2 phase showing that fluid inclusions of types 2 and 3 form two populations. B) Histogram of the melting temperature of CO_2.

equation of state of Bowers and Helgeson (1983). The difference in estimated pressure increases with decreased X_{CO2} and total pressure, especially below 2 kbar. In either cases, the calculated pressures are strongly dependent on visual estimates of the volume fraction of carbonic fluid, a value typically inaccurate due to uncertainty in the third dimension (Bodnar, 1983). Parry (1986), Schwartz (1989), and Brown and Lamb (1989) proposed iterative and/or graphical methods to deduce a set of thermodynamic data compatible with microthermometric measurements. These methods are based on P-T-X sections in the pseudobinary H_2O-CO_2 system at fixed NaCl concentration. The X_{CO2} and pressure estimated from these methods are also highly inaccurate because of the different thermodynamic data set used to construct the reference diagrams and the error introduced by linear intrapolation for intermediate salinities, temperatures of homogenisation, or CO_2 densities. The estimated pressure is that of the internal pressure of the inclusion on the liquid-vapour line (solvus) in the H_2O-CO_2-NaCl system. Therefore, the pressure estimates are valid for boiling fluids only, and are minimum estimates of the trapping pressure for other fluids.

With these limitations in mind it is, nevertheless, useful to make the exercise of estimating X_{CO2} and the trapping pressure. The histogram of X_{CO2} displays a mode at X_{CO2}=0.05, shouldered by values of X_{CO2} up to 0.3 (Fig. 4-4A). Estimates of X_{CO2} using other methods yield values in the same range although the numerical value for each inclusion is slightly different. A small number of type 2 inclusions display a wide range of X_{CO2} from 0.44 to 1.00 (Fig. 4-4A). Some of these data likely overestimates X_{CO2} due to error in visual estimate of volume ratio. Nevertheless, these data indicate that inclusions with high X_{CO2} values exist.

Bowers and Helgeson (1983) equation of state yields pressure estimates that have a

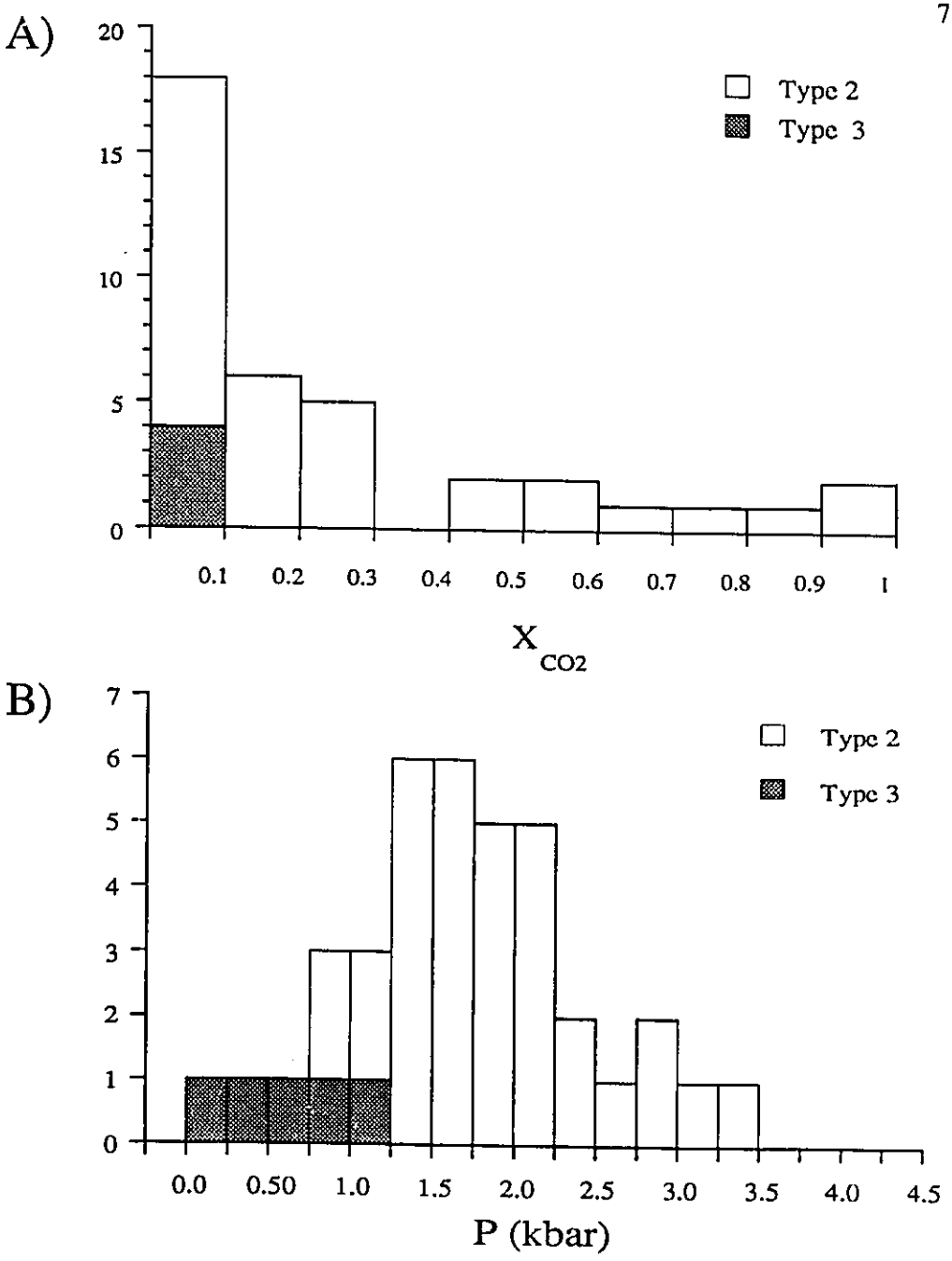

Figure 4-4. Histograms of X_{CO2} and pressure for fluid inclusions calculated using Bowers and Helgeson (1983) equation of state and FLINCOR (Brown, 1989). A) Mole fraction of CO_2 of fluid inclusions. B) Estimates of pressures.

normal distribution, and an average of 1.7±0.8 kbar (Fig. 4-4B), whereas Brown and Lamb (1989) equation of state yields pressure estimates with a large spread of values. Type 3 fluid inclusions yield low pressure of trapping using Bowers and Helgeson (1983) equation of state (Fig. 4-4B), but extremly variable and high pressures using Brown and Lamb (1989) equation of state. The equation of state of Bowers and Helgeson (1983) yields more consistent pressures and the average trapping pressure for most of the inclusions can be estimated at 1.7±0.8 kbar. There are, however, no geological criteria that constrain the trapping pressure of the Kokanee Range veins. Type 3 fluid inclusions were probably trapped during transient fluid pressure drop related to fault plane motions or migration along a pressure gradient. Assuming that the fluid was under lithostatic pressure, the average trapping pressure indicates a depth for mineralisation of 6±3 km. Hydrostatic load would yield a depth for mineralisation of about 18 km which is incompatible with the minimum metamorphic grade of the host rocks, i.e. deuteric alteration in the Nelson batholith.

Stable Isotopes

Analytical techniques

All mineral analyses were done on pure mineral concentrates handpicked under a binocular microscope. After pulverising to powder, whole rock sulphur was extracted with the Kiba solution and converted to Ag_2S (Sasaki et al., 1979). Sulphur isotope ratios were determined from SO_2 gas, produced by sulphide oxydation using cupric oxide at 1050°C, with a VG 602D mass spectrometer. Calcite, dolomite, and siderite were dissolved with HPO_3 following McCrea (1950) and Al-Aasm et al. (1990). Quartz, muscovite, and whole rock oxygen was extracted using BrF_5 or ClF_3 and converted to CO_2 by reaction with a hot graphite rod (Clayton and Mayeda,

1963; Borthwick and Harmon, 1982). $^{13}C/^{12}C$ and $^{18}O/^{16}O$ ratios of prepared CO_2 were determined with a VG SIRA 12 mass spectrometer. Sulphur, carbon, and oxygen isotope ratios are reported using the normal δ-notation relative to Cañon Diablo Troilite (CDT), PeeDee Belemnite (PDB), and Standard Mean Ocean Water (V-SMOW), respectively, in Tables 4-2 to 4-6. Routine precision on $^{34}S/^{32}S$, $^{13}C/^{12}C$, and $^{18}O/^{16}O$ ratios are 0.2‰, 0.1‰, and 0.2‰ respectively, and accurracy was monitored regularly during the course of analyses using internal standards.

Sulphur

Vein galena and sphalerite in each deposit plot as an elongate array on a $\delta^{34}S_{galena}$-$\delta^{34}S_{sphalerite}$ diagram (Fig. 4-5). Similar arrays are displayed by pairs of pyrite, galena, or sphalerite. Figure 4-5 shows that most of the data plot along the equilibrium 300ºC isotherm, in agreement with the pressure corrected average Th of fluid inclusions. Some galena-sphalerite pairs fall on the low or high temperature side of the 300ºC isotherm because of isotopic disequilibrium or because galena and sphalerite were not coexisting in some deposits and had to be extracted from different or deformed samples. The highest $\delta^{34}S$ values are from samples from the Bluebell deposit, and are similar to values reported by Ohmoto (1971). The gap between these and other data may result from a sampling bias, but, nevertheless, a large range of $\delta^{34}S_{sulphide}$ values is demonstrated for the deposits.

Histograms of galena, sphalerite, and pyrite average sulphur isotope ratio per deposit are shown on Figure 4-6. In order to test if $\delta^{34}S$ of galena, sphalerite, pyrite, and $\Delta_{galena\text{-}sphalerite}$ for deposits hosted by sedimentary or granitic rocks came from two populations with different means, Student's t test were conducted. Student's t tests were all below the critical value t_c at the level of significance of $2\alpha=0.01$. In consequence, there is no statistical evidence to suggest that $\delta^{34}S$

Table 4-2. Stable isotope data for mineralised and barren veins

Deposit	Sample	Gn	Sp	Py [Po]	Cpy [Tr]	Ba	Qz [Ms]	Sd		Do		Ca [Gf]	
		----------$\delta^{34}S$----------					$\delta^{18}O$	$\delta^{18}O$	$\delta^{13}C$	$\delta^{18}O$	$\delta^{13}C$	$\delta^{18}O$	$\delta^{13}C$
Mineralised veins													
Bosun	3-1						15.6						
	3-5	-8.3	-4.9					12.6	-6.7				
Monitor	4-1	-7.8	-5.1	-6.6			13.2	15.0	-7.7				
				-5.5			13.8						
Payne	K6-3	-5.6	-5.4				18.2	15.7	-7.0				
			-2.9										
	K6-7							15.1	-7.0				
Idaho	7-1	-7.2	-4.3				15.3	15.3	-7.3			-4.3	-1.9
	7-4									-8.9	-2.9		
Alamo	8-1		-7.2				13.6	11.4	-5.7				
	8-3	-8.3											
	8-5	-7.9	-6.4										
Highland	15-5						-5.9						
	15-6	-0.7	1.4										
			1.5	-0.1									
				-1.7									
Rambler	18-1						15.7						
	18-6	-2.4	-3.0										
Lucky Jim	23-1							12.4	-7.5				
	23-4	-2.8	-1.2										
McAllister	K25-7	-2.8	-3.5	-3.2	[-3.3]		16.2						
	K25-5						[12.2]						
Number-	F25-1									-4.2	-2.9	-5.3	-3.6
One	F25-2									4.1	-3.6		
	F25-4	-3.9	-1.6	-0.9									
Spokane	28-1							11.7	-6.7				
	28-2	-6.1	-1.9				-0.8						
	28-5						-5.8						
	28-6						-2.0						
Highlander	30-1						-2.8			-0.2	-4.8		
	30-5						-4.6						
	30-6	-0.5	1.6										
Whitewater	33-3						18.8						
	33-4		0.6				18.4	18.4	-7.4				
	33-5	-2.6	-0.6										

Table 4-2. Stable isotope data for mineralised and barren veins (continued)

Deposit	Sample	Gn	Sp	Py [Po]	Cpy [Tr]	Ba	Qz [Ms]	Sd		Do		Ca [Gf]	
		-----		$\delta^{34}S$ -----			$\delta^{18}O$	$\delta^{18}O$	$\delta^{13}C$	$\delta^{18}O$	$\delta^{13}C$	$\delta^{18}O$	$\delta^{13}C$
Noble Five	37-4	-5.1	-2.7				14.6	13.2	-7.5				
								13.4	-7.6				
	37-6						16.3						
Caledonia	41-6	0.7	2.4	3.2			18.7	15.1	-6.9				
Wonderful	W43-1		-5.6				11.3	13.8	-7.7				
							2.9						
Bluebell	E43-4	7.3	8.5	[8.7]			12.3					6.4	-7.7
	E43-5	7.6	9.4	[9.0]								7.5	-8.2
	E43-7		10.6										
Silvana	50-11	-7.1	-6.7					13.8	-6.7				
	50-12	-9.0	-6.0					15.8	-7.4				
	50-18	-7.8	0.1										
	50-27	-8.2											
	50-32	-8.5	-3.8					16.0	-6.8				
	50-36											1.1	-5.6
	50-40		-6.5					15.6	-7.5				
	50-42						-4.2						
	50-44		-4.8					14.3	-7.0				
	50-46		-6.4				7.2	15.1	-7.5				
	50-47	-10.5					6.9						
	50-49		-4.1					13.7	-6.5				
	50-50											14.1	-5.3
													[-20.4]
	50-51	-7.9	-3.7					13.3	-7.0				
	50-52		-3.7					15.6	-6.9			7.4	-6.1
Silversmith	53-2	-8.0	-7.6				-3.9	12.2	-7.4				
	53-4											5.5	-2.8
													[-18.0]
	53-5					26.9							
Richmond-	54-1	-6.5	-4.2		-6.4			13.9	-6.6				
Eureka								14.5	-6.4				
Panama	55-1						17.9						
Noonday	56-1	-10.5	-7.2					13.7	-6.9			-1.2	-5.6
Ivanhoe	57-4	-10.9	-6.2				11.9			3.5	-3.2	-3.5	-1.9
Mammoth	60-1		-13.4				14.6	16.8	-7.1			-5.1	-2.9
		-11.2	-8.6										

Table 4-2. Stable isotope data for mineralised and barren veins (continued)

Deposit	Sample	Gn	Sp	Py [Po]	Cpy [Tr]	Ba	Qz [Ms]	Sd		Do		Ca [Gf]	
		----------$\delta^{34}S$----------					$\delta^{18}O$	$\delta^{18}O$	$\delta^{13}C$	$\delta^{18}O$	$\delta^{13}C$	$\delta^{18}O$	$\delta^{13}C$
Van Roi	64-1	-13.7	-11.1		-11.8								
	64-3		-14.8				15.6	17.1	-6.3				
	64-3.1		-12.6				13.1						
	64-5											-5.8	-2.6
Hewitt	65-2	-12.2	-10.2										
	65-3						15.4						
							15.5						
Galena-	67-1	-12.9	-11.4				7.7						
Farm	67-3		-4.1				12.1	13.8	-6.4				
Comstock	77-1	-1.7	0.7										
Mountain-	81-1	-2.7					15.6	16.0	-7.1				
Con	81-2		-1.8										
Utica	86-1		1.1					15.9	-7.1			-0.8	-5.4
	86-2	-4.6	-1.9										
	86-3						16.6						
Cork-	94-1		-6.6				6.9	13.3	-7.4				
Province	94-2	-8.8	-5.4										
Wintrip	97-1	-9.4	-6.9	-9.4			-3.5						
							-3.2						
	97-2		-4.2					12.3	-7.7				
Scranton	112-2	-4.1	-2.1	-1.1	-1.1								
	112-4											-12.2	-5.2
	112-9						15.3						
Molly	121-6											-2.5	-0.9
Gibson	121-10	-2.6	-0.4		-0.2		7.5	10.3	-7.9				
				-0.4									
Alpine	127-1			0.7									
		-0.2	0.4	1.3									
	127-2						13.3						
	127-5						[10.8]						
	127-8						[9.4]						
Meteor	137-4	-0.7			-7.4		11.6						
Enterprise	148-1							13.3	-7.3				
			0.2							3.0	-4.2		
							-0.3						
	148-5	-3.0	0.2										

Table 4-2. Stable isotope data for mineralised and barren veins (continued)

Deposit	Sample	Gn	Sp	Py [Po]	Cpy [Tr]	Ba	Qz [Ms]	Sd		Do		Ca [Gf]	
		----------$\delta^{34}S$----------					$\delta^{18}O$	$\delta^{18}O$	$\delta^{13}C$	$\delta^{18}O$	$\delta^{13}C$	$\delta^{18}O$	$\delta^{13}C$
Enterprise (continued)	148-9		-5.7				11.0	13.4	-7.2	2.6	-3.6		
							-2.2						
			0.5							1.4	-3.5		
Arlington	152-3						-0.6			-1.7	-5.1	-2.0	-5.0
Ottawa	155-2	2.3	3.8	3.7									
	155-4	-2.2				10.7	-2.2			1.9	-3.2		
Standard	180-5						12.1	15.5	-6.5				
	180-7											-2.2	-2.8
	180-10	10.7	-8.4										
Victor	204-3	-6.3	-3.9				1.5	12.9	-7.6				
								12.4	-7.5				
Hamilton	SLF-8						9.8						
Barren veins													
Silvana	50-37						14.6						
Hamilton	SLF-4						-1.4					3.5	-3.5
Other	T1-10						15.9						
locations	T1-14						16.7						
	T2-3						11.3						
	T2-4			1.2			10.6						
	T3-8						17.7						
	T4-7						12.9						
	T5-2						16.8						
	T6-5						18.9						
	T7-10						16.8						
	T8-5						15.9						

Gn: galena; Sp: sphalerite; Py: pyrite; Po: pyrrhotite; CPY: chalcopyrite; Tr: tetrahedrite; Ba: barite; Qz: quartz; Ms: muscovite; Sd: siderite; Do: dolomite; Ca: calcite; Gf: graphite. Values between brackets are for the mineral in bracket in the heading of that column.

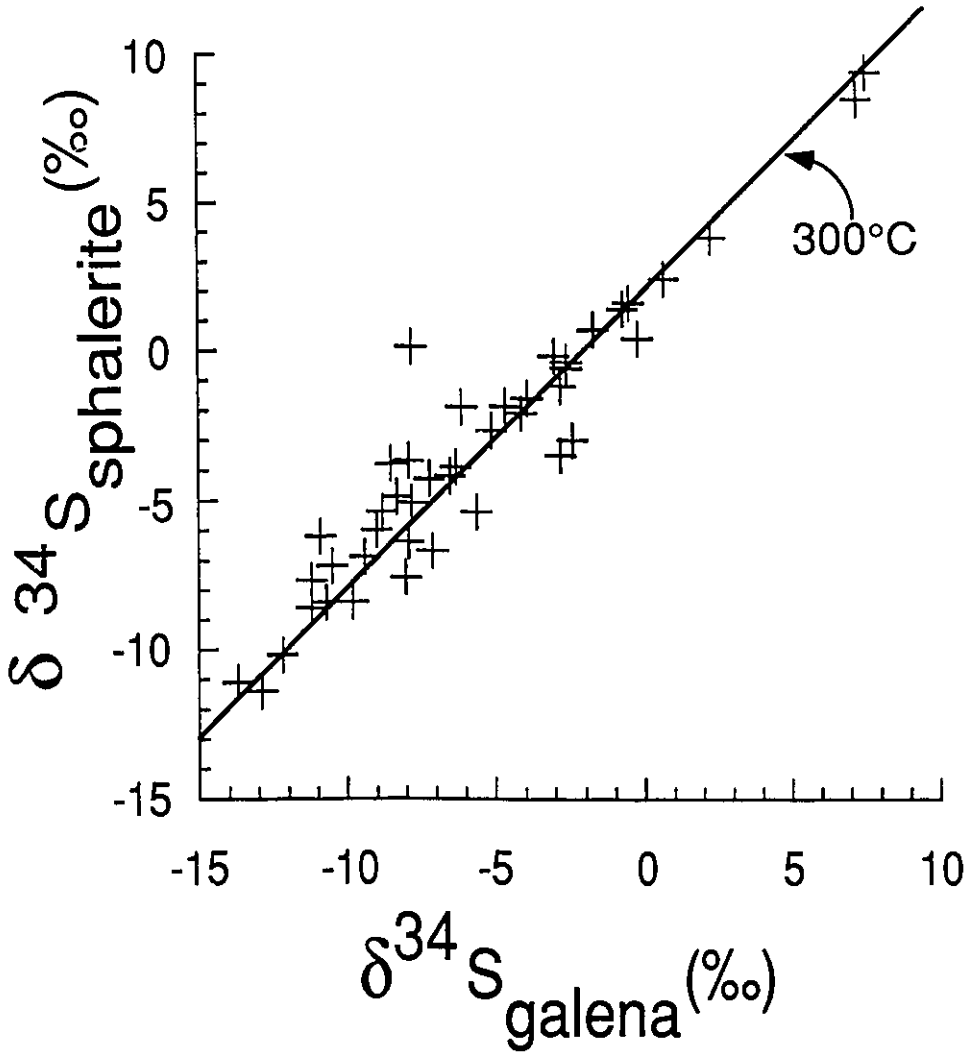

Figure 4-5. δ–δ plot of galena versus sphalerite in deposits of the Kokanee Range. Most of the data plot along an equilibrium isotherm of 300°C, indicating a large range of isotopic compositions for sulphur but similar temperatures of formation.

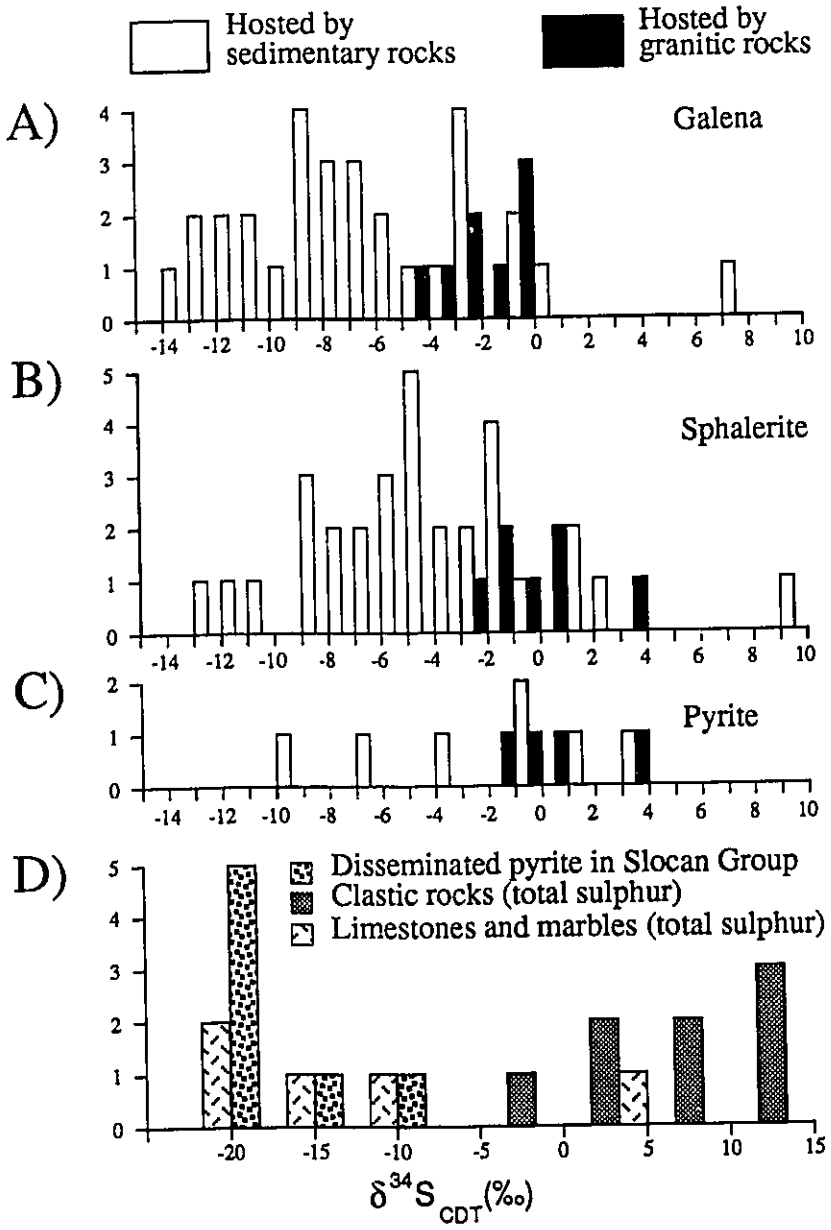

Figure 4-6. Histograms of $\delta^{34}S$. A) Average values for galena in a deposit hosted in sedimentary or granitic rocks. B) Average values for sphalerite in a deposit hosted in sedimentary or granitic rocks.C) Average values for pyrite in a deposit hosted in sedimentary or granitic rocks. D) Values for disseminated pyrite in clastic rocks of the Slocan Group, total sulphur from Paleozoic clastic rocks, and total sulphur in Mesozoic and Paleozoic limestones and marbles.

values from deposits hosted by sedimentary and granitic rocks come from two populations with different means.

Average $\delta^{34}S_{galena}$ value for each deposit is plotted on a map on Figure 4-7. Since pairs of galena and sphalerite or pyrite plot in a linear array in δ-δ space, the following description of the spatial variation in $\delta^{34}S_{galena}$ also applies to $\delta^{34}S_{sphalerite}$ and $\delta^{34}S_{pyrite}$. The $\delta^{34}S_{galena}$ contours display a general pattern of increasing $\delta^{34}S$, outward from a central area with $\delta^{34}S$ lower than -12 in Upper Triassic Slocan Group, towards deposits in sedimentary rocks as old as Cambrian (Fig. 4-7). The contours of $\delta^{34}S_{galena}$ are roughly concordant with lithologic boundaries (Fig. 4-7). Only one deposit hosted in sedimentary rocks north of the Nelson batholith has an average $\delta^{34}S_{galena}$ between -5.1 and -2.8. The apparent bimodal distribution of average $\delta^{34}S_{galena}$ (Fig. 4-6A) could be explained by bias in the sampling grid in view of the regular regional variation of $\delta^{34}S$ values. Deposits hosted by the Nelson batholith display a trend in which $\delta^{34}S_{galena}$ becomes higher, from -4.1 to 0.1, towards the centre of the batholith, opposite to the trend displayed by deposits hosted by sedimentary rocks (Fig. 4-7).

Barite is uncommon and usually forms a minor component of vein mineralisation. A small euhedral crystal of barite ($\delta^{34}S_{barite}$=26.9; Table 4-2) was found on a shear plane in graphitic schists in the Silversmith deposit, where siderite-galena-sphalerite occur in deformed lenses bounded by shear planes and transposed within the graphitic schists. Barite laths from the Ottawa deposit ($\delta^{34}S_{barite}$=10.7; Table 4-2) are intergrown with prisms of quartz and disseminated sulphides, but are in marked sulphur isotopic disequilibrium. The barite data are not readily explained in terms of either a hydrothermal origin or Triassic marine origin and, because they few in number, are not further discussed.

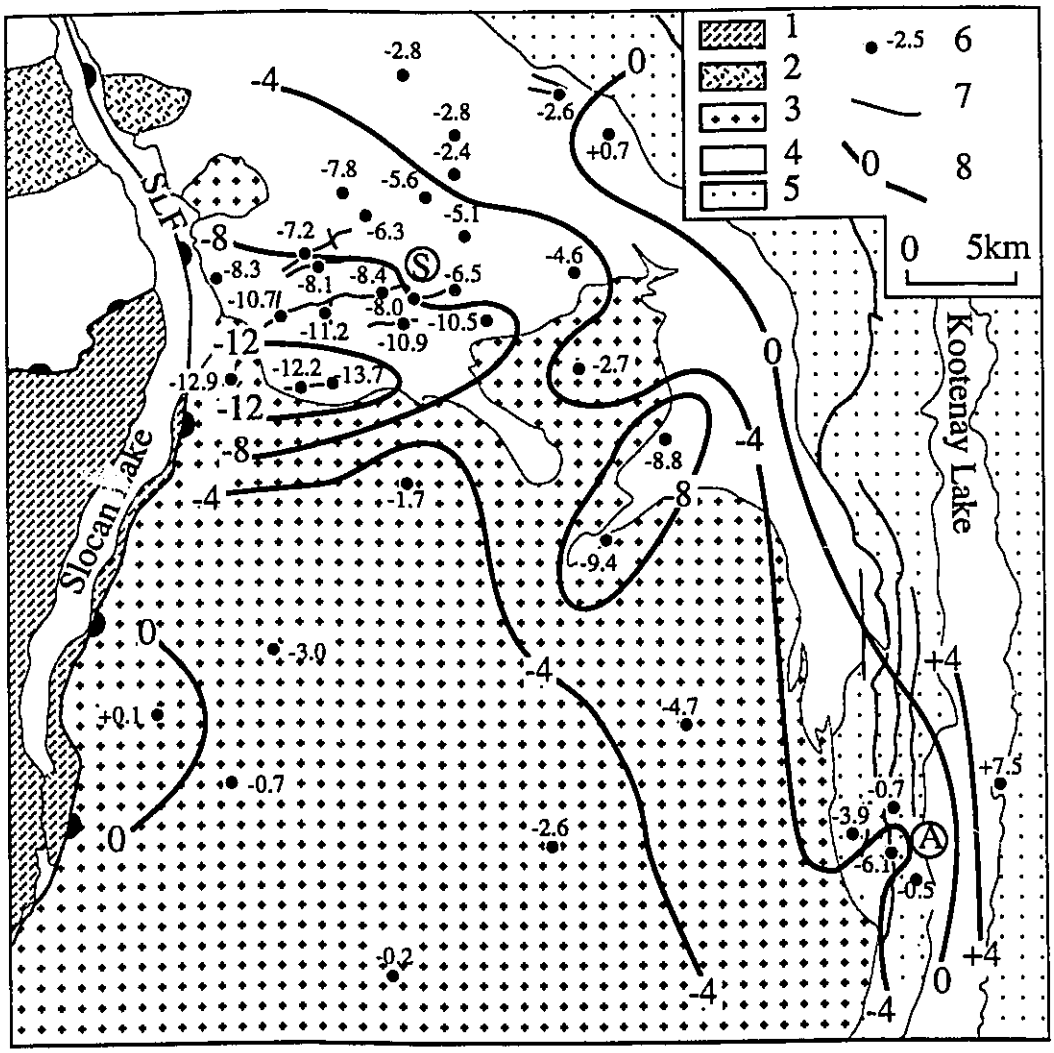

Figure 4-7. Geology map displaying the average $\delta^{34}S$ for galena in each deposit. The values are contoured and show a gradual increase in $\delta^{34}S$ towards older rocks. The contour pattern follows the distribution of lithological units. 1- Rocks of the Valhalla metamorphic core complex; 2-Granitic pluton of probable Cretaceous age; 3-Upper Triassic Slocan Group; 4-Middle Jurassic Nelson batholith; 5- Paleozoic sedimentary and metamorphic rocks; 6- Deposit location and average $\delta^{34}S$. 7- Faults. 8- Contour of $\delta^{34}S$.

Country rock sulphur

Disseminated pyrite in Upper Triassic Slocan Group pelites has low $\delta^{34}S$ values ranging from -19.5 to -6.7 (Table 4-3, Fig. 4-6D). The $\delta^{34}S$ of total sulphur from carbonate beds in Upper Triassic Slocan and Carboniferous Milford groups, and Lower Cambrain Badshot Formation are also low, ranging from -23.0 to +1.5 (Table 4-3, Fig. 4-6D). Micaceous sandstone, quartz-feldspar-biotite gneiss, and muscovite-biotite schists from the Upper Proterozoic-Lower Cambrian Hamill, Cambrian to Devonian Lardeau, and Carboniferous Milford groups have commonly low percentage of disseminated pyrite (to 2%), with $\delta^{34}S$ of total sulphur ranging from -4.4 to +11.9 (Table 4-3, Fig. 4-6D).

Carbon and oxygen

The carbon isotopic composition of siderite is homogeneous ($\delta^{13}C$=-7.1±0.5), whereas its oxygen isotopic composition is variable, $\delta^{18}O$ ranging from 10.3 to 18.4 (Table 4-2, Fig. 4-8). These siderites are from 26 deposits dispersed over an area of more than 1200 km^2, and hosted by granitic, sedimentary, and metamorphic rocks. Rare ore stage dolomite and common post-ore dolomite breccia cements have isotopic signatures distinct from siderite indicating two stages of carbonate precipitation from different fluids (Fig. 4-8). Carbon in dolomite has a higher $\delta^{13}C$ than siderite, ranging from -5.1 to -2.9, whereas $\delta^{18}O$ is lower, ranging from -8.9 to +4.1 (Table 4-2, Fig. 4-8). Ore stage calcite in the Bluebell deposit has an isotopic composition (Table 4-2) similar to the "early ore stage calcite" reported by Ohmoto and Rye (1970). Ore stage calcite from the Scranton has the lowest $\delta^{18}O$ of all deposits (Table 4-2), and probably indicates mineralising fluids dominated by meteoric water. Most commonly, however, calcite occurs as late veins cutting sulphide mineralisation or as cement to brecciated ore. These late calcites have $\delta^{13}C$ and

Table 4-3. Whole rock and disseminated pyrite $\delta^{34}S$ for sedimentary and metamorphic rocks

Sample	$\delta^{34}S_{CDT}$[1]	Lithology
Slocan Group		
T2-1	-23.0	Black limestone
T2-7	[-12.3]	Shale
T3-1	[-17.5]	Graphitic shale
T3-2	[-18.7]	Graphitic shale
T3-9	-19.9	Argillaceous limestone
T4-1	[-19.5]	Black shale
T4-6	1.0	Sandy limestone (2% disseminated pyrite)
T4-8	-22.0	Sandy limestone
T5-4	[-15.3]	Fine grained sandstone
T7-2	[-6.7]	Fine grained sandstone
T13-1	[-18.7]	Fine grained sandstone
Milford Group		
T9-2	1.5	Limestone
T9-3	4.5	Muscovite schist
T9-4	7.7	Micaceous sandstone
Lardeau Group		
T8-1	4.4	Muscovite schist
T8-2	5.0	Biotite-garnet schist
T8-9	11.9	Biotite schist
T9-11	11.2	Quartz-feldspar-biotite gneiss
Badshot Formation		
T9-10	-11.2	Crystalline marble
Hamill Group		
T9-9	11.9	Muscovite schist

1. Values for whole rock sulphur except those [in brackets] for disseminated pyrite.

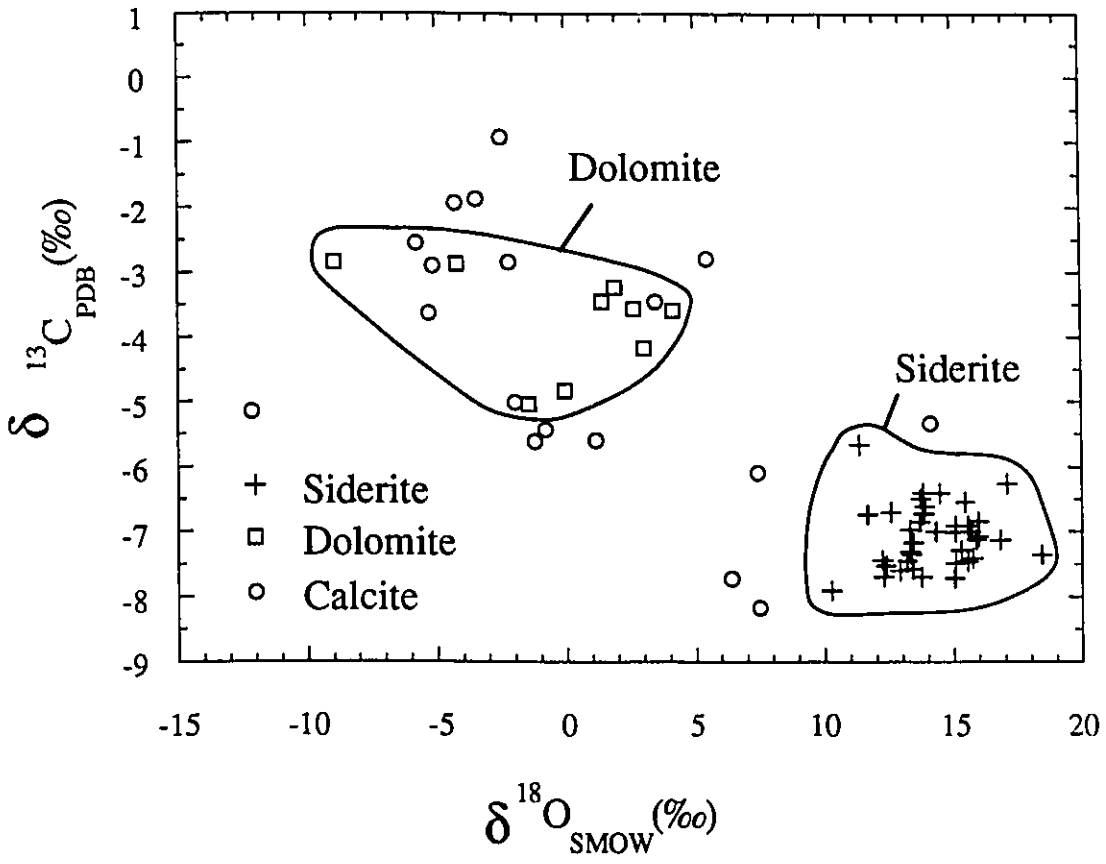

Figure 4-8. Isotopic composition of carbonates from the Kokanee Range. Siderite has an isotopic signature distinct than that of dolomite whereas calcite spans the entire range of values.

$\delta^{18}O$ values similar to, but more variable than, dolomite (Fig. 4-8). One exception, from a calcite cement in a siderite-sphalerite breccia from Silvana (50-52, Table 4-2) has an isotopic signature closer to siderite which suggest less admixed meteoric water and/or precipitation at a higher temperature than the other calcites. Two calcite lenses between shear planes in graphitic schists, nearby massive siderite-sphalerite-galena lenses in the Silversmith and Silvana deposits (Table 4-2), have $\Delta_{calcite\text{-}graphite}$ of 15.2 and 15.1‰, respectively. These could suggest isotopic equilibrium at 175ºC for these post deformation calcite, although the similarity of the Δ values may also be fortuitous.

$\delta^{18}O$ values for siderite and quartz in the deposits display two trends in δ-δ space (Fig. 4-9). The first trend is along an isotopic equilibrium isotherm at 300ºC; the large scatter on both sides of the isotherm indicates some disequilibrium. The second trend is characterised by $\delta^{18}O$ values for quartz as low as -5 for near constant values around -13 in siderite (Fig. 4-9). Commonly, this quartz occurs as a breccia cement. This marked isotopic disequilibrium results from admixture of meteoric water to the hydrothermal system during quartz precipitation; quartz and siderite are not cogenetic. Muscovite from narrow hydrothermal phyllic alteration halos surrounding mineralised veins in the Nelson batholith has $\delta^{18}O$ values ranging from 9.4 to 12.2 (Table 4-2) and δD values of -134 and -141.

Average $\delta^{18}O_{siderite}$ for each deposit is plotted on a map for Sandon area on Figure 4-11A. Contours of $\delta^{18}O$ display a concentric pattern of variation about a central area open to the west (Fig. 11A). A similar pattern is obtained for quartz using only those values that display no evidence of admixture of meteoric water (Fig. 4-9). The central area of low $\delta^{18}O_{siderite}$ is positioned on a east-west fault zone (Fig. 4-11A), locally referred to as the Main Lode, which

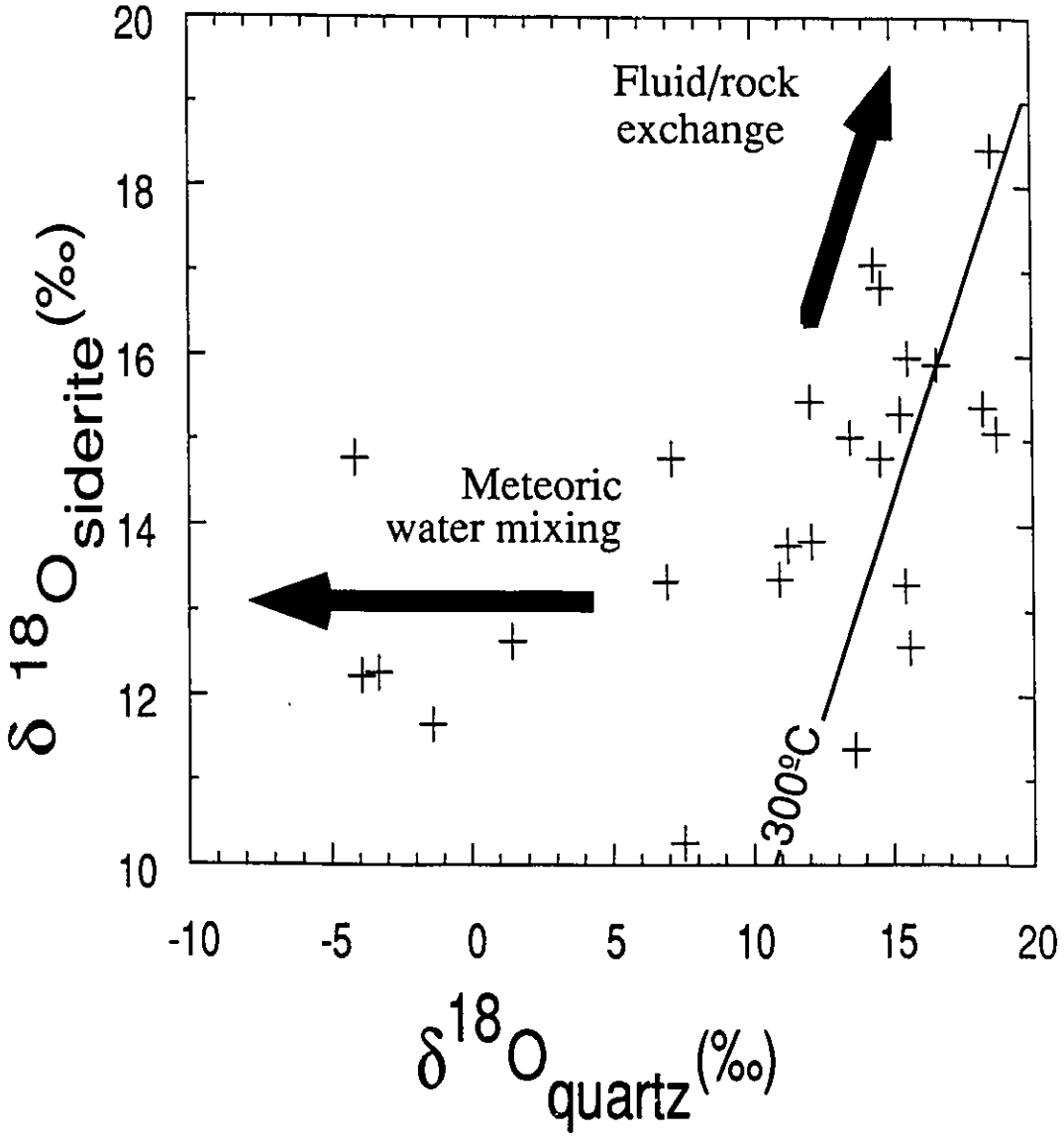

Figure 4-9. The oxygen isotopic composition of quartz and siderite display two trends, one along an equilibrium isotherm, indicating partial equilibrium, and the second, admixture of meteoric water.

contains many of the larger deposits of the Kokanee Range.

Barren veins

Barren quartz veins from widely spaced sampling sites display the same range of $\delta^{18}O$ values as mineralised veins (Table 4-2), and indicate that oxygen in the barren veins attained variable degrees of isotopic equilibrium with the wallrocks. The $\delta^{18}O$ values of barren veins do not permit differentiation from mineralised veins. Cairnes (1934) showed that the barren quartz veins were older than the Ag-Pb-Zn veins and this relative age is corroborated by $^{40}Ar/^{39}Ar$ data for a small quartz-muscovite veinlet near the McAllister deposit (Beaudoin et al., 1992a). The low $\delta^{18}O$ value of -1.4 for a quartz-calcite lense within the Slocan Lake Fault (SLF-4; Table 4-2) is discussed below.

Igneous rocks

Whole rock $\delta^{18}O$ values for the Nelson batholith range from +7.8 to +11.4‰ and average 9.5±1.0‰ (Table 4-4, Fig. 4-10A), similar to those (+9 to +12‰) reported by Magaritz and Taylor (1986). Two samples from nearby localities east of the Alpine deposit (Fig. 4-1) have $\delta^{18}O$ values of 6.7 and 6.1, and a sample from near the Arlington deposit, about 7km east of the trace of Slocan Lake Fault (Fig. 4-1), has a $\delta^{18}O$ of 4.8; these low $\delta^{18}O$ values indicate local exchange with meteoric water as they are surrounded by granitic rocks with normal $\delta^{18}O$ values. Oxygen isotope exchange between granitic rocks and meteoric water is evident adjacent to the Slocan Lake Fault. There, rocks of the Nelson batholith are variably altered to sericite-kaolinite-quartz-chlorite with, locally, hematite or pyrite, and cut by numerous small shear zones and faults with clay gouge. Whole rock $\delta^{18}O$ values range from 3.6, 300 m above the Slocan Lake Fault, to 0.1 less than 100 m from the fault plane, but no regular trend with distance from the Slocan Lake

Table 4-4. Whole rock, quartz, and feldspar $\delta^{18}O$ for igneous rocks

Sample	$\delta^{18}O$ (‰)	Lithology
Nelson batholith		
JL-18	9.0	KF porphyric HN granodiorite
JL-238	9.9	KF porphyric HN granodiorite
JL-273	10.5	Granodiorite
JL-375	8.7	KF porphyric HN granodiorite
JL-407	9.0	Granite
DB-49	8.1	Medium grained HN granodiorite
DB-70	9.7	Medium grained HN-BI granite
DB-74	4.8	KF porphyric HN granodiorite
DB-108	9.2	KF porphyric HN granodiorite
DB-274	9.4	Granite
DB-322	6.7	Fine grained HN granite
DB-324	6.1	Fine grained HN granite
DB-350	8.5	KF porphyric HN granodiorite
MA-207	10.9	KF porphyric HN granodiorite
MA-250	10.9	KF porphyric HN granodiorite
MA-354	9.2	KF porphyric HN granodiorite
MA-370	7.8	Granite
MS-28	9.3	KF porphyric HN granodiorite
T12-6	11.4	QZ-HN monzonite
T12-8	9.4	KF porphyric HN granodiorite
Nelson batholith, hangingwall of Slocan Lake Fault		
JL-57	3.6	KF porphyric HN granodiorite
SLF-1	0.4	KF porphyric granodiorite altered to sericite-kaolinite-quartz-chlorite-pyrite
SLF-2	1.0	Sheared KF porphyric granodiorite altered to sericite-kaolinite-quartz-chlorite-pyrite
SLF-5	0.1	Clay fault gouge
SLF-6	1.1	Hematitized granite
SLF-7	0.8	KF porphyric granodiorite altered to sericite and chlorite
SLF-16	9.8	Highly silicified, sericitized, and chloritized granite

Table 4-4. Whole rock, quartz, and feldspar $\delta^{18}O$ for igneous rocks (continued)

Sample	$\delta^{18}O$ (‰)	Lithology
Ladybird orthogneiss, footwall of Slocan Lake Fault		
SLF-9	1.0	Sericitized and kaolinitized foliated granite with MS porphyroblasts
SLF-10	2.1	Foliated BI granite with sericitized feldspar porphyroblasts
SLF-11	(9.6) [7.4]	QZ-KF-MS concordant metamorphic segregation
SLF-12	5.1 (12.2)	Sericitized foliated granite with discordant QZ vein
SLF-13	0.7	Foliated granite 3 m beneath a sub-concordant shear zone
Metasedimentary unit paragneiss, footwall of Slocan Lake Fault		
SLF-14	(9.9)	QZ-KF-MS concordant metamorphic segregation
Mulvey orthogneiss, footwall of Slocan Lake Fault		
SLF-15	(11.6) [9.8]	QZ-KF-MS concordant metamorphic segregation

Values for whole rock except those in (parentheses) and [brackets] which are for quartz and feldspar separates, respectively. KF: potassium feldspar; Qz: quartz; MS: muscovite; BI: biotite; HN: hornblende.

Fault is documented. About 1300 m above the fault, the Nelson batholith has a normal $\delta^{18}O$ of 8.1. A small lense of drusy quartz with central calcite bounded by shear planes has a $\Delta_{calcite\text{-}quartz}$ of +4.9‰ indicating an equilibrium temperature of 200ºC with a meteoric-derived fluid having a $\delta^{18}O_{fluid}$ of -13.1. One highly silicified granite sample (SLF-16, Table 4-4) within 20 cm of a mineralised quartz vein cut by small faults related to Slocan Lake Fault, has a $\delta^{18}O$ of 9.8, identical to vein quartz (SLF-8, Table 4-2), which suggests that in this case, hydrothermal alteration quartz, precipitated near the vein margin, did not exchange O with late meteoric fluids.

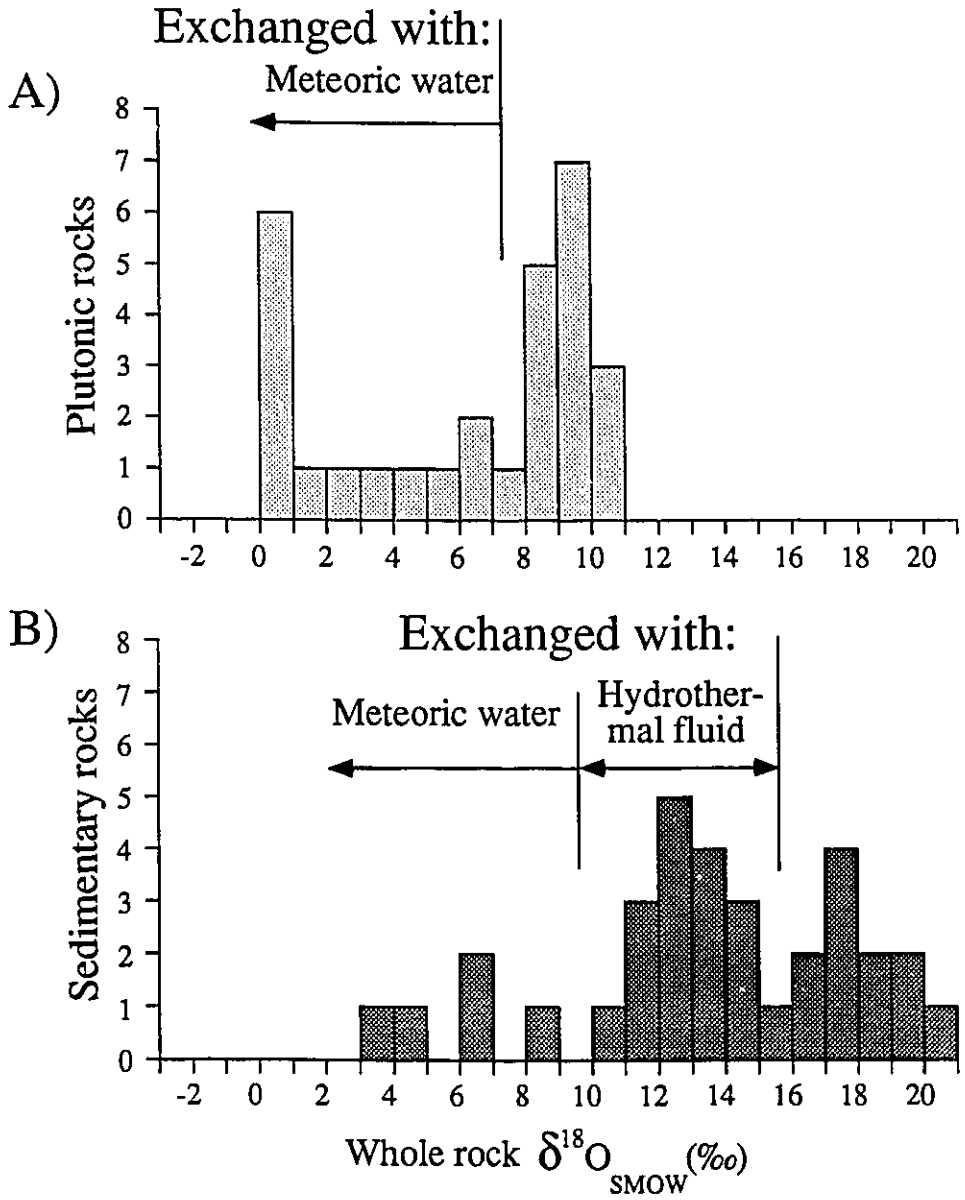

Figure 4-10. Histograms for whole rock $\delta^{18}O$ values. A) Granitic rocks, values below about 8‰ indicate exchange with meteoric water. B) Sedimentary and metamorphic rocks; values between between 10 and 16 are lowered by exchange with hydrothermal fluids whereas values below 10 indicate exchange with meteoric water.

In the footwall of the Slocan Lake Fault, the Ladybird orthogneiss is densely fractured and has a retrograde alteration characterised by muscovite porphyroblasts and sericitized felspars (Carr, 1985). Whole rock $\delta^{18}O$ values for Ladybird (Table 4-4) increase from 1.0 near Slocan Lake Fault to 5.1 about 400m below the fault, indicating decreased exchange with meteoric water away from the fault zone. A sample adjacent to thick shear zone that cuts the foliation of the Ladybird has a $\delta^{18}O$ value of 0.7, suggesting meteoric water migrated into late shear zones. Metamorphic segregations in the Ladybird, and underlying metasedimentary unit and Mulvey orthogneisses have feldspar and quartz $\delta^{18}O$ values ranging from 7.4 to 9.8 and from 9.6 to 12.2, respectively (Table 4-4). Two quartz-feldspar pairs have $\Delta_{quartz\text{-}feldspar}$ of 1.8 and 2.3, implying equilibrium temperatures of 240 and 170ºC with a meteoric-derived fluid having $\delta^{18}O$ values of 2.2 and -4.2, respectively, using fractionation factors from O'Neil and Taylor (1967) and Clayton et al. (1972). These temperatures and $\delta^{18}O_{fluid}$ values are similar to those calculated from the quartz-calcite lense in overlying Nelson batholith.

Sedimentary rocks in the Sandon area

Black shale, slate, siltstone, and sandstone were sampled along two north-south traverses in the Slocan Group west and east of Sandon (Fig. 11B). Along the 16 km long western traverse, whole rock $\delta^{18}O$ values range from 11.7 to 17.8 (Table 4-5) without a systematic trend. The eastern traverse is about 12 km long, and whole rock $\delta^{18}O$ values range from 16.3 to 20.3 (Table 4-5), also without a systematic trend. A Student's t test suggests that the two traverses are in rocks with different mean $\delta^{18}O$ values. Sedimentary rocks near the margin of Nelson batholith do not display evidence of exchange with low $\delta^{18}O$ noted above. The $\delta^{18}O$ values for Slocan Group sedimentary rocks decrease within a broad area that appears to emanate from the Slocan

Table 4-5. Whole rock $\delta^{18}O$ for Slocan Group in Sandon area

Western traverse			Eastern traverse		
Sample	$\delta^{18}O$(‰)	Lithology	Sample	$\delta^{18}O$(‰)	Lithology
T1-9	15.1	Black siltstone	T6-4	17.4	Black slate
T1-5	12.8	Black siltstone	T6-6	20.3	Siltstone
T1-3	11.7	Siltstone	T6-8	18.4	Sandstone
T1-1	12.3	Black shale	T13-9	16.4	Slate
T11-5	11.9	Black siltstone	T6-10	19.4	Sandstone
T11-11	14.6	Sandstone	T6-12	16.3	Slate
T3-3	14.5	Sandstone	T3-9	19.4	Sandstone
T11-10	12.7	Sandstone	T4-1	17.2	Sandstone
T11-13	13.9	Grey slate	T4-3	18.4	Sandstone
T12-10	13.4	Sandstone			
T12-5	13.6	Siltstone			
T12-9	17.8	Sandstone			
x=	13.7		x=	18.1	
s=	1.7		s=	1.4	
n=	12		n=	9	

Lake Fault (Fig. 4-11B).

Sedimentary and metamorphic rocks in Ainsworth area

Sedimentary and metamorphic rocks west of Ainsworth have whole rock $\delta^{18}O$ ranging from 11.6 to 17.7, whereas on both shores of Kootenay Lake, these rocks have lower whole rock $\delta^{18}O$ values ranging from 3.1 to 10.1 (Table 4-6). Crystalline marble from the Badshot Formation within the Bluebell deposit has a value of 22.5 (Table 6), similar to values reported for the "Bluebell limestone" by Ohmoto and Rye (1970). The broad range of $\delta^{18}O$ values in these metasedimentary rocks is partly due to lithological variation. The low $\delta^{18}O$ values are similar to those observed in rocks adjacent to the Slocan Lake Fault, and suggest as well that these rocks

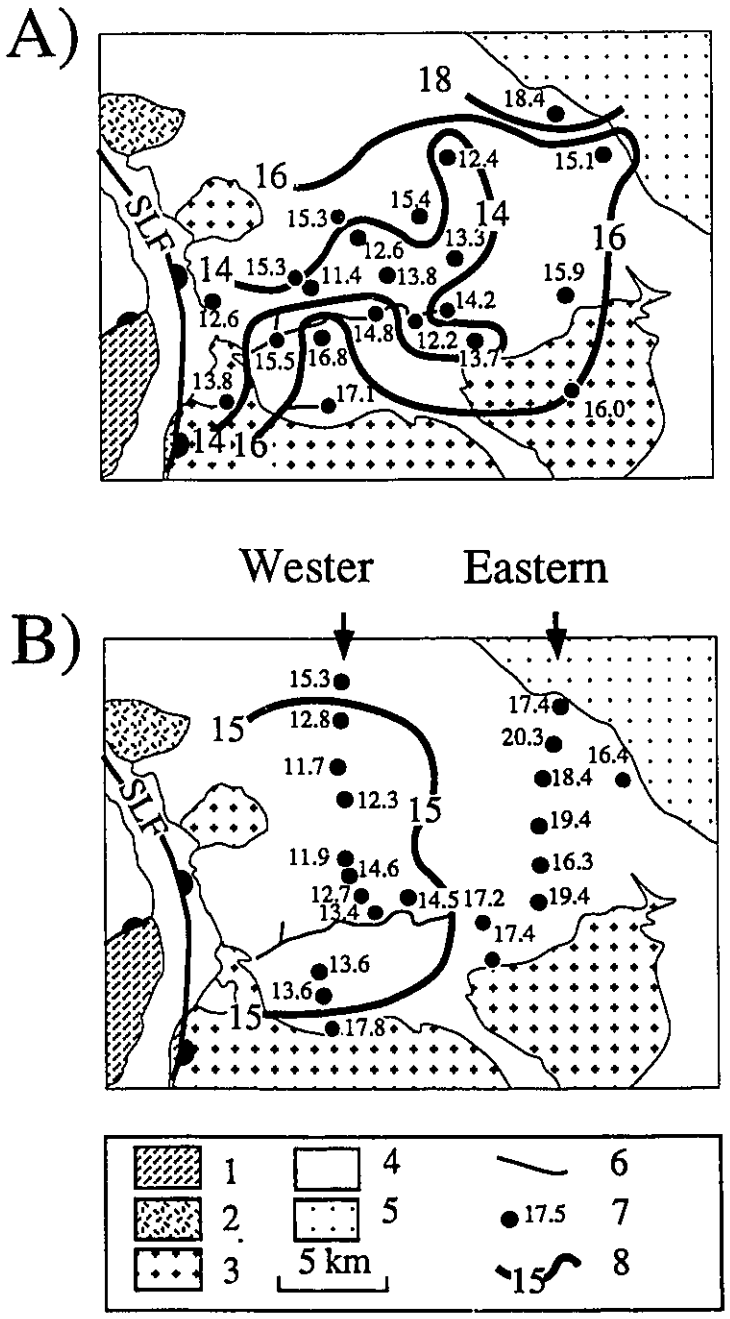

Figure 4-11.$\delta^{18}O$ zonation maps. A) Average value for siderite in each deposit display a pattern emanating from the Slocan Lake Fault (SLF) but also controlled, on a local scale, by the Main Lode fault zone. B) Whole rock for the western and eastern traverses in Slocan Group are contoured and show an area with values lower 15. 1- to 5- , see Figure 4-1.;6- Main Lode; 7- Deposits and whole rock samples locations and $\delta^{18}O$ value; 8-. Contour of $\delta^{18}O$.

Table 4-6. Whole rock $\delta^{18}O$ for sedimentary and metamorphic rocks in Ainsworth area

Sample	$\delta^{18}O$(‰)	Lithology
Slocan Group		
T8-7	14.7	Sandstone
T9-1	13.0	Biotite-muscovite schist
Milford Group		
T8-4	11.6	Biotite-muscovite schist
T9-7	17.7	Biotite-garnet schist
T9-3	14.0	Muscovite schist
T9-4	3.1	Micaceous sandstone
Lardeau Group		
T8-2	12.2	Biotite-garnet schist
T8-9	8.2	Biotite schist
T8-1	6.8	Muscovite schist
T9-11	4.4	Quartz-feldspar-biotite gneiss
Badshot Formation		
T9-10	22.5	Crystalline marble
Mohican Formation		
T9-9	6.5	Muscovite schist
Hamill Group		
T9-8	10.1	Micaceous metasandstone

exchanged oxygen with low $\delta^{18}O$ meteoric water.

Source of Sulphur

The regional trend of variation in the abundance of ^{34}S in sulphides (Fig. 4-7) and the near

isotopic equilibrium of galena and sphalerite in δ-δ space (Fig. 4-5) indicate a large variation (22.2‰) in $\delta^{34}S_{H2S}$ in the Kokanee Range deposits, which most likely derives from the mixing of two or more sulphur reservoirs with different isotopic compositions. In an open system, sulphide precipitation could lead to a large isotopic fractionation of the residual aqueous sulphur. However, a sulphur reservoir with a $\delta^{34}S$ of -14 would require more than 99% of the original sulphur to have been precipitated as sulphide in order to account for galena with a $\delta^{34}S$ of -2.8, such as in the Lucky Jim deposit (Table 4-2, Fig. 4-7). This scenario is considered unlikely, especially since the Lucky Jim represents about 10% of the total production in the Kokanee Range. Regular variation in redox state of the hydrothermal fluid by reaction with wallrocks is considered unlikely at the scale of the district because of the sluggish kinetics of sulphur isotopic equilibrium at temperatures around 300ºC (Ohmoto and Lasaga, 1982).

Whole rock and disseminated pyrite sulphur (Fig. 4-6D) span more than the entire range of ore sulphide $\delta^{34}S$ and display two peaks at high (+10 to +15) and low (-20 to -15) $\delta^{34}S$, each representative end members of isotopically different sulphur stored in the sedimentary rocks of the area. Because the local country rocks contain sulphur with a range of $\delta^{34}S$ values larger than found for vein sulphides, wallrock sulphur could account for the variation of $\delta^{34}S_{sulphides}$. There is a correlation between $\delta^{34}S$ of country rocks and average $\delta^{34}S$ per deposit (Fig. 4-7) which indicates that the hydrothermal fluid acquired S through reaction with regional country rocks. The Bluebell deposit has the highest $\delta^{34}S_{galena}$ (+7.5; Table 4-2) and is hosted by the Cambrian Badshot Formation. A sample of pure crystalline Badshot marble yielded a low, total sulphur, $\delta^{34}S$ (-11.2; Table 4-3). This indicates that sulphur in the Bluebell was not derived from its immediate wallrock, which is only 30 to 50 m thick (Höy, 1980), but sulphur was more likely

derived from the Cambrian to Carboniferous clastic rocks in the area. $\delta^{34}S_{sulphide}$ values for deposits hosted in the Nelson batholith could result from variation in mixing proportions of isotopically light sulphur leached from surrounding Slocan Group pelites with a heavier sulphur source, close to 0‰, possibly representing a third sulphur reservoir.

Three geologically discrete sulphur reservoirs thus are identified, of which the first two display a large range of $\delta^{34}S$: 1) disseminated pyrite and total S in impure limestone beds in Cambrian Badshot Formation, and Carboniferous Milford and Upper Triassic Slocan groups, and characterised by low $\delta^{34}S$; 2) Carboniferous to Cambrian sedimentary clastic rocks and metamorphic equivalents, characterised by high $\delta^{34}S$ for total sulphur; 3) magmatic sulphur represented by disseminated sulphides in the Nelson batholith or deep-seated igneous rocks or magmatic fluids, characterised by a $\delta^{34}S$ near 0.

Source of Carbon

The homogeneity of the carbon isotopic composition of siderite and the large area where carbon was sampled require a large and homogeneous carbon reservoir and/or an extensive homogenisation process. In contrast with sulphur which is dominated by reaction with local country rocks, carbon is dominated by a hydrothermal fluid rich in carbonate which buffers carbon leached from country rocks. A carbonate-rich hydrothermal fluid is also indicated by ore stage siderite deposition, and CO_2-rich, CH_4-poor fluid inclusions.

Precise estimation of $\delta^{13}C_{fluid}$ in equilibrium with siderite at 300ºC is not possible at present due to lack of experimental data at high temperature. Reduced partition functions for siderite, calculated by Golyshev et al. (1981), suggest fractionation factors for calcite and dolomite at temperatures below 323ºC that are comparable to those calculated by Bottinga (1969),

and the empirical data from Sheppard and Schwarcz (1970). Above this temperature, agreement is less satisfactory. For siderite and calcite, Golyshev et al. (1981) estimate a per mil fractionation for carbon (1000 ln α(siderite-calcite)) of ≈2.3 at 300ºC. Extrapolation of experimental data of Carothers et al. (1988) to 300ºC indicates a per mil fractionation (+5.5‰) which is much larger than that of Golyshev et al. (1981). Carothers et al. (1988) did not discuss this discrepancy between the two data sets. Therefore, we estimate that the minimum and maximum values for $\delta^{13}C_{CO2}$ in the hydrothermal fluid using, respectively, the results of Golyshev et al. (1981) for siderite, and of Bottinga (1969) for calcite; at 300ºC, carbonate-CO_2 fractionations are +0.7 and -2.1. The values for $\delta^{13}C_{fluid}$ range from -7.8 to -5.0. Note that the uncertainty in $\delta^{13}C_{fluid}$ is larger than the standard deviation about the mean $\delta^{13}C_{siderite}$.

The inferred size, isotopic composition, and required homogeneity of the CO_2 reservoir constrains its nature. Either this reservoir was formed by large scale, high grade metamorphism in the middle or lower crust by mixing decarbonation CO_2 with oxydised graphitic carbon, or it resulted from mantle CO_2 degassing. The following arguments, however, suggest that CO_2 degassing from the mantle is more likely: 1) the low CH_4 content in inclusion fluids indicate that reduced carbon was not abundant in the source area or along the path of the hydrothermal fluid; 2) a widespread suite of lamprophyre dykes, coeval with mineralisation, and considered by-products of Paleocene-Eocene crustal extension in southeastern British Columbia (Beaudoin et al., 1992a) indicates mantle melting and, therefore, degassing either during extension-driven mantle upwelling or ascent of mafic melts; 3) extension resulted in crustal thinning and mantle upwelling beneath the Kokanee Range. The upper mantle and lower crust both display low resistivity probably caused by electrical conduction by a fluid phase mainly located in

deformation zones (Gough, 1986; Jones et al., 1988). Gough (1986) suggested that the fluid phase was derived from mantle degassing and/or partial melting; 4) a large transcrustal fault zone, Slocan Lake Fault, has been seismically imaged to the Moho (Cook et al., 1988) and likely provided the channel to transfer hydrothermal fluids from deep-seated reservoirs to higher crustal levels. This role of the Slocan Lake Fault is evidenced by isotope zonations, as discussed later.

Origins and Evolution of the Hydrothermal Fluids

Origin of the hydrothermal fluids

Fluid inclusion data, and stable and Pb isotope data, indicate multiple fluids that reacted with discrete geologic reservoirs and mixed in various proportions. At least three different fluids were involved during the various stages of mineralisation (Fig. 4-12). A fluid with a low $\delta^{18}O$ can be uniquely identified as meteoric water with a short history of water/rock oxygen exchange. Fluid inclusions from quartz with low $\delta^{18}O$ typically display low temperatures (190-241ºC) and salinities (2.0-4.4 wt. % NaCl eq.; Table 4-1). These trapping temperatures are similar to those temperatures calculated from calcite-graphite pairs (175ºC) in the Main Lode, and a quartz-calcite lense (200ºC), and the apparent temperature of reequilibration of quartz-feldspar pairs (170-240ºC) in the Slocan Lake Fault (Tables 4-2 and 4-4), suggesting that no significant temperature correction is necessary for these late-stage inclusions. The calculated $\delta^{18}O$ values for the meteoric-dominated fluid based on quartz-water fractionation (Clayton et al., 1972), range from -14.6 to -12.3, and are higher than the value (-20) calculated for a Tertiary meteoric water having a δD of -152, as determined from measurements on inclusion waters by Ohmoto and Rye (1970). Some water/rock oxygen exchange is required for the late stage fluid if they originated with a $\delta^{18}O$ of -20. The extent of oxygen isotope exchange between meteoric water and country rocks

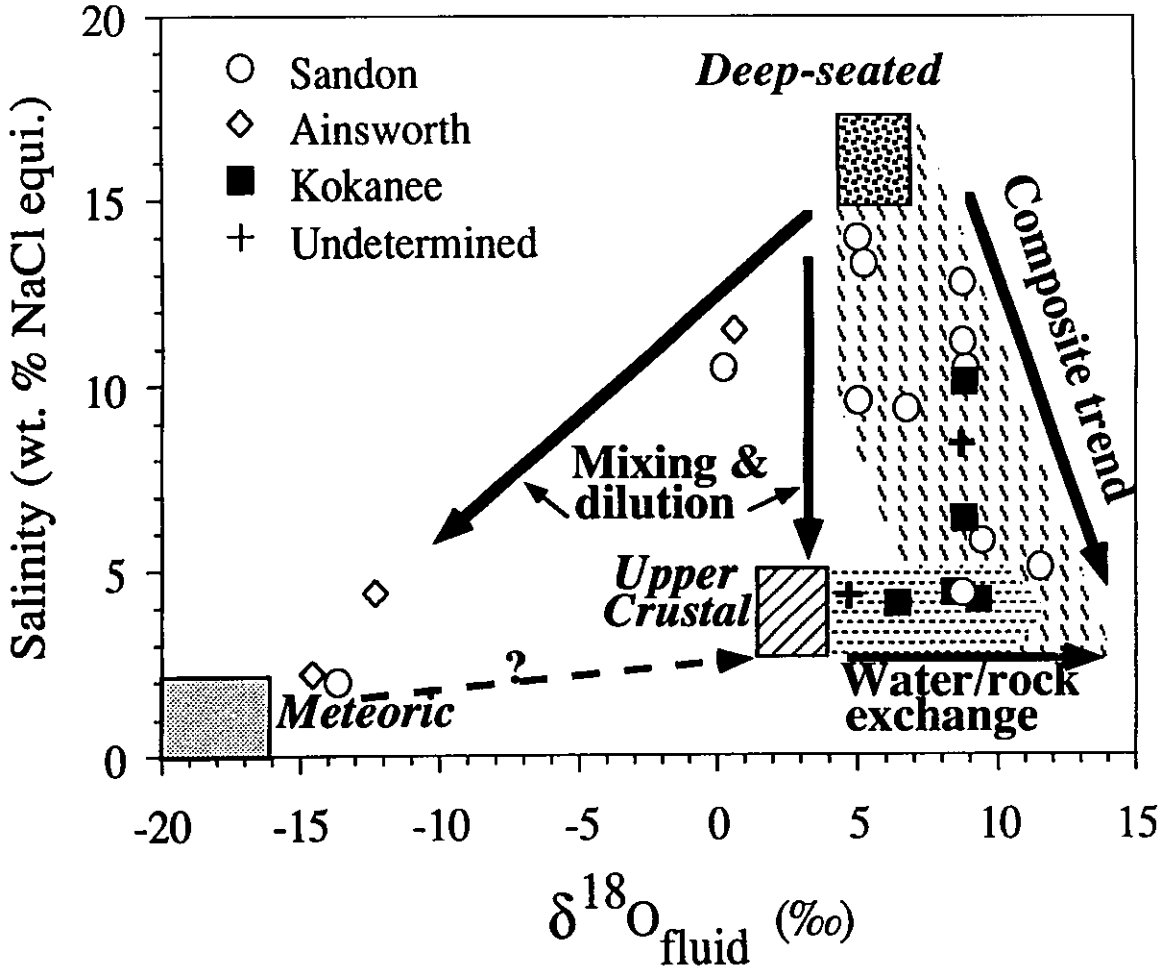

Figure 4-12. Salinity-$\delta^{18}O$ diagram displaying the approximate isotopic composition and salinity of the meteoric, upper crustal, and deep-seated fluids, and the mixing and water/rock exchange trends. Sandon, Ainsworth, and Kokanee groups are based on Pb isotopic compositions (Beaudoin et al., 1992b); deposits not analysed for Pb isotopes are labelled undetermined.

depends on the attained water/rock ratio, which was particularly high immediatly adjacent to Eocene extensional faults, such as the Slocan Lake Fault; low $\delta^{18}O$ values in rocks along the shores of Kootenay Lake also suggest a major fault beneath the lake. Magaritz and Taylor (1986) identified meteoric hydrothermal alteration with high water/rock ratios only across traces of the large Eocene fault zones of southern British Columbia. Elsewhere in the Kokanee Range, no evidence of widespread O exchange between meteoric water and country rocks has been identified. The meteoric-dominated hydrothermal fluid invaded the fracture network during the late stages of hydrothermal activity. This suggests that meteoric water permeated deeper levels of the crust and invaded the fracture network in the waning stage of the hydrothermal system, possibly during uplift of the crustal block in which mineralisation was taking place.

The isotopic composition of Tertiary meteoric water (δD=-152) determined by Ohmoto and Rye (1970) is significantly different from that (δD=-115) calculated by Magaritz and Taylor (1986) from biotite and hornblende from the Nelson batholith. Magaritz and Taylor (1986) suggested that the Nelson batholith was pervasively altered by a meteoric-hydrothermal fluid at high temperature (>400°C), and that this system resulted either from proximity to buried Tertiary plutons or represented exhumation of deep segments of the batholith. Paleocene-Eocene extension and uplift recorded in the area (Parrish et al., 1988) argues for the latter hypothesis. It is more likely that the meteoric-hydrothermal alteration of the Nelson batholith took place during the cooling of the batholith in the Middle-Late Jurassic, possibly before accretion to North America, and therefore accounting for the heavier meteoric water than that proposed for the Tertiary by Ohmoto and Rye (1970).

Salinity-$\delta^{18}O_{fluid}$ data (Fig. 4-12), and δD values for hydrothermal alteration muscovite

suggest two additional hydrothermal fluids. The δD_{fluid} is calculated to be -90 at 300ºC for equilibrium with hydrothermal alteration muscovite, by extrapolation of Suzuoki and Epstein (1976) fractionation factors. Taylor (1979) suggested, based on empirical data, that below 400ºC the slope of the fractionation curves becomes shallower, which would yield a value of δD_{fluid} closer to -105. We therefore estimate that δD_{fluid} during hydrothermal alteration was in the range of -105 to -90, and likely represents the earliest hydrothermal fluids flowing in the veins. These δD values are intermediate between those for Tertiary meteoric water (-152; Ohmoto and Rye, 1970) and deep-seated fluids in isotopic equilibrium with metamorphic and magmatic rocks.

Salinity-$\delta^{18}O_{fluid}$ data (Fig. 4-12) require that two fluids with slightly different $\delta^{18}O_{fluid}$ but constrasting salinities (≈4 and 15 wt. % NaCl eq.) were involved during mineralisation. These end member fluids are respectively labelled "upper crustal" and "deep-seated" on Figure 4-12, and two hypotheses can be envisaged for their origins: 1) both fluids are ultimately of meteoric origin but have experienced different histories of water/rock exchange and, possibly, have resided in different lithospheric segments for some period of time. The upper crustal fluid would display an evolved $\delta^{18}O$ signature but relatively unmodified δD because of a shorter water/rock history correlated by its location in the upper crust. The deep-seated fluid would display evolved $\delta^{18}O$ and δD signatures due to a long water/rock exchange history in deep lithospheric segments at higher temperatures than the upper crustal fluid; 2) the upper crustal fluid is an evolved meteoric water as in the first hypothesis but the deep-seated fluid has a different origin. The source of the water for the deep-seated fluid can be sought in metamorphic dehydration reactions or degassing of magmatic rocks formed by partial melting of lower crustal or mantle rocks. That fluids may presently reside in the lower crust and upper mantle beneath the Kokanee Range is suggested by

their low electrical resistivity and low upper mantle density (Gough, 1986). The mantle processes responsible for the generation of these fluids were likely initiated at the beginning of Paleocene-Eocene extensional collapse of the Cordillera in southeastern British Columbia, and were maintained by the presence of an elongate mantle upflow beneath the interior of the Canadian Cordillera (Majorowicz and Gough, 1991). It has been argued that unroofing of a metamorphic core complex involves retrograde metamorphism of its lower plate and, therefore, that metamorphic reactions will take up, rather than release, water through hydration reactions (Reynolds and Lister, 1987; Smith et al., 1991). Although this is reasonable for the lower plate, juxtaposition of a hot lower plate beneath a cooler upper plate is, however, likely to induce prograde metamorphic dehydration of the latter, and these fluids would be expected to migrate upward in the crust.

The value of $\delta^{18}O$ calculated for the deep-seated fluid, at 300°C in equilibrium with quartz using the fractionation factor of Clayton et al. (1972), is around +5 to +6 (Fig. 4-12). This $\delta^{18}O_{fluid}$ is atypical and can found in waters equilibrated with magmatic or metamorphic rocks, or highly evolved meteoric waters. Although it is unlikely that evolved meteoric waters reached the lower crust and mantle, it is possible that they mixed with metamorphic dehydration fluids derived from the lower crust or magmatic fluids derived from the mantle.

Fluid mixing

Mixing between fluids of different salinities is clearly indicated by the wide range, and gradual change, in salinities documented in the Kokanee Range (Table 4-1; Fig. 4-12). Within one thin section, the standard deviation (1σ) about the mean salinity of one population of inclusions ranges from 0.1 to 2.9 wt. % NaCl eq. (Table 4-1). For example, at the Ivanhoe

deposit, two clusters of inclusions were studied at the base (early) and top (late) of a large zoned sphalerite grain. Early sphalerite precipitated from a fluid with a salinity of 14.0 wt. % NaCl eq. whereas the fluid that deposited late sphalerite had a salinity of 9.6 wt. % NaCl equi. (Table 4-1): a decrease in salinity for late sphalerite suggests dilution of a saline hydrothermal fluid.

The range and small scale heterogeneity of salinities does not appear to result from post-trapping modification. For example, leakage of fluids in the inclusions could alter the salt concentration but this generally occurs where a fracture plane intercepts older inclusions (Roedder, 1984) and evidence for this was not observed.

Beaudoin et al. (1992b) showed that deposits in Kokanee Range can be divided into four groups on the basis of Pb isotope ratios in galena: deposits are plotted with different symbols according to their Pb isotope group in Figure 4-12. Pb isotope systematics in galena indicate that upper crustal Pb from local country rocks was leached by different hydrothermal fluids than those that transported Pb from lower crustal and mantle sources (Beaudoin et al., 1992b). The reservoirs of S and C are also distinct and the assumption can be made that S was leached by the same fluids that leached upper crustal Pb whereas C was carried by the fluids associated with deep-seated Pb sources. The Pb in deposits of the Sandon group was shown to be a mixture between a lower crustal and an upper crustal source, whereas Pb in deposits of the Kokanee group was leached from the upper crustal source only. Zoning of Pb isotope ratios in the Sandon group was interpreted to result from introduction, along fault zones, of a hydrothermal fluid carrying lower crustal Pb with high $^{208}Pb/^{206}Pb$ ratios, and mixing of this Pb with that leached from country rocks having a low $^{208}Pb/^{206}Pb$ as the fluid migrated away from the fault zones (Beaudoin et al., 1992b). Figure 4-12 show that deposits of the Kokanee group generally do not

display evidence of mixing with the deep-seated hydrothermal fluid. One exception is the Rambler deposit that has two populations of inclusions with different salinities but both are within the mixing trend between the deep-seated and upper crustal fluids (Fig. 4-12). This conflict can be explained by mass balance considerations if the deep-seated fluid, on its way to the Rambler, leached enough country rocks Pb to lose its Pb isotopic signature or if much of its original lower crustal Pb was precipitated early but the fluid remained saturated relative to galena by leaching Pb from country rocks.

A schematic mixing trend between the deep-seated and meteoric water is shown on Figure 4-12. This trend is poorly defined, in part because mixing occurred late in the evolution of the hydrothermal system when the fracture network was flooded by meteoric water, and perhaps by sampling bias. It is significant that all the deposits of the Ainsworth group plot along the mixing trend between the deep-seated and meteoric fluids. The Spokane vein of the Ainsworth group cut a 44 Ma lamprophyre dyke: this is the youngest relative age for a deposit (Beaudoin et al., 1992a). It is therefore reasonable to consider that deposits of Ainsworth group are younger than the other deposits, and were formed during, or after, dilution of the deep-seated hydrothermal fluid by meteoric water, possibly following uplift.

Oxygen water/rock exchange

$\delta^{18}O$ maps for vein siderite and quartz, and sedimentary rocks (Fig. 4-11) display patterns of variation, although less pronounced for the country rocks, that are broadly similar and open to the west. Increase in $\delta^{18}O$ of siderite and quartz outward from the central area results from increased exchange between the hydrothermal fluids and sedimentary rocks whereas a decrease in $\delta^{18}O$ for the sedimentary rocks indicates higher water/rock ratios (Fig. 4-11). The geometric

relation between the Slocan Lake Fault and the $\delta^{18}O$ zonation patterns could be interpreted to indicate that the Slocan Lake Fault cut the contour patterns or that the fault zone was a major conduit for hydrothermal fluids. The identical ages of deformation along the Slocan Lake Fault and of mineralisation (Beaudoin et al., 1992a) argues for a direct link between the Slocan Lake Fault and the patterns of $\delta^{18}O$ values for siderite, quartz, and country rocks. The apparent crosscutting relation may have resulted from the emanation of the hydrothermal fluids exclusively into the hangingwall rocks of the shallow dipping fault zone, or from late stage displacement along the fault zone. Indeed, the Slocan Lake Fault is a late stage brittle feature overprinting an earlier ductile fabrics (Carr et al., 1987). The "composite trend" on Figure 4-12 suggests that mixing between deep-seated and upper crustal hydrothermal fluids was accompanied by water/rock reaction and isotopic exchange. Similar patterns for Pb (Beaudoin et al., 1992b) and O isotope zoning, and mixing between deep-seated and upper crustal fluids, demonstrate control of the hydrologic regime at first order or regional scale by Slocan Lake Fault and at the second order or local scale by the Main Lode fault zone in channeling deep-seated hydrothermal fluids in the upper crust.

Deposits hosted in Nelson batholith display no pattern of $\delta^{18}O$ variation. The absence of large scale ^{18}O depletion in the granitic rocks must indicate channeled flow and lower water/rock ratios as suggested by narrow hydrothermal alteration halos.

CO_2 immiscibility and boiling

CO_2 immiscibility in the hydrothermal fluids is proved by the coexistence of inclusions rich in CO_2 phases with contrasting densities within a thin section. The high density CO_2 phase in type 2 inclusions (Fig. 4-3A) was trapped at higher pressures than the low density CO_2 phase

in type 3 inclusions (Fig. 4-4B). This suggest that depressurization produced a low density CO_2 vapour phase. Type 3 inclusions probably trapped variable, but small, amounts of that immiscible CO_2 vapour phase together with the aqueous fluid. Type 2 inclusions display large variations of vapour/liquid volume ratios which yield a large range of X_{CO2} (Fig. 4-4A). These observations also suggest that type 2 inclusions trapped an heterogeneous fluid comprised of an aqueous and an immiscible CO_2 phase. In some cases, types 1, 2, and 3 inclusions coexist in the same crystal (Table 4-1).

A small number of inclusions homogenised to vapour, suggesting that boiling occurred during trapping of all three types of inclusions. In general, the vapour/liquid volume ratios of type 1 and 3 inclusions are constant but extremly variable for type 2 inclusions which appear to be due to trapping various amounts of an immiscible CO_2 phase rather than boiling.

Boiling of hydrothermal fluids can be an efficient mechanism for mineral deposition (Drummond and Ohmoto, 1985). In the Kokanee Range, exsolution of a CO_2 phase appears to have been widespread whereas evidence for water boiling is more limited. Two main chemical effects may result from removing CO_2 from a hydrothermal fluid and both probably promoted precipitation of siderite: an increase of pH and a decrease of the partial pressure of CO_2. Lynch (1989a) showed that only a small percentage of boiling will drastically reduce X_{CO2} and readily result in deposition of siderite. Because siderite is a major gangue mineral in deposits clustered along the Main Lode, extensive CO_2 exsolution and minor boiling probably occurred in this fault zone.

Summary: Crustal Hydrology during Extension

The isotopic and fluid inclusion data permit the identification of distinct H, C, O, S, and

Pb reservoirs which are located in separate lithospheric segments: the upper crust, the lower crust, and the mantle (Fig. 4-13). The principal reservoir for S and part of the Pb is in the local upper crustal country rocks. The dominant reservoir for C is most likely the upper mantle which has also been shown to be a Pb reservoir (Beaudoin et al., 1992b). The salinity-$\delta^{18}O_{fluid}$ data (Fig. 4-12) require three contrasting fluids: 1) a high salinity, deep-seated fluid with crust-buffered $\delta^{18}O$; 2) an upper crustal fluid of low salinity also with crust-buffered $\delta^{18}O$; 3) a slightly evolved meteoric water derived fluid characterised by low salinity, $\delta^{18}O_{fluid}$, and δD_{fluid}.

The different fluids migrated through, and exchanged H, C, O, S, and Pb with the rocks in the various reservoirs. This complex process of exchange, mixing, and precipitation involving various fluids and rock reservoirs, and the relative mass balance involved are schematically illustrated on Figure 4-13. The upper crustal fluids which had exchanged O and leached S and Pb from the local upper crustal rocks formed the Kokanee group of deposits; they contain no Pb derived from the lower crust or mantle (Beaudoin et al., 1992b). Because deposits of the Kokanee group typically do not contain siderite the contribution of deep-seated C as CO_2 cannot be ascertained for these deposits.

The Sandon, Ainsworth, and Bluebell groups of deposits all display contributions of Pb from the lower crust and mantle (Beaudoin et al., 1992b) and therefore are interpreted to have involved the deep-seated fluid illustrated on Figures 4-12 and 4-13. Deposits of these three groups all have identical mantle C isotopic signatures. Salinity-$\delta^{18}O$ data (Fig. 4-12) for Sandon and Ainsworth groups of deposits suggest mixing of the deep-seated with the upper crustal and the meteoric fluids. Evidence for dilution of an early saline fluid by dilute, late stage fluids in the Bluebell deposit was documented by Ohmoto and Rye (1970). The association of the high

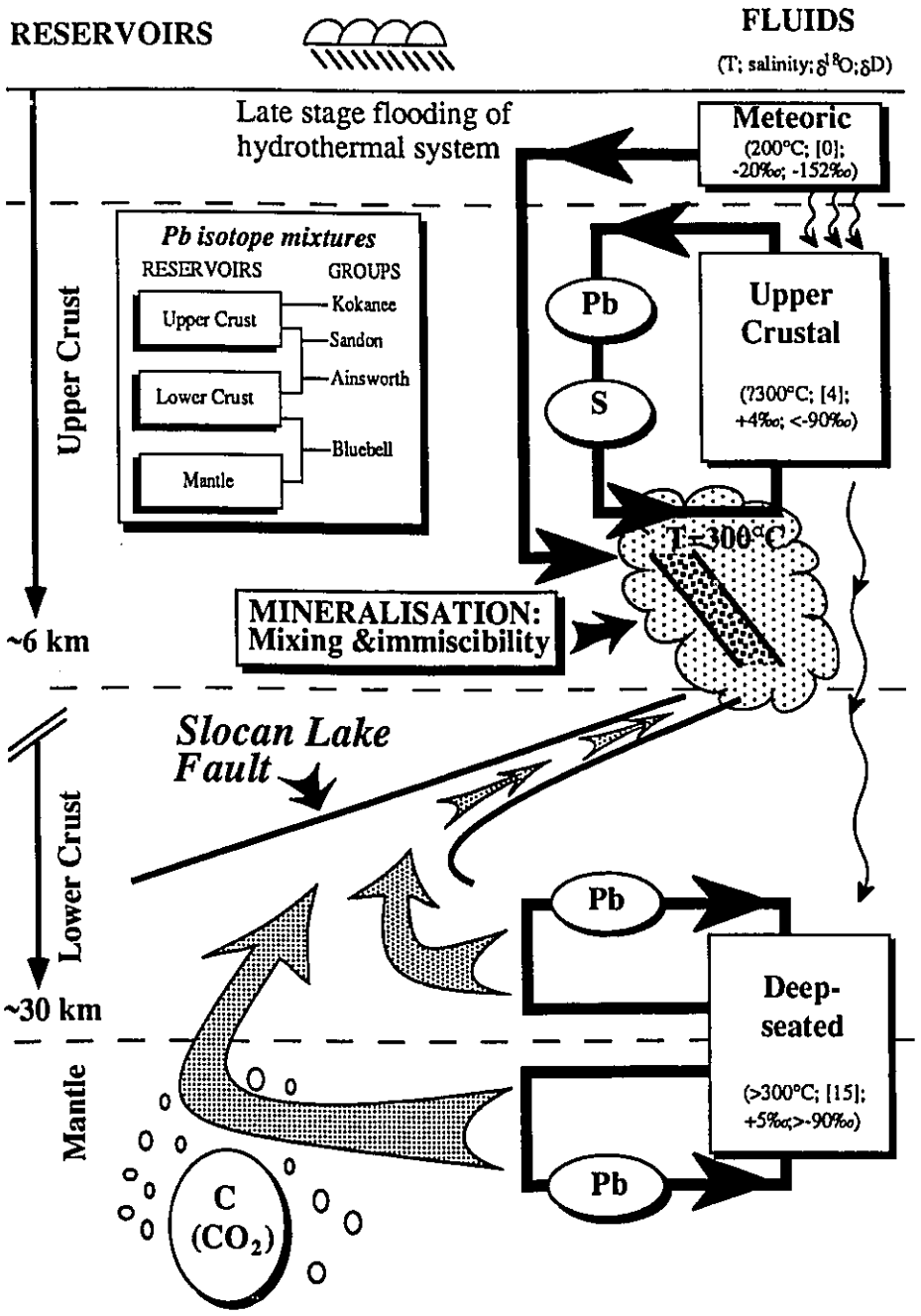

Figure 4-13. Summary diagram displaying the location of the C, S, and Pb reservoirs and the fluids that migrated through them. Slocan Lake Fault provided the channelway to connect the deep-seated fluids with the upper crust.. Thick lines and arrows display the associations between the hydrothermal fluids and the sources of Pb and S. C is derived by mantle CO_2 degassing. Mineralisation occurred by mixing and immiscibility at an estimated depth of 6 km in a thermally equilibrated aquifer. Meteoric water flooded the mineralised fracture network at a late stage of hydrothermal activity. The Pb isotope mixtures in galenas are shown in inset (modified from Beaudoin et al., 1992b).

salinity, deep-seated fluid with the lower crustal Pb, mantle Pb, and C reservoirs is therefore well established (Fig. 4-13).

Influx of meteoric water during the late stages of mineralisation was widespread (Fig. 4-13). The Ainsworth group veins were deposited by a mixed meteoric and the deep-seated fluid (Fig. 4-12). The fact that these deposits have probably younger ages than the others (Beaudoin et al., 1992a) suggests that meteoric fluids progressively displaced the crustal fluids.

The migration of fluids, equilibrated with lower crustal and mantle rocks, into the upper crust has been mapped using O and Pb isotopes. Both isotopic tracers show the dominant influence of crustal faults in connecting deep-seated reservoirs with the upper crust. A first order and essential control was provided by the Slocan Lake Fault which channeled fluids towards higher crustal levels. Smaller faults which host the veins, such as the Main Lode fault zone, provided a second order control on the detailed O (Fig. 4-11) and Pb (Beaudoin et al., 1992b) zonation patterns.

The deposition of siderite early and nearby the Main Lode fault zone was probably controlled by CO_2 immiscibility. The dominant fluid process occurring during mineralisation, however, was mixing and dilution (Fig. 4-12) and it is likely that mixing and dilution played a significant role in precipitating the hydrothermal minerals (Fig. 4-13). No temperature zonation within the hydrothermal system can be demonstrated at the scale of the Kokanee Range. This suggests that fluids and their aquifers were thermally equilibrated and that the upper crustal and deep-seated fluids had similar temperatures by the time they reached the level of mineralisation, which is estimated to be about 6 km below paleosurface.

Crustal migration of the hydrothermal fluids occurred during early stages of Paleocene-

Eocene crustal extension as shown by similar ages (58-59 Ma), for mineralisation (Beaudoin et al., 1992a) and extension (Parrish et al., 1988). The earliest ages for extensional deformation in the Kokanee Range are those for syndeformational cooling of the Ladybird orthogneiss within a ductile shear zone, precursor, at deeper levels, of the Slocan Lake Fault. Partial melting of the source of the Ladybird magma therefore occurred before Late Paleocene. It is likely that melting was triggered as a result of, and early in, crustal extension. Heating and uplift probably provided the driving force for hydrothermal fluid flow and fostered mineralisation processes relatively early in the extensional history. Tilting of crustal-scale aquifers of low permeability as little as 5º is sufficient to induce fluid migration (Criss and Hofmeister, 1991). Indeed, Bardoux and Irving (1989) suggested as much as 37º of tilting for Eocene intrusions near the Slocan Lake Fault, based on paleomagnetic data. Therefore, tilting of lithosphere segments during extension is an attractive driving force for hydrothermal fluid flow in the Kokanee Range.

The isotopic and fluid inclusion data identify several reservoirs for H, C, O, S along the paths of several hydrothermal fluids. Mineralisation is genetically related to crustal extension and uplift which opened fluid flow paths and provided the energy for fluid migration. Different isotopic tracers identify single or varied multiple sources. Sources which are identified for one isotopic tracer cannot, therefore, be identified as sources for other elements, such as gold, without isotopic signatures, even if they were present at the same time in the same environment.

CHAPTER 5

A Descriptive Model for Silver-Lead-Zinc Veins

Introduction

A widely held concept in metallogeny is that silver-lead-zinc veins, which are commonly spatially associated with felsic intrusions, typically of batholithic dimensions, are also genetically related to them (Lindgren, 1933; Bateman, 1959; Routhier, 1963, Guilbert and Park, 1986). Such intrusions may be found in proximity to, or within, the mineralised area; otherwise, buried plutons have been inferred. A typical case is the Freiberg district, Germany, in which a granitic intrusion occurs at the margin of the district but has not been linked to mineralisation, whereas considerable efforts have been devoted to find a buried pluton inferred from mineralogical zoning studies and gravimetric modelling (Baumann, 1965). For example, in 1955, four 1800 m deep holes were drilled in search of the hypothetic, ore-producing Freiberg pluton (Baumann, 1965). Laznicka (1985) likely referred to that hypothetic intrusion when he mentioned a "cryptobatholith" in the district.

My dissatisfaction with the various theories of a genetic link between the intrusion of granitic magmas and silver-lead-zinc veins arose from this detailed regional geological and geochemical study of the deposits of the Kokanee Range. The Kokanee Range includes the Slocan camp, which has been frequently referred to in economic geology textbooks and has been widely regarded as genetically related to the Middle Jurassic Nelson batholith. Dating of vein and

hydrothermal alteration muscovite, however, has demonstrated that mineralisation was Eocene, 110 Ma younger than the age of cooling of the batholith (Beaudoin et al., 1992a). The sources of H, C, O, S, and Pb are varied and the fluid flow paths, rather than originating from the Nelson batholith, are controlled by a transcrustal fault zone formed as a result of crustal extension triggered by the collapse of the Cordilleran orogen (Beaudoin et al., 1992b; 1992c). Research in the Kokanee Range, combined with recent geochronological and geochemical data for the Keno Hill, Coeur d'Alène, Harz Mountains, Freiberg, and Příbram districts and a review of the literature, provide the basic information described and discussed in this chapter.

Previous Classifications of Veins

Vein deposits were the subject of the first attempts to classify mineral deposits. Early classifications were based mainly on the shape of the deposit such as vein, bed, dissemination, etc. Later, for example in Beck and Weed (1909), a first order division was made by determining if the deposits were primary or secondary, i.e., formed from mechanical or chemical destruction and transposition of primary deposits. Primary deposits were subdivided according to the age relations between mineralisation and the formation of the country rock: syngenetic or epigenetic. Epigenetic deposits were further subdivided by shape into veins and others. Finally, the veins were classified according to their metal association: hence, Beck and Weed (1909) had a class of silver-lead veins which they subdivided according to dominant mineral assemblages.

This general scheme of classification is still widely used although the lower order subdivisions have been frequently reorganised and renamed, and deposits within these subdivisions have changed according to new geological observations or current theories. Lindgren (1933) subdivided epigenetic hydrothermal deposits into categories (hypo-, meso-, epithermal)

based on pressure and temperature of formation and considered that these deposits had a magmatic affiliation. Silver-lead veins were considered to be part of the mesothermal category and were further subdivided into different mineral assemblages: Lindgren (1933) recognised that silver-lead veins included "*many types between which so many transitions exist that a classification is difficult*" (p. 565). Routhier (1963) placed some of the silver-lead-zinc veins discussed in this paper into a "péri-plutonique" category commonly associated with granitic or monzonitic plutons and regarded them as grading outward from a pyrometasomatic zone. Laznicka (1985) made a class of "Pb-Zn (Ag) deposits in granite aureoles" that included the deposits discussed in this paper as well as other deposits considered to be different. Laznicka (1985, p. 1236) stated that "*when a granite hosts orebodies, it is an old granite acting as a passive host, genetically unrelated to the mineralization*". Guilbert and Park (1986), on the other hand, created a large class of "Cordilleran vein type deposits" which were formed by ascending hydrothermal fluids of magmatic or meteoric origin, but which they considered to be related to adjacent igneous activity. They held that this class could be recognised world-wide but, of the vein districts discussed in this paper, only the Coeur d'Alène district was given as an example. Graybeal et al. (1986) classified the silver-lead-zinc veins discussed in this paper as "Paleozoic and Mesozoic base metal veins", hosted in sedimentary, plutonic, or volcanic rocks, and related to coarse grained intrusions. Graybeal et al. (1986) considered that these veins were formed at relatively high temperature and pressure in relation to the common proximity of the coarse grained intrusions which were believed to supply heat and possibly some ore constituents. They considered that the Coeur d'Alène district was unique and formed a class of its own.

Previous classifications of veins generally resulted in the placing of deposits with

enormous ranges of geological characteristics within each class. Veins are small and represent local geochemical anomalies which have potential to display much variability. It is suggested here that selection of subsets comprising classical vein districts bearing many similar geological parameters will permit a better classification and, ultimately, understanding of the geological processes responsible for the formation of each class.

Definition of Silver-Lead-Zinc Veins

Silver-lead-zinc veins are defined according to their form and their dominant economic metal content. Deposits of this type form tabular to lenticular orebodies, called veins or lodes. The order of the metals is arbitrary as market values fluctuate. Silver is put first to distinguish them from veins in which it can be a minor constituent, but in which it has never been a major economic commodity. Lead is before zinc because, in general, lead production has been greater than that of zinc. This is in part an economic artifact from historic times when zinc was not a commodity sought after and actually brought penalties from smelters when it occurred in the lead ore concentrate. There are, however, many accounts of reclaiming old dumps and refilled stopes rich in zinc and the bias in zinc production is therefore difficult to estimate precisely.

The above definition is essentially descriptive and makes no genetic inference. It distinguishes from veins with other metal associations, and from veins with additional important metals, such as gold. The vein morphology also permits distinction from mantos, skarns, etc., although the same metal assemblages can be present. Replacement of limestone is present in some silver-lead-zinc vein districts, however. Although it is possible that some districts, such as Tintic, that are mainly or solely characterised by massive sulphide bodies replacing limestones are of the same type as those containing silver-lead-zinc veins, this discussion is limited to

dominantly vein districts. Indeed, after defining and characterising a class of silver-lead-zinc veins, further studies may prove that there are justifications for enlarging the definition of that class of deposits.

Summary of Selected Geological Features

In order to construct a descriptive model, six district were selected as classical examples of silver-lead-zinc veins. These districts are the Kokanee Range and Keno Hill, Canada; Coeur d'Alène, U.S.A.; the Harz Mountains and Freiberg, F.R.G.; and Příbram, Czechoslovakia (Fig. 5-1). In these districts, the following geological features were selected for comparison (Tables 5-1 to 5-3).

Mineralogy

Silver-lead-zinc veins consist of galena and sphalerite in a gangue of siderite, quartz, dolomite, or calcite. Galena and sphalerite are commonly associated with minor pyrite, chalcopyrite, and a diverse and complex suite of sulphosalt minerals, always including tetrahedrite, and silver minerals (Table 5-1). Siderite and/or quartz are dominant gangue species. Calcite is an important gangue in the Harz Mountains, whereas dolomite and ankerite are common in the Coeur d'Alène district. In the Kokanee Range and Keno Hill districts, calcite and/or dolomite are typically, but not exclusively, late stage minerals associated with flooding of the hydrothermal system by meteoric water (Beaudoin et al., 1992c; Lynch, 1989a). Silver-lead-zinc veins have long been the subject of mineralogical zoning studies (Park, 1955; Dahlgrün, 1950; Baumann, 1965). In some cases, the mineral zones were formed by multiple hydrothermal events or a telescoped single event (Kutina, 1963) rather than by regular zoning about a single point. In the Keno Hill district, Lynch (1989b) argued that there is a mineralogical zonation that

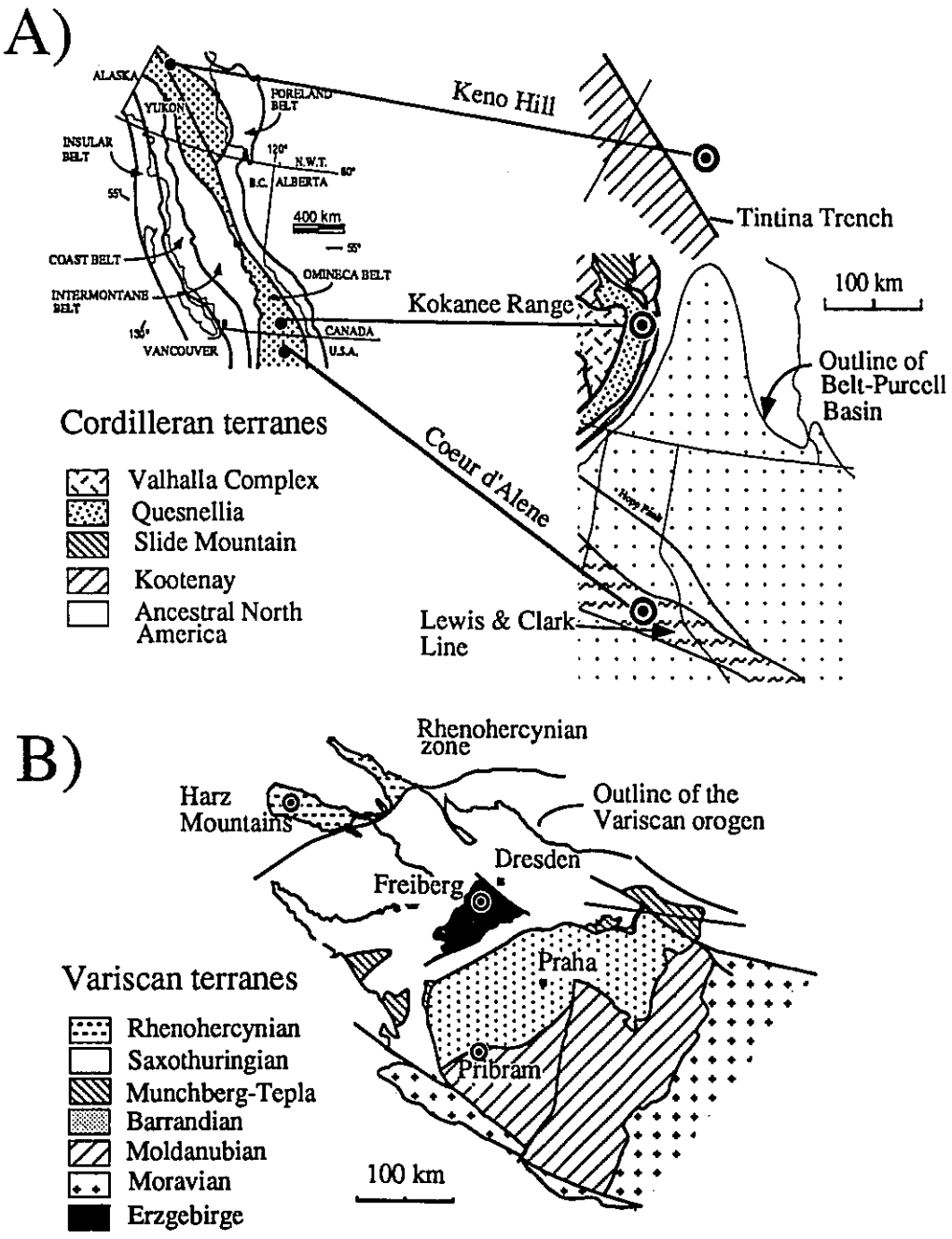

Figure 5-1. Location map of the six classical silver-lead-zinc vein districts, selected for establishing the descriptive model, in relation to the terrane assemblage in: A) the Cordilleran Orogen of North America; B) the Variscan Orogen of Central Europe.

closely matches the classical zoning models of Spurr (1912) and Emmons (1924).

Metal ratios

The metal ratios for silver-lead-zinc vein districts are compared with those from other types of Ag-Pb-Zn deposits (Fig. 5-2). The former are characterised by Pb/(Pb+Zn) ratios ranging from 0.51 to 0.72 and (Ag*100)/((Ag*100)+Pb) ratios ranging from 0.22 to 0.63 (Table 5-1). In ternary Ag-Pb-Zn space (Fig. 5-2A), lead-zinc skarns have high Zn ratios whereas porphyry-Cu and volcanic hosted epithermal vein districts have Ag ratios similar to, or higher than, those of silver-lead-zinc vein districts. Carbonate replacement and manto deposits plot in a large field overlapping that of silver-lead-zinc vein districts. In Mexico, Megaw et al. (1988) demonstrated, for carbonate replacement and mantos, a gradual change from high zinc ratio skarn ores to subequal Pb-Zn ratio sulphide chimneys and mantos, the latter being further characterised by higher Ag ratios. In ternary Ag-Pb-Au space (Fig. 5-2B), carbonate replacement and manto deposits are distinctly enriched in Au relative to silver-lead-zinc vein districts, although Au data are available from only two silver-lead-zinc vein districts. There is no evidence that significant amounts of Au are present in those districts that lack Au production statistics. This is particularly true for the Keno Hill district which has a modern mining history.

Hostrocks and associated intrusions

Silver-lead-zinc veins have been genetically related to the intrusion of granitic plutons or batholiths. Little attention, however, has been directed to the sedimentary rocks which host most veins. These are typically thick and monotonous sequences dominated by fine to medium grained clastic rocks, and minor carbonate, mafic volcanic and tuff units (Table 5-2). Another common feature is that most of these sedimentary rocks have been metamorphosed to the greenschist

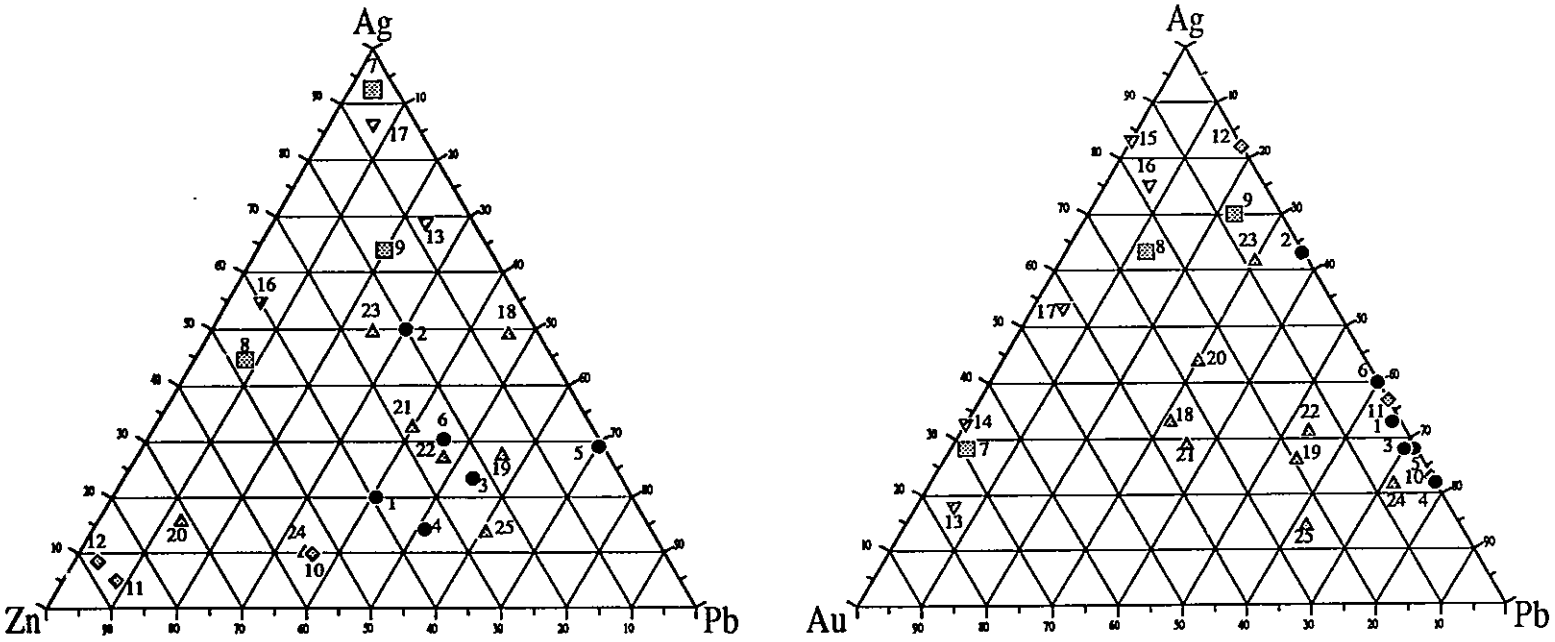

● Ag-Pb-Zn vein districts

1. Kokanee Range
2. Keno Hill
3. Coeur d'Alene
4. Harz Mountains
5. Freiberg
6. Pribram

▩ Porphyry-Cu

7. Bisbee
8. Butte
9. Morococha

◈ Pb-Zn skarn

10. Typical Pb-Zn skarn
11. Nakatatsu
12. Hanover

▽ Volcanic hosted epithermal vein districts

13. Comstock
14. Tayolita
15. Creede
16. Arcata
17. Orcopampa

△ Carbonate replacement and mantos

18. Main Tintic
19. East Tintic
20. Gilman
21. Leadville
22. Park City
23. Fresnillo
24. San Francisco del Oro
25. Bingham (non-porphyry)

Figure 5-2. Comparison of the metal ratios for silver-lead-zinc vein districts with those of other types of deposits mined for Ag, Pb, or Zn. A) Ag-Pb-Zn ternary space. B) Ag-Pb-Au ternary space. Values for typical "Pb-Zn skarn" from Einaudi and Burt (1982).

facies (Table 5-2). Freiberg is an exception because it occurs solely in gneiss.

The sedimentary basins containing the host sequences are part of Pb-Zn metallogenic provinces that typically contain large sediment hosted, commonly sedimentary exhalative (SEDEX), massive sulphide deposits. The Selwyn basin hosts both the Keno Hill district and a suite of SEDEX deposits that include the Tom, Jason, and Howards Pass. The Belt-Purcell basin contains the Coeur d'Alène district and the Sullivan deposit. In fact, both are near the base of the Belt-Purcell stratigraphic sequence. The Harz Mountains and Příbram districts are in sedimentary basins containing the famous Rammelsberg and Meggen deposits in Germany and the Zlaté Hory and Horní Benešov deposits in Czechoslovakia. In the Kokanee Range, the carbonate rocks of the ancient North America passive margin contain several small SEDEX deposits, such as the Jersey and the Reeves-Macdonald.

The characteristics of the granitic intrusions spatially associated with silver-lead-zinc veins are briefly reviewed below. In the Kokanee Range, the Nelson batholith is a large, syn to late orogenic, dioritic to granitic complex dominated by a hornblende-biotite granodiorite phase that commonly contains megacrystic potassium feldspar. The Nelson batholith displays a calc-alkaline differentiation trend and was intruded during the Middle Jurassic (165-170 Ma) (Ghosh, 1986; Carr et al., 1987). A significant component of the batholith was derived from a mantle source (Ghosh, 1986). In the Keno Hill district, the Mayo Lake pluton comprises a core of megacrystic potassium feldspar granodiorite and a marginal granite phase. The Mayo Lake pluton intruded the Mayo Lake shear zone but is not deformed (Lynch, 1989a) and postdates regional metamorphism (Boyle, 1965). A bimodal suite of extension-related, alkaline, A-type, and compression-related, S-type plutons (Anderson, 1987) intruded the Selwyn basin during the

Table 1. Geological parameters of Ag-Pb-Zn veins districts

District	Metal production (10^3t) and ratios						
	Ag	Pb	Zn	Au	Pb/(Pb+Zn)	(Ag*100)/ [(Ag*100)+Pb]	
Kokanee, Canada	2.6	530	510	0.001	0.51	0.33	Galena, *chalcop* *tetrahe* *silver*, *bourno*
Keno Hill, Canada	6.4	380	250	-	0.60	0.63	Galena, *chalcop* *tetrahe* *polybas*
Coeur d'Alène, U.S.A.	29.1	6970	2770	0.016	0.72	0.29	Galena *marcas* *jameso* *polyba* *bourno* *magnet*
Harz Mountains, F.R.G.	>5	>1820	>1220	-	0.60	0.22	Galena *chalcop*
Freiberg, F.R.G.	>7 0.018 (1901)	>1700 2.1 (1901)	-	-	-	0.29 0.46 (1901)	Galena *arseno* *tetrahe* *silver*
Příbram, Czechoslovakia	>3.5 0.039 (1898)	>520 4.8 (1898)	>260	-	0.67	0.40 0.45 (1898)	Galena *chalcop* *silver*,

1. L: length; D: depth; T: thickness. References - Kokanee Range: Beaudoin et al. (1991c), Cairnes (1934); Keno Hi
Leach et al., (1988); Harz Mountains: Beck and Weed (1909), Walther (1986), Möller et al. (1984); Freiberg: Bau

Table 1. Geological parameters of Ag-Pb-Zn veins districts

District	Metal production (10^3t) and ratios						Miner
	Ag	Pb	Zn	Au	Pb/(Pb+Zn)	(Ag*100)/ [(Ag*100)+Pb]	Sulphides
Kokanee, Canada	2.6	530	510	0.001	0.51	0.33	Galena, sphalerite, *pyrite, chalcopyrite, arsenopyrite, tetrahedrite, pyrargyrite, silver, jamesonite, boulang bournonite, stephanite, sc*
Keno Hill, Canada	6.4	380	250	-	0.60	0.63	Galena, sphalerite, *pyrite, chalcopyrite, arsenopyrite, tetrahedrite, pyrargyrite, polybasite, stephanite, silv*
Coeur d'Alène, U.S.A.	29.1	6970	2770	0.016	0.72	0.29	Galena, sphalerite, *pyrite, marcasite, chalcopyrite, a jamesonite, tetrahedrite, p polybasite, silver, boulang bournonite, gold, meneghi magnetite, hematite, urani*
Harz Mountains, F.R.G.	>5	>1820	>1220	-	0.60	0.22	Galena, sphalerite, *pyrite, chalcopyrite, tetrahedrite,*
Freiberg, F.R.G.	>7 0.018 (1901)	>1700 2.1 (1901)	-	-	-	0.29 0.46 (1901)	Galena, sphalerite, *pyrite, arsenopyrite, chalcopyrite, tetrahedrite, pyrargyrite, silver*
Příbram, Czechoslovakia	>3.5 0.039 (1898)	>520 4.8 (1898)	>260	-	0.67	0.40 0.45 (1898)	Galena, sphalerite, *pyrite, chalcopyrite, tetrahedrite, silver, stephanite, stibnite*

1. L: length; D: depth; T: thickness. References - Kokanee Range: Beaudoin et al. (1991c), Cairnes (1934); Keno Hill: Boyle (1965), Ly
Leach et al., (1988); Harz Mountains: Beck and Weed (1909), Walther (1986), Möller et al. (1984); Freiberg: Baumann (1965), Beck

	Mineralogy (*minor in italics*)		Alteration	Maximum size of vein structure[1]	Depth of mineralisation
	Sulphides	Gangue			
	Galena, sphalerite, *pyrite, pyrrhotite, chalcopyrite, arsenopyrite, tetrahedrite, pyrargyrite, acanthite, silver, jamesonite, boulangerite, bournonite, stephanite, scheelite*	Siderite, quartz, dolomite, calcite, *barite, fluorite, muscovite*	Local phyllic: sericitisation, silicification, pyritisation	L: 6 km D: 600 m T: 45 m	≈1.7 kbar ≈6 km
	Galena, sphalerite, *pyrite, pyrrhotite, chalcopyrite, arsenopyrite, jamesonite, tetrahedrite, pyrargyrite, acanthite, polybasite, stephanite, silver*	Siderite, quartz, calcite, *barite*	Local pyritisation, silicification	L: 5 km D: 340 m T: 30 m	≈1.6 kbar ≈6 km
	Galena, sphalerite, *pyrite, pyrrhotite, marcasite, chalcopyrite, arsenopyrite, jamesonite, tetrahedrite, pyrargyrite, polybasite, silver, boulangerite, bournonite, gold, meneghinite, magnetite, hematite, uraninite*	Siderite, quartz, dolomite, ankerite, *barite, adularia, tourmaline, muscovite, chlorite, gahnite*	Widespread bleaching (due to loss of Fe)	L: 3 km D: 2300 m T: 3 m	1-3 kbar 3-10 km
	Galena, sphalerite, *pyrite, marcasite, chalcopyrite, tetrahedrite, bournonite*	Quartz, calcite, *barite, siderite, dolomite, sericite, adularia*	Local sericitisation and silicification, vein clay-slate (gangthonscheifer)	L: 15 km D: 1000 m T: 80 m	?
	Galena, sphalerite, *pyrite, arsenopyrite, chalcopyrite, tetrahedrite, pyrargyrite, acanthite, silver*	Quartz, *siderite, calcite, barite, fluorite*	Local sericitisation, disseminated sulphides	L: 7 km D: 650 m T: 2 m	?
	Galena, sphalerite, *pyrite, chalcopyrite, tetrahedrite, pyrargyrite, silver, stephanite, stibnite*	Siderite, quartz, calcite	?	L: D: 1500 m T: 8 m	? <2 km

4); Keno Hill: Boyle (1965), Lynch (1989b), Watson (1986); Coeur d'Alène: Bennett and Venkatakrishnan (1982), Fryklund (1964), eiberg: Baumann (1965), Beck and Weed (1909), Laznicka (1985); Příbram: Beck and Weed (1909), Žák and Dobeš (1991).

Table 2. Regional geological setting of Ag-Pb-Zn vein districts

District	Tectonic setting	Hostrocks (*italics host ore*)	
		Volcanic & Sedimentary	Plutonic
Kokanee, Canada	Crustal extension; Valhalla metamorphic core complex; hangingwall of a transcrustal low angle Slocan Lake Fault	*Cambrian to Upper Triassic shale, sandstone, greywacke, limestone,* tholeiitic basalts	*Nelson batholith (165-170 Ma): granodioritic, K-spar megacrystic, calc-alkaline; kersantite (40-52 Ma)*
Keno Hill, Canada	Mayo Lake Shear zone: transcurrent dextral fault overprinting a regional thrust	*Mississippian Keno Hill Quartzite, upper (?) and Lower Jurassic schist (graphitic, muscovite and chlorite)*	Mayo Lake pluton (≈81 Ma): granite to granodiorite; lamprophyre
Coeur d'Alène, U.S.A.	Lewis and Clark line: major fault zone active from Middle Proterozoic to Holocene	*Proterozoic Belt Supergroup (1.85 to 0.85 Ga): argillite, slate, quartzite*	Gem stocks (≈100 Ma): zoned monzonite to syenite; lamprophyre (Eocene)
Harz Mountains, F.R.G.	Set of parallel dextral strike-slip faults with normal component	*Siluro-Carboniferous greywackes and shales*	Broken-Oker granite, and Harzburg layered, tholeiitic intrusion (292±9 Ma); diabase; kersantite
Freiberg, F.R.G.	Summit of a gneiss dome, possibly in footwall of a low angle normal fault bounding a metamorphic core complex	Not present	Neiderbobritzsch (317±4 Ma): monzogranite; *dykes: mica diorite, mica syenite, quartz porphyry, kersantite, minette*
Příbram, Czechoslovakia	Terrane boundary: the Central Bohemian Shear zone, mineralisation in a secondary fault, the Lettenkluft	*Precambrian to Cambrian greywacke and shales, spilite, keratophyres and tufs*	*Central Bohemian Pluton (331±4 M granodiorite; diabase dykes*

1- Positive numbers indicate mineralisation is older than intrusion whereas negative numbers are for mineralisation younger than intrusion. References Bennett and Venkatakrishnan (1982), Leach et al., (1988); Harz Mountains: Beck and Weed (1909), Hannak (1981), Mertz et al., (1989), Posepny (19(and Förster (1990); Příbram: Matte et al., (1990), van Breemen et al., (1982), Žák and Dobeš (1991).

Hostrocks (*italics host ore*)			Age of mineralisation	Difference in age between mineralisation and granite intrusion[1]
	Plutonic	Metamorphic rocks or grade		
,	*Nelson batholith (165-170 Ma): granodioritic, K-spar megacrystic, calc-alkaline; kersantite (40-52 Ma)*	*Greenschist to sillimanite-kyanite,* Valhalla metamorphic core complex (Eocene)	≈58-59 to <44 Ma	≈-110 Ma
, *ist*)	Mayo Lake pluton (≈81 Ma): granite to granodiorite; lamprophyre	*Greenschist*	? (see text)	? (see text)
;	Gem stocks (≈100 Ma): zoned monzonite to syenite; lamprophyre (Eocene)	*Greenschist (>0.85 Ga)*	>870 Ma	≈+770 Ma
	Broken-Oker granite, and Harzburg layered, tholeiitic intrusion (292±9 Ma); diabase; kersantite	*Greenschist*; Ecker gneiss	≈123 Ma	≈-170 Ma
	Neiderbobritzsch (317±4 Ma): monzogranite; *dykes: mica diorite, mica syenite, quartz porphyry, kersantite, minette*	*Freiberg gneiss dome (Freiberger gneiskuppel): Precambrian biotite gneiss, mica schist, phyllite*	270-290 Ma	? (see text)
	Central Bohemian Pluton (331±4 Ma): granodiorite; diabase dykes	*Greenschist*	<330 Ma >260 Ma	0 to -70 Ma

alisation younger than intrusion. References: Kokanee Range: Beaudoin et al. (1991a) ; Keno Hill: Lynch (1989a); Coeur d'Alène: k (1981), Mertz et al., (1989), Posepny (1902); Freiberg: Baumann (1965), Gerstenberger (1989), Matte et al., (1990), Tischendorf

Cretaceous (81-109 Ma; Sinclair et al., 1980). The Mayo Lake pluton is affiliated with the S-type plutons (Lynch, 1989a).

In the Coeur d'Alène district, the Gem stocks are small, zoned monzonitic to syenitic bodies intruded during the Late Cretaceous (100 Ma; Schalck, 1989). The monzonite locally contains megacrystic potassium feldspar. In the Harz Mountains, a post-orogenic suite of three dioritic to granitic plutons (Brocken, Oker, Ramberg) and the Harzburg gabbronorite intruded during the Late Carboniferous (292±9 Ma; Schoell, 1970; Mertz et al., 1989). The Harzburg gabbronorite, interpreted to be a layered, tholeiitic intrusion (Vinx, 1982), and the Brocken pluton are spatially separated by the Ecker gneiss (Möller et al., 1984) whose origin is unknown. In the Příbram district, the Central Bohemian pluton (331±4; van Breemen et al., 1982) was intruded along the boundary between the Barrandian and Moldanubian terranes and sealed the Central Bohemian shear zone (Žák and Dobeš, 1991). The Central Bohemian pluton is a large intrusive complex ranging in composition from gabbro and diorite to, and dominated by, a biotite granodiorite that locally contains megacrystic potassium feldspar. An initial $^{87}Sr/^{86}Sr$ ratio of 0.7089 was interpreted by van Breemen et al. (1982) to indicate either a mixed mantle-upper crustal or lower crustal origin for the magma of the Central Bohemian pluton. The Erzgebirge forms a domal structure dominated by biotite gneisses that are cut by a granitic complex that was intruded in less than 4 Ma (Gerstenberger, 1989) and comprised of an older, monzogranitic, collision-related, S-type suite possibly originating from a lower crustal source, and a younger peraluminous, syenogranitic suite with a geochemical affinity to within plate granites (Tischendorf and Förster, 1990). Although it is clear that these plutons intruded the gneiss, it is not stated whether or not they are deformed. The Neiderbobritzsch pluton, which is adjacent to

the Freiberg district, is a member of the older intrusive complex and has a Rb/Sr age of 317±4 Ma and an initial $^{87}Sr/^{86}Sr$ ratio of 0.7068 (Gerstenberger, 1989).

Alteration

Hydrothermal alteration associated with silver-lead-zinc veins has commonly not been the subject of detailed petrological and geochemical studies. The earliest geochemical work was intended to prove or disprove the lateral secretion theory in the Freiberg and Příbram districts (Beck and Weed, 1909). Typically, hydrothermal alteration is restricted to the vicinity of the veins and extends as much as a few metres into the wallrocks. In the Coeur d'Alène district, however, large zones of hydrothermal bleaching, as much as a few kilometres wide, are typical (Fryklund, 1964).

The alteration is typically phyllic, characterised by sericitisation, silicification, and pyritisation of the wallrocks (Table 5-1). Bleaching in the Coeur d'Alène district resulted from removal of iron oxides but apparently not from addition of sericite (Fryklund, 1964).

Age of mineralisation

The age of mineralisation in a silver-lead-zinc vein district is typically a complex problem to address because of the common lack of datable ore stage material, although, in some areas, age can be constrained using crosscutting relations with ages for dated intrusive or metamorphic events. In the Příbram district, Žák and Dobeš (1991) noted that mineralisation was younger than the Variscan granitic intrusions but older than uranium veins which have U-Pb uraninite ages ranging from 260 to 275 Ma. Mineralisation is therefore younger than the Central Bohemian pluton by as much as 70 Ma (Table 5-1). Routhier (1980) noted a 100 Ma age difference between granite intrusion and mineralisation in the Příbram district and concluded that the age difference

precluded any genetic link between intrusion and mineralisation, even if only as a heat source. Žák and Dobeš (1991), however, noted that the marginal facies of the Central Bohemian pluton are similar to high heat production granite and may therefore have maintained a higher geothermal gradient for a longer period of time at the margins of the pluton.

It the Freiberg district, veins cut the Freiberg gneiss dome which is interpreted to result from extensional collapse of the Variscan orogen (Matte et al., 1990). The gneiss dome has been intruded by the 317 Ma Neiderbobritzsch pluton of the "older intrusive complex" (Gerstenberger, 1989). There are, however, no crosscutting relations between the veins and the adjacent pluton apparent on maps. Tischendorf and Förster (1990) estimated that Freiberg mineralisation occurred between 270 and 290 Ma and considered that the Freiberg veins were genetically related to the "younger intrusive complex" which they considered to be significantly younger than the "older intrusive complex". Gerstenberger (1989), however, suggested that both granitic suites were intruded in less than 4 Ma and that the ages for the "younger intrusive complex" were decreased by late Rb autometasomatism. The data therefore suggest that hydrothermal mineralisation in the Freiberg district is 30 to 50 Ma younger than the adjacent Neiderbobritzsch pluton.

For the other districts, various stages of mineralisation have been dated with variable accuracy. In the Kokanee Range, K-Ar and step heating $^{40}Ar/^{39}Ar$ data for vein and hydrothermal alteration muscovite yield identical 58-59 Ma ages; the youngest age for mineralisation is from a vein that cuts a 44 Ma lamprophyre dyke (Beaudoin et al., 1992a). There is a ~110 Ma interval between the emplacement of the Nelson batholith and mineralisation, which precludes any genetic link between the two. In the Harz Mountains, Mertz et al. (1989) dated vein adularia from the late stages of the main phase of mineralisation in the area of St. Andreasberg using Rb/Sr and

$^{40}Ar/^{39}Ar$ methods. The age data prove that mineralisation is Early Cretaceous (~123 Ma) and about 170 Ma younger than the Brocken pluton.

A positive age difference of over 770 Ma between mineralisation and emplacement of the Gem stocks (100 Ma) in the Coeur d'Alène district was suggested by Leach et al. (1988), on the basis of K-Ar dates for post-ore stage vein sericite. Sericite yielded ages ranging from 77 to 876 Ma: young ages could be reset older ages or represent young sericite unrelated to mineralisation (Leach et al., 1988). They also noted that their oldest ages for mineralisation broadly correlates with regional metamorphism of the Belt basin. A Proterozoic age for mineralisation was also suggested by Zartman and Stacey (1971) on the basis of 1.2 to 1.5 Ga model ages for galena Pb isotopic compositions. It is unlikely that the Coeur d'Alène Pb isotopic composition could have resulted from Mesozoic remobilisation of Proterozoic Pb in galena without adding significant amounts of radiogenic Pb to the Coeur d'Alène galena.

The age of mineralisation in the Keno Hill district is contentious. Lynch (1989a) showed that the faults containing the mineralisation were conjugate to the Mayo Lake transcurrent dextral shear zone and that hydrothermal mineral precipitation coincided with brittle faulting subsequent to ductile deformation. District scale mineralogical and stable isotopic studies indicate that the hydrothermal system is zoned away from both the Mayo Lake shear zone and pluton, but Lynch (1989a) favoured the latter association in view of geochronological data indicating that mineralisation was slightly younger than regional metamorphism (Sinclair et al., 1980). Lynch (1989b) considered that the Mayo Lake pluton acted only as a heat source for the hydrothermal system. The pluton, however, is unaltered and the question arises as to how heat transfer occurred between the cooling granitic magma and the hydrothermal fluids. Significant thermal conduction

was limited to the contact metamorphic aureole which could have exchanged heat with hydrothermal fluids. A high water/rock ratio in the contact metamorphic aureole of the Mayo Lake pluton has not been demonstrated. Lynch (1989a, p. 179), however, recognised that "*the large scale of the hydrothermal system corresponds more closely to the scale and distribution of the structural domains, and the mineral zoning may alternatively be interpreted as being associated to broad hydrothermal metasomatism related to the formation of the Mayo Lake shear zone, with the intrusion of the pluton as a further late stage consequence*".

The link between the intrusion of the Mayo Lake pluton and mineralisation therefore relies heavily on the data of Sinclair et al. (1980). These authors attempted to date mineralisation by comparing whole rock K-Ar model ages from massive quartzite cut by mineralised stockwork with those from quartzite distant from mineralisation. They concluded that the stockwork had slightly younger ages than the unmineralised country rocks, a difference which they imparted to overprinting by hydrothermal alteration. One of the "unmineralised country rock" samples of Sinclair et al. (1980), however, is cut by a pyrite-siderite veinlet and was collected 1.5 m from the fault-bounded Ruby vein. If this sample is included in the mineralised stockwork category, the two groups (stockwork and unmineralised) do not have a statistically valid difference in K-Ar model ages. Previous K-Ar ages for granitic rocks in the Selwyn basin were compiled and recalculated by Sinclair et al. (1980), and yield ages ranging from 81 to 109 Ma, similar to those for mineralised stockwork and unmineralised massive quartzite. Sinclair et al. (1980) considered these Cretaceous ages representated cooling following regional greenschist metamorphism. The K-Ar data of Sinclair et al. (1980) therefore are not considered to lead to an estimate of the age of mineralisation; silver-lead-zinc veins in the Keno Hill district could be either older or younger

than the intrusion of the Mayo Lake pluton. The structural analysis by Lynch (1989a) suggests that mineralisation is coeval with brittle deformation in conjugate structures to the Mayo Lake shear zone which, in turn, has been intruded by the undeformed Mayo Lake pluton.

Tectonic setting

The classical silver-lead-zinc vein districts are found in two orogens: the Cordilleran Orogen of North America and the Variscan Orogen of Europe (Fig. 5-1). The vein districts, except Freiberg which is in gneiss, are in sedimentary basins dominated by clastic rocks that have been deformed, metamorphosed, and intruded by igneous rocks. The Belt and Selwyn basins, that contain, respectively, the Coeur d'Alène and Keno Hill districts, are epicratonic embayments in the passive margin of Ancestral North America (Harrison, 1972; Abbott et al. , 1986). The Harz Mountains and Příbram districts are in two opposing Paleozoic basins about a central block, the Barrandian terrane, which were closed along intracontinental or intraoceanic subduction zones with opposing polarities (Matte et al., 1990). Příbram is at the collision boundary between the Barrandian and Moldanubian terranes (Žák and Dobeš, 1991) whereas the Kokanee Range overlaps several accreted terranes (Gabrielse and Yorath, 1989).

The silver-lead-zinc vein minerals were deposited late in the tectonic evolution of the orogens. In the Selwyn basin, the faults containing mineralisation are conjugate structures related to a dextral transcurrent fault zone, the Mayo Lake shear zone, which, it has been suggested, overprinted a ramp on an older thrust fault (Lynch, 1989a). In the Harz Mountains, mineralisation is contained in sets of parallel and wedge-shaped oblique, dextral strike-slip and normal faults (Beck and Weed, 1909) which cut Upper Carboniferous Variscan thrusts and isoclinal folds (Hannak, 1981). The other districts are located at plate boundaries. The Kokanee Range is in the

upper plate of the Valhalla metamorphic core complex which was unroofed during extension resulting from the collapse of the Cordilleran Orogen (Parrish et al., 1988). The Freiberg district bears similarities in its tectonic setting to that of the Kokanee Range insofar as it has been proposed that the host Erzgebirge gneiss forms the lower plate of a low angle extensional shear zone (Matte et al., 1990). At Freiberg, veins are contained in a conjugate set of shear and tension fractures that cuts the summit of the Freiberg gneiss dome (Baumann, 1965). Příbram is located at the boundary between the Barrandian and Moldanubian terranes in a major, dextral transpression fault zone: the Central Bohemian shear zone (Rajlich, 1987). Mineralisation is contained in structures related to the Lettenkluft high angle reverse fault that is peripheral to the Central Bohemian shear zone (Žák and Dobeš, 1991). This shear zone, in turn, has been intruded by the 331±4 Ma Central Bohemian pluton (van Breemen et al., 1982). Mineralisation cuts the pluton at Vrančice and, therefore, is later than the Variscan transpressional and plutonic regimes.

For the Coeur d'Alène district, the tectonic setting at the time of mineralisation is not clear. If mineralisation occurred in the Late Precambrian (~0.87 Ga), it could have been coeval with a metamorphic event that resulted in regional greenschist facies metamorphism (Leach et al., 1988). The nature of the tectonic regimes that drove Upper Proterozoic metamorphism and deformation in the Belt basin is enigmatic at present (Gabrielse and Yorath, 1989). The Coeur d'Alène district is located within the Lewis and Clark line which is considered to be a major intracontinental plate boundary that was probably initiated as Early Proterozoic synsedimentary faults which have remained active to the Holocene, including a major event of dextral strike-slip deformation in the Late Cretaceous that overprinted earlier structures (Bennett and Venkatakrishnan, 1982; Wallace et al., 1990).

Fluid inclusions

Fluid inclusion homogenisation temperatures for four of the silver-lead-zinc vein districts range from 170 to 450ºC and have modes between 250 and 300ºC (Table 5-3). Inclusion fluids display a wide range of salinities from almost pure water to saline fluids with as much as 26 wt. % NaCl eq., although the range in salinities for each district is smaller (Table 5-3). In the Kokanee Range, a meteoric water and an upper crustal, low salinity (4 wt. % NaCl eq.) hydrothermal fluid were both mixed with a high salinity (15 wt. % NaCl eq.) hydrothermal fluid of deep-seated origin (Beaudoin et al., 1991c). Similarly, Žák and Dobeš (1991) suggested that low salinities in calcite fluid inclusions resulted from admixture of meteoric water. For the Keno Hill district, Lynch et al. (1990) argued that the range in salinities was a product of boiling off more than 50% of the initial mass of a hydrothermal fluid that had an initial salinity of 5 wt. % NaCl eq.

CO_2 and variable, but minor, amounts of CH_4 are common gas phases in the Kokanee Range, Keno Hill, and Coeur d'Alène districts, but CO_2 is not present at Příbram (Table 5-3). Žák and Dobeš (1991) reported that some ice crystals did not melt at temperatures above 0ºC and interpreted this as metastable, superheated ice. It is also possible that small amounts of CO_2 were present and crystallised a CO_2-H_2O clathrate. In the Coeur d'Alène district, N_2 and light chain hydrocarbons were identified by microthermometry and laser Raman spectrography (Bijak, 1985; Leach et al., 1988). Leach et al. (1988) interpreted a systematic change, from older veins rich in zinc and characterised by CH_4-C_nH_m gases to younger veins rich in Ag and characterised by CO_2, to be due to the oxydation of a metamorphic fluid.

Boiling and/or CO_2 immiscibility have been inferred for the Kokanee Range, Keno Hill,

Table 3. Isotopic and fluid inclusion data for Ag-Pb-Zn vein districts

District	Vein mineralisation			
	Pb in galena	$\delta^{34}S_{sulphides}$(‰)	$\delta^{18}O_{quartz}$(‰)	Carbo
Kokanee, Canada[1]	$^{206}Pb/^{204}Pb$: A: 17.351-17.790; B: 17.406-17.510; K: 18.819-19.254; S: 18.619-19.031 $^{207}Pb/^{204}Pb$: A: 15.473-15.523; B: 15.467-15.489; K: 15.626-15.684; S: 15.599-15.684 $^{208}Pb/^{204}Pb$: A: 38.159-38.354; B: 37.747-38.084; K: 38.721-39.183; S: 38.818-39.175	Gn: -13.7 to +7.6 Sp: -14.8 to +10.6 Py: -9.4 to +3.7	-5.6 to +18.8	Sd: $\delta^{13}C$: -7. $\delta^{18}O$: 10 Do: $\delta^{13}C$: -5. $\delta^{18}O$: -8. Ca: $\delta^{13}C$: -8. $\delta^{18}O$: -1
Keno Hill, Canada	$^{206}Pb/^{204}Pb$: 19.038-19.320 $^{207}Pb/^{204}Pb$: 15.626-15.713 $^{208}Pb/^{204}Pb$: 38.960-39.445	Gn: -21.1 to +1.6 Sp: -12.0 to +0.7 Py: -3.6 to +4.9	Early 10.5 to 20.1 Late -5.4 to 10.5	Sd: $\delta^{13}C$: -1 $\delta^{18}O$: 12. Ca: $\delta^{13}C$: -9. $\delta^{18}O$: -8.
Coeur d'Alène, U.S.A.	$^{206}Pb/^{204}Pb$: 16.147-16.304 $^{207}Pb/^{204}Pb$: 15.367-15.406 $^{208}Pb/^{204}Pb$: 35.886-35.990	Gn: -3.0 to +8.2 Py: 0.0 to +17.8 Cpy & Td: 0.0 to +7.0	+13.2 to +13.2	Sd: $\delta^{13}C$: -8. $\delta^{18}O$: 11.
Harz Mountains, F.R.G.	$^{206}Pb/^{204}Pb$: 18.452-18.527 $^{207}Pb/^{204}Pb$: 15.636-15.662 $^{208}Pb/^{204}Pb$: 38.484-38.586	Gn: -23.6 to +10.7 Sp: -20.9 to +16.0	?	Ca: $\delta^{13}C$: -1 $\delta^{18}O$: 11.
Freiberg, F.R.G.	$^{206}Pb/^{204}Pb$: 18.051-18.072 $^{207}Pb/^{204}Pb$: 15.580-15.597 $^{208}Pb/^{204}Pb$: 38.154-38.248	?	?	
Příbram, Czechoslovakia	$^{206}Pb/^{204}Pb$: 18.01-18.12 $^{207}Pb/^{204}Pb$: 15.53-15.61 $^{208}Pb/^{204}Pb$: 38.23-38.03	Gn: -15 to -1 Sp: -9 to +1	?	Sd: $\delta^{13}C$: -8. $\delta^{18}O$: 15. Do: $\delta^{13}C$: -1 $\delta^{18}O$: 13

1. A, B, K, S: groups of deposits defined by their Pb isotopic composition, respectively Ainsworth, Bluebell, Kokanee, and Sandon. 2. Range of
Sp: sphalerite; Py: pyrite; Cpy: chalcopyrite; Po: pyrrhotite; Td: tetrahedrite; Sd: siderite; Do: dolomite; Ca: calcite; WR: whole rock. Referenc
et al. (1982), Lynch et al. (1990); Coeur d'Alène: Bijak (1985), Constantopoulos and Larson (1991), Criss and Fleck (1990), Harris et al. (1981
Bielicki and Tischendorf (1991), Möller et al. (1979), Neilsen (1968), Sperling and Neilsen (1973); Freiberg: Bielicki and Tischendorf (1991)

		Hostrocks	Fluid inclusion[2]
$\delta^{18}O_{quartz}$(‰)	Carbonates (‰)	$\delta^{34}S$ (‰)	
-5.6 to +18.8	Sd: $\delta^{13}C$: -7.9 to -5.7 $\delta^{18}O$: 10.3 to 18.4 Do: $\delta^{13}C$: -5.1 to -2.9 $\delta^{18}O$: -8.9 to +4.1 Ca: $\delta^{13}C$: -8.2 to -0.9 $\delta^{18}O$: -12.2 to +14.1	WR: -23.0 to +11.9 Py: -19.5 to -12.3	200-450 (300), [0.9-17.2] X_{CO2}: mainly below 0.3, several CO_2-rich Mixing, boiling, CO_2 immiscibility
Early 10.5 to 20.1 Late -5.4 to 10.5	Sd: $\delta^{13}C$: -11.3 to -7.9 $\delta^{18}O$: 12.3 to 19.1 Ca: $\delta^{13}C$: -9.7 to -5.4 $\delta^{18}O$: -8.3 to +14.1	Py: -5.1 to +14.9	Sd: 225-325 (270), [0.0-19.8] Qz: 205-365 (300), [0.0-17.3] X_{2CO2}: below 0.28, few CO_2-rich Boiling, CO_2 immiscibility
+13.2 to +13.2	Sd: $\delta^{13}C$: -8.3 to -4.4 $\delta^{18}O$: 11.7 to 19.0	?	Qz: 250-320 (260) Sp: 320-350 [5-13] CO_2-N_2-CH_4 Boiling, CO_2 immiscibility
?	Ca: $\delta^{13}C$: -13.5 to -5.6 $\delta^{18}O$: 11.4 to 23.5	WR: -6.6 to +9.4 Py: -19.8 to +4.9 Po: -4.7 to +12.9	?
?	?	?	?
?	Sd: $\delta^{13}C$: -8.0 to -14.0 $\delta^{18}O$: 15.4 to 20.6 Do: $\delta^{13}C$: -13.0 to -5.0 $\delta^{18}O$: 13.3 to 21.6	Py: -34.0 to +23.0	170-300 (250), [13-26] $CaCl_2$-NaCl-$MgCl_2$

l, Kokanee, and Sandon. 2. Range of temperature in °C (mode), [range of salinities, in wt. % NaCl eq.]. Abbreviations: Gn: galena; ı: calcite; WR: whole rock. References: Kokanee Range: Beaudoin et al. (1991b; 1991c); Keno Hill: Boyle et al.(1970), Godwin and Fleck (1990), Harris et al. (1981), Leach et al. (1988), Yates and Ripley (1985), Zartman and Stacey (1971);Harz Mountains: ɛrg: Bielicki and Tischendorf (1991); Příbram: Bielicki and Tischendorf (1991), Žák and Dobeš (1991).

and Coeur d'Alène districts, but no evidence for boiling was observed at Příbram (Table 5-3). Lynch et al. (1990) argued that boiling was a major process of ore deposition in the Keno Hill district, but this process was much less important in the Kokanee Range and Coeur d'Alène districts (Beaudoin et al., 1992c; Leach et al., 1988).

Pressure estimates from volumetric properties of H_2O-CO_2-NaCl fluids are typically imprecise due to lack of experimental data at elevated temperature and pressure. For the Kokanee Range and the Keno Hill districts, the estimated pressure during trapping of boiling fluids is identical at 1.6 to 1.7 kbar (Beaudoin et al., 1992c; Lynch et al., 1990). The range of pressures calculated in both districts is also similar to that estimated by Leach et al. (1988) for the Coeur d'Alène district. Assuming that the hydrothermal fluids were under lithostatic load, the depth of mineralisation was between 3 and 10 km and averaged around 6 km (Table 5-2). Such estimates are not possible in the Příbram district because boiling has not been documented. Žák and Dobeš (1991) estimated a maximum of 2 km of erosion since mineralisation occurred. This is likely a minimum estimate of the depth of emplacement.

Stable isotopes

Sulphur

The sulphur isotope compositions of galena, sphalerite, and pyrite are typically variable, and the $\delta^{34}S$ values for these sulphides display a range from 16 to 26‰ in each of the classical districts for which there are data (Table 5-3). The range in $\delta^{34}S_{sulphides}$ is nearly duplicated to exceeded by the range of $\delta^{34}S$ values for disseminated pyrite and pyrrhotite or total sulphur in local sedimentary or plutonic country rocks (Table 5-3). This led Nielsen (1968), Boyle et al. (1970), Žák and Dobeš (1991), and Beaudoin et al. (1992c) to suggest that sulphur was primarily

derived from leaching of local country rocks. In the Kokanee Range, Keno Hill, and the Harz Mountains districts, sulphur isotope ratios display more or less regular district scale changes. In the Harz Mountains (Nielsen, 1968) and the Kokanee Range (Beaudoin et al., 1991c) the change in $\delta^{34}S_{sulphides}$ is correlated with values for sulphur in the country rock. Lynch et al. (1990) suggested that the sulphur isotope zonation in the Keno Hill district was a result of a gradually changing oxydation state of the hydrothermal fluid. This hypothesis is not favoured here because it involves maintaining isotopic equilibrium between sulphur aqueous species in the fractures and pores along the 25 km length of the hydrothermal system at temperatures below 300°C.

Vertical changes of $\delta^{34}S_{sulphides}$ have been documented in the Příbram and Coeur d'Alène districts. At Příbram, the Δ value between galena and sphalerite decreases towards the surface over a vertical distance of 1500 m, indicating that the vertical zoning in not controlled by decreasing temperature (Žák and Dobeš, 1991). These authors suggested, instead, that it was controlled by a change in the oxydation state of the hydrothermal fluids. In the Coeur d'Alène district, an isotope shift of about 4‰ in pyrite within a vertical distance of less than 400 m was documented by Harris et al. (1981). They, too, suggested that the isotopic shift resulted from an increase in either pH or oxygen fugacity, but favoured the latter and suggested it resulted from mixing a reduced, H_2S-bearing brine with an oxygenated, deeply circulating groundwater.

Oxygen

The $\delta^{18}O$ values for vein siderite, quartz, dolomite, and calcite indicate that variable degrees of oxygen isotope exchange occurred between the hydrothermal fluids and hostrocks. When plotted on a map, $\delta^{18}O$ values for quartz and siderite display regular zoning patterns in both the Kokanee Range and Keno Hill districts and have been interpreted to reflect decreased

water/rock ratios away from the major hydrothermal fluid channels (Beaudoin et al., 1992c; Lynch et al., 1990). In the Kokanee Range, ^{18}O depletion of sedimentary rocks in the area of highest water/rock ratios further demonstrate the control of oxygen isotope exchange between hydrothermal fluids and hostrocks on the $\delta^{18}O$ values of vein minerals (Beaudoin et al., 1992c). $\delta^{18}O$ values, as low as -12.2‰, for quartz, dolomite, and calcite are due to late stage admixture and subsequent flooding of the hydrothermal system by meteoric water in the Kokanee Range and Keno Hill districts (Beaudoin et al., 1992c; Lynch et al., 1990). In the Příbram district, Žák and Dobeš (1991) also suggested that late stage calcite precipitated following admixture of meteoric water.

Depletion of ^{18}O downward along a vertical profile has been demonstrated for quartz in the Coeur d'Alène district (Constantopoulos and Larsen, 1991) and dolomite in the Příbram district (Žák and Dobeš, 1991). In the Coeur d'Alène district, Constantopoulos and Larsen (1991) could not determine whether boiling, CO_2 effervescence, variation in water/rock exchange, temperature gradient, or fluid mixing was responsible for the vertical change of $\delta^{18}O_{quartz}$. According to Žák and Dobeš (1991), the vertical ^{18}O depletion in the Příbram district resulted from a temperature gradient, a suggestion corroborated by fluid inclusion data. Siderite and calcite, however, display no vertical ^{18}O gradient. Siderite is the early gangue mineral but Žák and Dobeš (1991) proposed that the isotopic shift due to the thermal gradient was exactly compensated by admixture of low $\delta^{18}O$ meteoric water from the upper part of the profile. This is a very complicated scenario and it seems unlikely that meteoric water was added to the hydrothermal fluids during precipitation of siderite, not during that of dolomite, but again during precipitation of late stage calcite as suggested by Žák and Dobeš (1991).

Carbon

Siderite in the Kokanee Range displays a very narrow range of $\delta^{13}C$ values (2.2‰), whereas those in Příbram display the largest (6.0‰; Fig. 5-3). The isotopic signatures of siderite in the Kokanee Range and Coeur d'Alène districts largely overlap each other, but those for Keno Hill and Příbram are more distinct and the siderite is more depleted in ^{13}C than in the other districts (Fig. 5-3). Ore stage calcite in the Harz Mountains and dolomite in Příbram have $\delta^{13}C$ values covering the total range displayed by siderite. Late stage calcite in Keno Hill, and dolomite and calcite in the Kokanee Range have larger ranges of $\delta^{13}C$ which extend to higher values than those for siderite in these districts (Table 5-3). In the Kokanee Range, Beaudoin et al. (1992c) concluded that dolomite and most of the calcite were precipitated from a fluid with a $\delta^{13}C$ distinct from that of the fluid that precipitated siderite. In the Příbram district, Žák and Dobeš (1991) documented a ^{13}C depletion for siderite and dolomite, but not for calcite, downward along a vertical profile for 1500 m. Žák and Dobeš (1991) related the $\delta^{13}C$ trend to a temperature gradient of nearly 100ºC. There is no correlated trend for $\delta^{18}O_{siderite}$, however. Žák and Dobeš (1991) suggested that the vertical trend for galena and sphalerite resulted from a changing oxydation state of the fluids and this process, therefore, likely influenced the C isotopic compositions of the carbonates as well.

Two sources have been proposed for carbon. The first is organic carbon leached from local country rocks. Organic C dominated the isotopic composition of siderite and calcite at Keno Hill (Lynch et al., 1990) and Příbram (Žák and Dobeš, 1991), and of calcite in the Harz Mountains (Möller et al., 1979; 1984). At Keno Hill, a regional change of $\delta^{13}C_{siderite}$ was proposed to result from either progressive carbon exchange between hydrothermal fluids and the graphitic

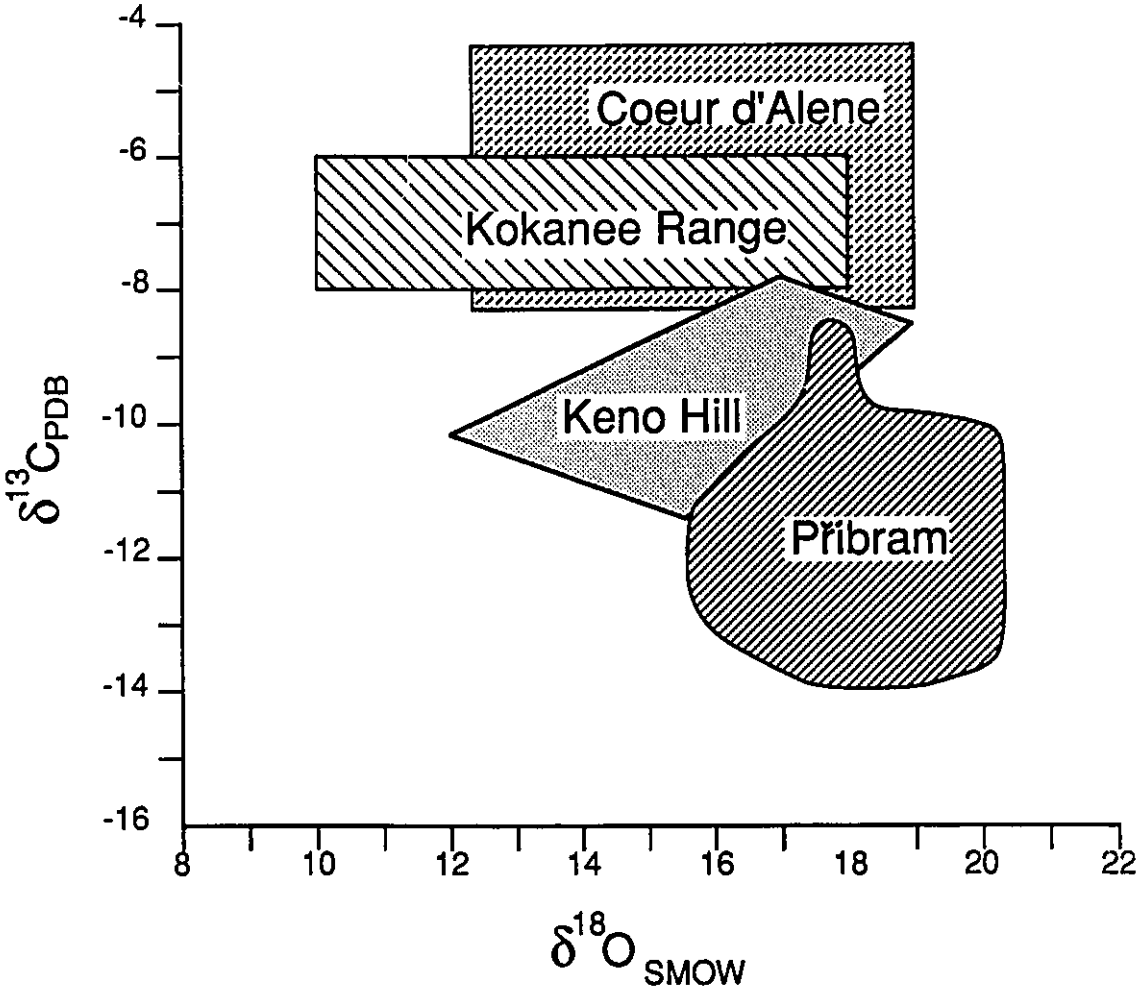

Figure 5-3. Carbon-oxygen isotopic composition of siderite in silver-lead-zinc vein districts. Data sources in Table 5-3.

quartzite or from loss of gaseous species during boiling (Lynch et al., 1990). The second source is juvenile or magmatic carbon and is best documented in the Kokanee Range. In contrast to locally derived and variable sulphur isotopic signature, $\delta^{13}C_{siderite}$ is homogeneous (-7.1±0.5‰) for 26 deposits within a 1200 km^2 area, leading Beaudoin et al. (1992c) to suggest a large and homogeneous reservoir of deep-seated carbon, possibly CO_2 degassed from the mantle. This is corroborated by a significant component of Pb, in most of the deposits, derived from a depleted upper mantle or the lower crust, and the coeval intrusion of a widespread suite of lamprophyre dykes (Beaudoin et al., 1992b; 1992c). A mantle source for carbon has also been suggested for the Coeur d'Alène district (Yates and Ripley, 1985), but has yet to be thoroughly documented. Similarly, in the Příbram district, a deep-seated carbon reservoir has been suggested for dolomite, ankerite, and calcite, mainly on the basis of homogeneous and suitable carbon isotopic signatures (Žák and Dobeš, 1991). This hypothesis, however, is weakened by the late deposition of dolomite, ankerite, and calcite relative to early siderite, which is dominated by locally derived carbon of organic origin, and would require tapping of a deep-seated carbon reservoir late in the evolution of the hydrothermal system. In the Harz Mountains, a contribution of magmatic carbon from granitic intrusions has been suggested by Möller et al. (1979; 1984), but would seems unlikely in view of the age difference between the intrusions and mineralisation (Mertz et al., 1989) and the typically non-distinctive isotopic composition of carbon in granitic melts.

Pb isotopes

The Pb isotopic compositions of galena in silver-lead-zinc vein districts (Table 5-3) is displayed in Figure 5-4. Data for each district are of variable quality and quantity. By far the most thoroughly studied district is the Kokanee Range in which 147 analyses are available from

74 deposits, including all the large producers (Beaudoin et al., 1992b). For the other districts, galenas from less than twelve deposits have been analysed.

In all districts except Kokanee Range, the Pb isotopic data defines one linear (Coeur d'Alène, Harz Mountains) or scattered (Keno Hill, Freiberg, Příbram) array (Fig. 5-4). In the Kokanee Range, four groups of deposits are defined by their Pb isotopic composition, each with a distinct geographic distribution and each forming a linear array (Beaudoin et al., 1992b).

The most striking feature of Figure 5-4 is that nearly all the data plot between the orogene and upper crust curves of Zartman and Doe (1981) in $^{207}Pb/^{204}Pb$ versus $^{206}Pb/^{204}Pb$ space. This suggests that Pb in silver-lead-zinc veins is mainly derived from mixtures of rocks which have been stored in the upper crust for long periods of time (upper crust curve) and rocks which have been formed (deformed) and mixed during repeated orogenic cycles (orogene curve). Data from the Coeur d'Alène district plot slightly below the orogene curve, but this probably reflects a discrepancy between model and real "orogene" Pb isotopic compositions in that area. A notable exception is the Kokanee Range district, where two of the four groups of deposits (Bluebell and Ainsworth) plot distinctly below the orogene curve and are considered to contain significant amounts of Pb derived from the lower crust and depleted upper mantle (Beaudoin et al., 1992b).

In $^{208}Pb/^{204}Pb$ versus $^{206}Pb/^{204}Pb$ space, most of the data plot close to, but above, the orogene curve (Fig. 5-4). For three of the groups of deposits in the Kokanee Range (Bluebell, Ainsworth, and Sandon), this was interpreted to indicate variable contributions of lower crustal Pb (Beaudoin et al., 1992b). For other deposits, this probably represents orogene Pb comprised of a mixture of rock Pb different than that given by the model curve. This is shown by Bielecki and Tischendorf (1991) for the Příbram district. For Freiberg, Bielecki and Tischendorf (1991)

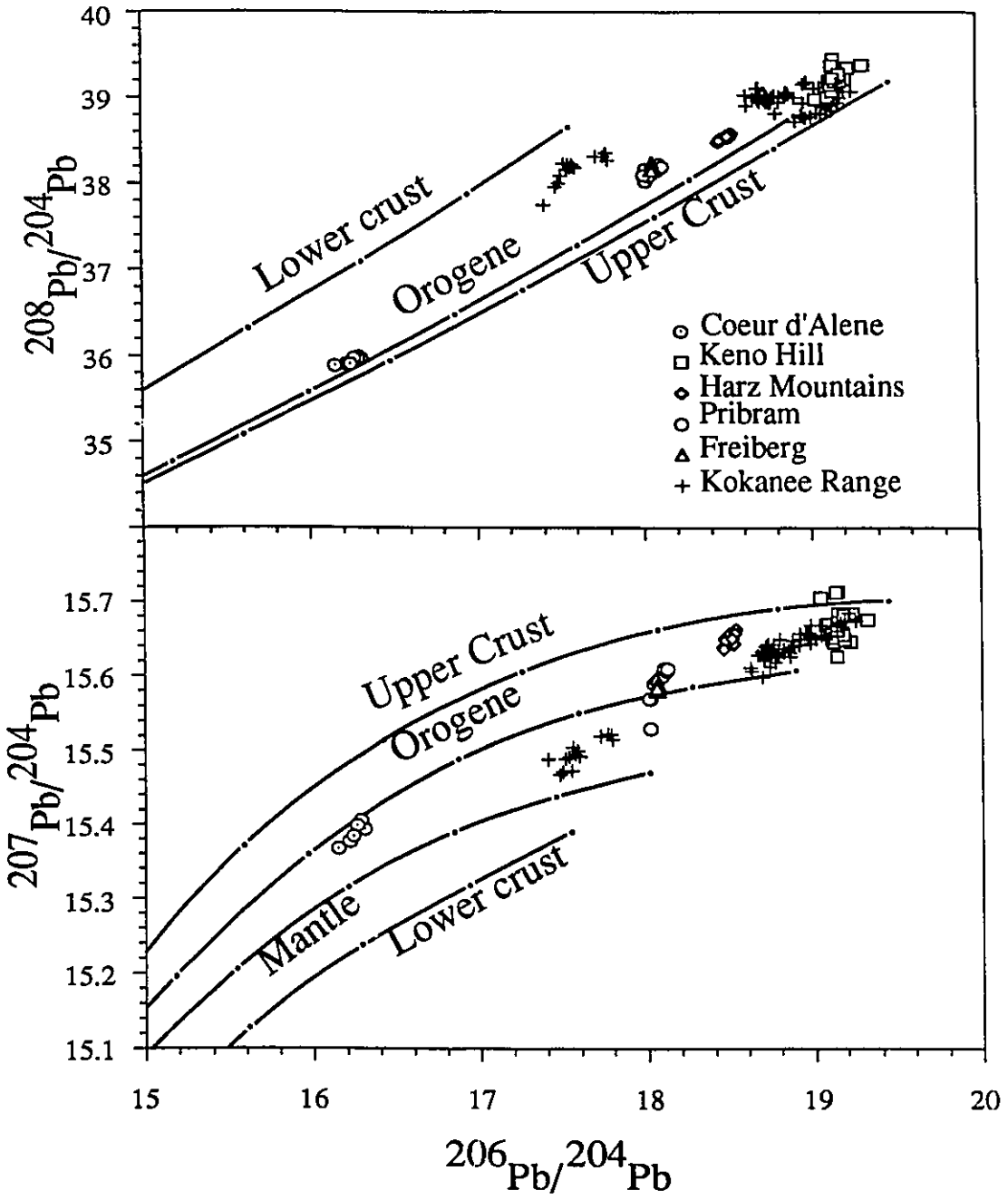

Figure 5-4. Pb isotopic composition of galena in silver-lead-zinc districts. Data for Coeur d'Alene, the Harz Mountains, and Freiberg represent single analyses whereas those for the Kokanee Range are the average isotopic compositions for individual deposits and those for Pribram comprise both single analyses and deposit averages. Data sources in Table 5-3. Growth curves are those of the Plumbotectonics model II of Zartman and Doe (1981); dots represent 0.4 Ga age intervals.

suggested a lower crustal component of Pb because deposits of various ages from the Saxothuringian domain of the Variscan orogen of Central Europe plot along a trend suggesting a decreasing contribution of lower crustal Pb in younger deposits.

The Pb isotopic data for each district display either a linear spread of ratios (Kokanee Range) or are tightly clustered (Freiberg). In the Kokanee Range, the arrays were interpreted to lie on mixing lines between Pb reservoirs with different isotopic compositions and to indicate that mixing occurred through leaching of Pb from its reservoirs by several hydrothermal fluids (Beaudoin et al., 1992b). In general, the homogeneity of the Pb isotopic compositions in one district can be correlated with the diversity of hostrocks lithologies. An end member with great lithological diversity could be represented by the Kokanee Range, which is located at the collision boundary between an old Precambrian craton and accreted Paleozoic and Mesozoic terranes of diverse origin. The end member with low lithological diversity could be represented by the Freiberg district, in which the veins are hosted by gneisses that have locally reached the granulite grade of metamorphism; metamorphic homogenisation of the Pb isotopic compositions is therefore possible, in addition to a lithological assemblage that was initially homogeneous.

Descriptive Model

A summary of the common features of silver-lead-zinc veins is presented in Table 5-4 and will be used to outline a descriptive model. Silver-lead-zinc veins are comprised of massive galena and sphalerite in a gangue of siderite, quartz, dolomite, or calcite. Quartz, dolomite, or calcite also commonly occur as late stage minerals precipitated during meteoric water flooding of the hydrothermal system. Alteration is restricted to the immediate vicinity of the veins and is typically phyllic, characterised by sericitisation, silicification, and pyritisation.

Table 5-4. Descriptive model for silver-lead-zinc veins.

Feature	Summary
Metal ratios: **Pb/(Pb+Zn)** **(Ag*100)/((Ag*100)+Pb)**	 0.51 to 0.72 0.22 to 0.63
Mineralogy: **Sulphides** **Gangue**	 Galena and sphalerite Siderite, quartz, dolomite, and calcite
Alteration	Local sericitisation, silicification, pyritisation
Hostrocks: **Sedimentary** **Plutonic** **Metamorphism**	 -Precambrian to Mesozoic fine to medium grained clastic rocks with minor volcanic rocks -Granite, granodiorite (most common), monzonite, syenite. I- and S-type. Collision to post collision -Greenschist, exceptionally to granulite
Age of mineralisation	Precambrian to Eocene
Maximum size of vein structure	Length: 15 km; Depth: 2300 m; Thickness: 15 m
Depth of mineralisation	0 to 10 km; probable average: 6 km
Tectonic setting	In faults conjugate or secondary to crustal shear zones which often are terrane boundaries. Late tectonic in orogen history, after compression, during or after crustal extension
Fluid inclusion	Temperature: 250-300°C; salinity: 0-26 wt. % NaCl eq. CO_2 abundant but not universal, minor CH_4, N_2
S	Highly variable $\delta^{34}S$, correlated with local country rocks
C	-Variable, $\delta^{13}C$ between -14 and 0; probably C leached from local country rocks -Homogeneous, $\delta^{13}C$ between -8 and -5; probably deep seated C from mantle CO_2 degassing
Pb	Linear or scattered arrays, one to four groups of deposits. Upper crustal to orogen Pb, lower crustal and upper mantle components present locally.

Silver-lead-zinc veins have a limited range of Pb/(Pb+Zn) ratios between 0.51 and 0.72 and (Ag*100)/((Ag*100)+Pb) ratios ranging from 0.22 to 0.63. They have Ag-Pb-Zn-Au ratios distinct from those for Pb-Zn skarns, volcanic hosted epithermal veins, and veins associated with porphyry-Cu deposits. Silver-lead-zinc vein districts and carbonate replacement and manto deposits have similar ratios in ternary Ag-Pb-Zn space, although carbonate replacement and manto deposits are characterised by metal compositions distinctly richer in Au in ternary Ag-Pb-Au space (Fig. 5-2).

Silver-lead-zinc veins are typically hosted in monotonous fine to medium grained clastic rocks, as well as minor associated carbonate rocks and felsic to mafic volcanic rocks. These sedimentary sequences are found in Precambrian to Mesozoic basins with origins ranging from epicratonic embayments in passive margins to back arc basins to island arcs. These sedimentary and volcanic rocks have been typically folded and thrust during collision events, and metamorphosed to the geenschist facies. They have been intruded by granitic to ultramafic rocks, of alkaline to calc-alkaline affinity. The granitic plutons can be classified as I, S, and within-plate types, and were intruded during, but more commonly after, plate collision. The only common significant feature of the hostrocks is that they lie within Pb-Zn metallogenic provinces characterised by sediment-hosted, Pb-Zn, massive sulphide deposits. The diversity of types and tectonic settings of the sedimentary basins and igneous rocks containing the mineralisation clearly indicate that they bear little control on ore formation. The lack of igneous and tectonic specialisation of the plutons spatially associated with mineralisation contrasts with that observed for porphyry-Cu, Cu-Au, and Mo, stockwork Sn-W, or skarn deposits (Mutschler et al., 1981; Westra and Keith, 1981; Einaudi and Burt, 1982; Eckstrand, 1984; Strussi, 1989).

The most common temperature of fluid trapping is in the range 250-300°C. The hydrothermal fluids display a large range in salinity, form 0 to 26 wt. % NaCl eq., although each district has a narrower range of salinities. CO_2 is abundant in some deposits; other gaseous species identified include CH_4 and N_2.

Sulphur in vein sulphides displays a wide range of $\delta^{34}S$ values, which are correlated with those for local country rocks, and thus suggest that sulphur was derived from local country rock sources. Carbon displays two groups of isotopic compositions: i) variable $\delta^{13}C$ between -14 and 0, reflecting various C sources leached from the local country rocks; ii) homogeneous $\delta^{13}C$ between -8 and -5, indicating deep seated sources, possibly mantle CO_2 degassing. Pb isotope data define one to four linear or scattered arrays in each district. The main Pb reservoir appears to have been in the local country rocks, which have imparted Pb isotopic compositions intermediate between upper crust and orogene Pb evolution model curves (Fig. 5-4). Distinct, and occasionally major, components of Pb derived from depleted upper mantle or lower crustal sources are identified in some groups of deposits.

Silver-lead-zinc veins are contained within all types of faults, which have strike length as great as 15 km. The faults have vertical to shallow dips and mining has been pursued down to 2300 m. The veins are narrow massive structures (<2 m) or form stockworks in deformation zones as wide as 80 m. The best estimate of the depth of mineralisation is 6 km but is still poorly constrained at present.

The faults containing the veins are commonly nearby, or mechanically related to, transcrustal shear zones at terrane boundaries. The age of mineralisation ranges from Precambrian to Eocene but mineralisation was emplaced later than the collision tectonic events in the area.

Where data are available, mineralisation is coeval with, or later than, crustal extension initiated by the collapse of orogens. This tectonic lineage cannot be shown to be exclusive at present.

Genetic Models

Genetic models for silver-lead-zinc veins are varied and contrasted; none has yet emerged as a popular and useful guide to understanding the processes that formed these deposits and for exploration purposes. Recently proposed genetic models for silver-lead-zinc veins can be grouped into three categories: i) magmatic differentiation; ii) magmatic heat source; iii) deep crustal faults.

A magmatic differentiation model has been applied to the Freiberg district and the Erzgebirge of Germany in general (Tischendorf and Förster, 1990). Briefly, this model states that incompatible elements such as Sn, W, Mo, Bi, Li, etc, are associated with the felsic products of extreme fractional crystallisation of initially mafic magmas, wheras compatible, chalcophile elements such as Cu, Pb, Zn, Ag, Co, Ni, etc., are concentrated in the intercumulate fluid phase of the accumulating crystal pile at the base of the mafic magma chamber (Tischendorf, 1989; Tischendorf and Schwab, 1989). Expulsion of the intercumulate fluid phase coeval with intrusion of mafic and lamprophyric dykes eventually yields the so-called "melanocratic metallogenesis" which comprises the silver-lead-zinc veins of Freiberg (Tischendorf, 1989; Tischendorf and Schwab, 1989; Tischendorf and Förster, 1990). I consider that most aspects of this model remain to be demonstrated.

The second model calls for the spatially associated intrusion to act as a heat source driving the hydrothermal system and suggests there was no, or only limited, input of metals or fluids to the hydrothermal system from the intrusion. This model bears many similarities to magmatic-hydrothermal systems (Criss and Taylor, 1986) and has been proposed for the Harz

Mountains (Möller et al., 1979; 1984), the Keno Hill district (Sinclair et al., 1980; Lynch, 1989b), and the Coeur d'Alène district (Criss and Fleck, 1990). This model can now be discounted for the Harz Mountains on the basis of a 170 Ma age difference between intrusion and mineralisation (Mertz et al., 1989). At Keno Hill, this model is a distinct possibility, but other hypotheses are just as likely (Lynch, 1989a), especially in view of the inconclusive dating of mineralisation (Sinclair et al., 1980). In the Coeur d'Alène district, this model relates mineralisation to the Idaho batholith, which is at least 60 km away from the district, and neglects to take into account the offset of the deposits due to Cretaceous strike-slip deformation in the Lewis and Clark line (Bennett and Venkatakrishnan, 1982; Wallace et al., 1990), and the age and Pb isotope data which indicate that mineralisation is Proterozoic (Zartman and Stacey, 1971; Leach et al., 1988).

The third model relates deep crustal faults and metamorphic events to the formation of silver-lead-zinc veins. The metamorphic part of the model has been outlined for the Coeur d'Alène district by Leach et al. (1988) and Constantopoulos and Larsen (1991) and the relation to deep crustal faults was demonstrated in detail by Beaudoin et al. (1992a; 1992b; 1992c) for the Kokanee Range. The deep crustal fault model is based on the close association of silver-lead-zinc veins with major structural breaks, commonly at terrane boundaries. These deep crustal fault zones are considered to be first order hydrothermal fluid channels that connected deep seated C, Pb, and fluid reservoirs with upper crustal C, S, Pb, and fluid reservoirs. Mixing of two to three different hydrothermal fluids that had exchanged with the C, S, and Pb reservoirs has been demonstrated in most districts. Three hydrothermal fluids have been demonstrated by fluid inclusion salinity data and $\delta^{18}O$-δD isotopic signatures from vein and alteration minerals in the Kokanee Range (Beaudoin et al., 1992c) and two from inclusion waters in the Coeur d'Alène

district (Constantopoulos and Larsen, 1991). Both studies suggest the mixing of a deep seated hydrothermal fluid, with oxygen and hydrogen isotopic signatures indicative of extensive and high temperature isotopic exchange with crustal rocks, possibly as a result of metamorphism, with a second fluid with a ^{18}O-shifted, but only slightly modified δD, probably ultimately of meteoric origin but having experienced a long history of oxygen isotope exchange with upper crustal country rocks. The third hydrothermal fluid is characterised by low temperatures and salinities and is dominated by meteoric water; it is commonly dominant in the waning stages of the hydrothermal system. Mixing between deep seated and upper crustal fluids is a major, district scale, cause of ore deposition. Boiling and CO_2 immiscibility are widespread in some districts and can be effective precipitation mechanisms (Drummond and Ohmoto, 1985), but their influence was limited to temporal, areal, and vertical domains. The role of metamorphism is mainly in the generation of fluids either through dehydration or high temperature water/rock exchange. The metallogenic importance of magmatic relative to metamorphic processes needs to be further evaluated. CO_2 degassing of the upper mantle is advocated in the Kokanee Range district (Beaudoin et al., 1992c). Similarly, the crustal processes responsible for the mechanical, thermal, and chemical destabilisation of the lithosphere are not well constrained. In the Kokanee Range, crustal extension as a result of the collapse of the Cordilleran orogen appears to have been the triggering process that led to mineralisation. A tectonic setting similar to that of the Kokanee Range has been suggested for the Freiberg district (Tischendorf and Schwab, 1989; Matte et al., 1990). Extension results in a thinned crust and upwelled upper mantle, thermal disequilibrium, deep seated fracture zones, new or renewed fracture porosity, and magmatic and metamorphic events. This is a highly unstable and dynamic geological environment of which

mineralisation can be a by-product. A further consequence of extension is crustal block tilting (Bardoux and Irving, 1989). Criss and Hofmeister (1991) showed that crustal blocks tilted to a small angle (5º) undergo fluid convection even for low permeability aquifers.

In summary, further work is required in many districts to clarify which processes were more likely responsible for mineralisation. Deep crustal faults are a common feature in four of the classical silver-lead-zinc vein districts and may have yet to be recognised in the two remaining districts. For example, it is only recently (Parrish, 1984; Parrish et al., 1988) that the size and profound importance of the Slocan Lake Fault in the geological evolution of the Kokanee Range has been demonstrated.

Comparison with Ag-Pb-Zn Carbonate Replacement and Manto Deposit Type

In the preceding discussion, silver-lead-zinc veins have been shown to possess distinct geological and geochemical characteristics which justify grouping them into one class (Table 5-4). This class is compared with the Ag-Pb-Zn carbonate replacement and manto deposit type. Because replacement of limestone by massive sulphide bodies along fractures is known in some silver-lead-zinc vein districts, for example the Bluebell deposit in the Kokanee Range (Ohmoto and Rye, 1970), it is appropriate to review the major geological and geochemical characteristics of carbonate replacement and manto deposits. In Mexico, these deposits commonly grade from skarn to massive sulphide bodies in the form of either mantos or chimneys away from the associated intrusion (Megaw et al., 1988). They are characterised by irregular shapes and sharp contacts, and display textural evidence indicating replacement. The skarn ores have slightly higher homogenisation temperatures (280 to 560ºC) and very high salinities (3 to 58 wt. % NaCl eq.) relative to the massive sulphide bodies, which display temperatures (200 to 450ºC) and

salinities (1 to 26 wt. % NaCl eq.) similar to silver-lead-zinc vein districts. In Leadville and Gilman, however, the hydrothermal fluids are characterised by low salinities ranging from 2 to 5 wt. % NaCl eq. (Beaty et al., 1990). Carbonate replacement and manto deposits formed at shallower levels, under pressures ranging from 0.3 to 0.8 kbar (Megaw et al., 1988), compared to silver-lead-zinc veins (6 km; 1.6 kbar). Sulphur isotopic compositions at Leadville and Gilman are tightly clustered around 0‰ (Beaty et al., 1990), but can also be variable as in some Mexican deposits (Megaw et al., 1988). A genetic link between carbonate replacement and manto deposits and nearby intrusions has been suggested, based on zonation from skarn to chimneys, spatial association, and geochemical data (Megaw et al., 1988; Beaty et al., 1990). Such a genetic link for silver-lead-zinc veins is not supported by the present study. Silver-lead-zinc veins (Table 5-4) therefore appear to be a type of ore deposit distinct from carbonate replacement and manto deposits but no single deposit scale feature can be shown to be distinctive; rather, a district scale comparison appears to be required. Carbonate replacement and manto deposits were also considered distinct from silver-lead-zinc veins by Megaw et al. (1988).

Conclusion

A descriptive model for silver-lead-zinc veins shows that they form a distinct class of mineral deposits (Table 5-4). They are characterised by their mineralogy, metal ratios and local phyllic alteration. The veins are in faults that are commonly associated with deep crustal breaks at terrane boundaries. The veins are hosted by monotonous sequences of clastic rocks deposited in basins within various tectonic settings and that have been intruded by granitic to gabbroic plutonic rocks. The veins occur late in the tectonic evolution of the orogen and, in some cases, are associated with the extensional collapse of the orogen. The vein minerals were precipitated

by mixing and local boiling of different hydrothermal fluids. These fluids commonly include a deep seated fluid of ultimate metamorphic or magmatic origin, a hydrothermal fluid chemically and isotopically equilibrated with the upper crust and of ultimate meteoric origin, and a fluid dominated by meteoric water. Mineralisation occurred at temperatures around 250-300°C from dilute to saline fluids. Sulphur is derived from the local country rocks, whereas carbon can have a dual origin, either as organic carbon from the local country rocks or as deep seated carbon produced by mantle CO_2 degassing. Pb is mainly derived from local upper crustal rocks but significant lower crustal or mantle contributions are identified in some groups of deposits.

Conclusion

The Ag-Pb-Zn vein and replacement deposits of Kokanee Range have long been thought to be genetically related to the intrusion of the Nelson batholith. Step heating $^{40}Ar/^{39}Ar$ spectra and K-Ar analyses indicate an age of crystallisation of vein and hydrothermal alteration muscovite of 59 Ma in the Kokanee Range. Coeval lamprophyre dykes indicate that hydrothermal system in the Kokanee Range was active for at least 15 Ma but likely shorter in each deposit. Mineralisation is coeval with Paleocene-Eocene crustal extension during which the Valhalla metamorphic core complex was rapidly uplifted along the Slocan Lake Fault, a transcrustal low angle normal fault. An age interval of at least 100 Ma has documented between batholith emplacement and mineralisation which makes any genetic link between the two unlikely.

The isotopic and fluid inclusion data permit the identification of distinct H, C, O, S, and Pb reservoirs which are located in distinct lithospheric segments: the upper and lower crust, and the mantle. The reservoir for S and for part of the Pb is in the local upper crustal country rocks. The reservoir for C is most likely the upper mantle but could also be in the lower crust; both of which have been shown to be Pb reservoirs. The salinity-$\delta^{18}O_{fluid}$ data require three contrasting fluids. A high salinity, deep-seated fluid is well equilibrated with the crust, whereas an upper crustal fluid display a low salinity and evolved meteoric oxygen isotopic signature. A fluid characterised by low salinity, $\delta^{18}O_{fluid}$, and δD_{fluid} is uniquely identified as slightly evolved meteoric water.

The different fluids migrated through, and exchanged H, C, O, S, and Pb with the rocks in the different reservoirs identified. The deposits of the Kokanee group were formed by the

upper crustal fluid only, which exchanged O, and leached S and Pb from the local upper crustal rocks. Deposits of the Sandon, Ainsworth, and Bluebell groups of deposits have identical mantle C isotopic signatures, and were formed by mixing the upper crustal fluid with the high salinity, deep-seated fluid characterised by $\delta^{18}O$ and δD values typical of metamorphic or magmatic fluids, that had leached Pb from the lower crustal and mantle reservoirs. Influx of a fluid dominated by meteoric water in the waning stages of the hydrothermal system is widespread. The Ainsworth group is the result of mixing the meteoric fluid with the deep-seated fluid. The dominant fluid process occurring during mineralisation was mixing and dilution.

Crustal migration of the hydrothermal fluids occurred in the early stages of Paleocene-Eocene crustal extension as shown by similar ages, around 58-59 Ma, for mineralisation and extension. Slocan Lake Fault channeled fluid flow towards higher crustal levels but more local structures host mineralisation. It is suggested that thermal destabilisation of the crust, or crustal scale block tilting, early in the crustal extension process triggered and provided the energy to sustain hydrothermal fluid flow. Mineralisation is therefore genetically related to crustal extension.

A descriptive model for silver-lead-zinc veins shows that they form a distinct type of mineral deposits. They are characterised by their mineralogy, metal ratios and local phyllic alteration. The veins are in faults that are commonly associated with deep crustal breaks at terrane boundaries. The veins are in monotonous sequences of clastic rocks that have been intruded by granitic to gabbroic plutonic rocks. The veins occur late in the tectonic evolution of the orogen and, in some cases, are associated with the extensional collapse of the orogen. The vein minerals were precipitated by mixing and local boiling of different hydrothermal fluids.

These fluids commonly include a deep seated fluid of ultimate metamorphic or magmatic origin, a hydrothermal fluid chemically and isotopically equilibrated with the upper crust of ultimate meteoric origin, and a fluid dominated by meteoric water. Mineralisation occurred at temperatures around 250-300°C from dilute to saline fluids. Sulphur is derived from the local country rocks, whereas carbon can have a dual origin, either as organic carbon from the local country rocks or as deep seated carbon produced by mantle CO_2 degassing. Pb is mainly derived from local upper crustal rocks but significant lower crustal or mantle contributions are identified in some groups of deposits.

References

Abbott J.G., Gordey S.P., and Tempelman-Kluit D.J., 1986: Setting of stratiform, sediment-hosted lead-zinc deposits in Yukon and northeastern British Columbia. In Morin J.A., ed., Mineral deposits of the northern Cordillera, C.I.M. Special Volume 37: 1-18.

Al-Aasm I.S., Taylor B.E., and South B., 1990: Stable isotope analysis of multiple carbonate samples using selective acid extraction. Chemical Geology, **80**: 119-125.

Anderson R.G., 1987: Plutonic rocks of the Dawson map area, Yukon Territory. Geological Survey of Canada, Paper 87-1A: 689-697.

Andrew A., Godwin C.I., and Sinclair A.J., 1984: Mixing line isochrons: A new interpretation of galena lead isotope data from southeastern British Columbia. Economic Geology, **79**: 919-932.

Archibald D.A., Glover J.K., Price R.A., Farrar E., and Carmichael D.M., 1983: Geochronology and tectonic implications of magmatism and metamorphism, southern Kootenay Arc and neighbouring regions, southeastern British Columbia. Part I: Jurassic to mid-Cretaceous. Canadian Journal of Earth Sciences, **20**: 1981-1913.

Archibald D.A., Krogh T.E., Armstrong R.L., and Farrar E., 1984: Geochronology and tectonic implications of magmatism and metamorphism, southern Kootenay Arc and neighbouring regions, southeastern British Columbia. Part II: Mid-Cretaceous to Eocene. Canadian Journal of Earth Sciences, **21**: 567-583.

Armstrong R.L., 1988: Mesozoic and Early Cenozoic magmatic evolution of the Canadian Cordillera. Geological Society of America Special Paper 218: 55-91.

Bardoux M., and Irving E., 1989: Paleomagnetism of Eocene rocks of the Kelowna and Castelgars areas, British Columbia: studies in determining paleohorizontal. Canadian Journal of Earth Sciences, **26**: 829-844.

Bateman A.M., 1925: Notes on silver-lead deposits of Slocan district, British Columbia, Canada, Economic Geology, **20**: 554-572.

Bateman A.M., 1959: Economic mineral deposits. John Wiley, Second Edition, 916 p.

Baumann L., 1965: On the zonal distribution of mineralization in the ore veins of the Freiberg ore district. Symposium. Problems of Postmagmatic Ore Deposition, Prague, **2**: 56-66.

Beaty D.W., Landis G.P., and Thompson T.B., 1990: Carbonate-hosted sulfide deposits of the central Olorado mineral belt: Introduction, general discussion, and summary. In Beaty D.W., Landis G.P., and Thompson T.B., eds., Carbonate-hosted sulfide deposits of the Colorado mineral belt, Economic Geology Monograph **7**: 1-18.

Beaudoin G., 1990: Geological compilation map, northern Kokanee and southern Goat Ranges, British Columbia. British Columbia Ministry of Energy, Mines and Petroleum Resources, Open File 1990-18.

Beaudoin G., and Sangster D.F., 1990: Preliminary report on the Silvana Mine and other Ag-Pb-Zn vein deposits, northern Kokanee Range, British Columbia. British Columbia Ministry of Energy, Mines and Petroleum Resources, Geological Fieldwork, Paper 1990-1: 251-255.

Beaudoin G., and Sangster D.F., 1991: The use of production data as an exploration guideline

for Ag-Pb-Zn-Au vein and replacement deposits, northern Kokanee Range, southeastern British Columbia. British Columbia Ministry of Energy, Mines and Petroleum Resources, Geological Fieldwork 1990, Paper 1991-1: 171-178.

Beaudoin G., Roddick J.C., and Sangster D.F., 1992a: Eocene age for Ag-Pb-Zn-Au vein and replacement deposits of the Kokanee Range, British Columbia. Canadian Journal of Earth Sciences, in press.

Beaudoin G., Sangster D.F., and Godwin C.I., 1992b: Isotopic evidence for complex Pb sources in the Ag-Pb-Zn-Au veins of the Kokanee Range, British Columbia. Canadian Journal of Earth Sciences, in press.

Beaudoin G., Taylor B.E., and Sangster D.F., 1992c: Silver-lead-zinc veins and crustal hydrology during Eocene extension, southeastern British Columbia, Canada. Geochimica and Cosmochimica Acta, submitted.

Beaudoin G., and Sangster D.F., 1992d: A descriptive model for silver-lead-zinc veins. Economic Geology, submitted.

Bevier M.L., 1987: A Pb isotopic study of the Valhalla complex and its surrounding rocks, southeastern British Columbia: preliminary interpretations. *in* Radiogenic Age and Isotopic Studies: Report 1, Geological Survey of Canada, Paper 87-2, p. 13-20.

Beck R., and Weed W.H., 1909: The nature of ore deposits. McGraw-Hill, 685 p.

Bennett E.H., and Venkatakrishnan R., 1982: A palinspatic reconstruction of the Coeur d'Alene mining district based on ore deposits and structural data. Economic Geology, **77**: 1851-1866.

Bijak M.K., 1985: A fluid inclusion study of the Bunker Hill mine, Coeur d'Alene district, Idaho. Unpublished M.Sc. thesis, New Mexico Institute of Mining and Technology, 153 p.

Bielicki K.-H., and Tischendorf G., 1991: Lead isotope and Pb-Pb model age determinations of ores from Central Europe and their metallogenic interpretation. Contributions to Mineralogy and Petrology, **106**: 440-461.

Bodnar R.J., 1983: A method of calculating fluid inclusion volumes based on vapor bubble diameter and P-V-T-X properties on inclusion fluids. Economic Geology, **78**: 535-542.

Bonhomme M.G., Baubron J.-C., and Jebrak M., 1987: Minéralogie, géochimie, terres rares et âge K-Ar des argiles associées aux minéralisations filoniennes. Chemical Geology, **65**: 321-339.

Borthwick J., Harmon R.S., 1982: A note regarding ClF_3 as an alternative to BrF_5 for oxygen isotope analysis. Geochimica et Cosmochimica Acta, **46**: 1665-1668.

Bottinga Y., 1969: Calculated fractionation factors for carbon and hydrogen isotope exchange in the system calcite-CO_2-graphite-methane-hydrogen and water vapor. Geochimica et Cosmochimica Acta, **33**: 49-64.

Bowers T.S., and Helgeson H.C., 1983: Calculation of the thermodynamic and geochemical consequences of nonideal mixing in the system H2O-C)2-NaCl on phase relations in geologic systems: Equation of state for H2O-CO2-NaCl fluids at high pressures and temperatures. Geochimica et Cosmochimica Acta, **47**: 1247-1275.

Boyle R.W., 1965: Geology, geochemistry, and origin of the lead-zinc-silver deposits of the Keno Hill-Galena Hill area, Yukon Territory. Geological Survey of Canada Bulletin **111**.

Boyle R.W., Wanless R.K., and Stevens R.D., 1970: Sulfur isotope investigation of the lead-zinc-silver-cadmium deposits of the Keno Hill-Galena Hill area , Yukon, Canada.

Economic Geology, **65**: 1-10.

Bozzo A.T., Chen J.R., and Barduhu A.J., 1973: The properties of the hydrates of chlorine and carbon dioxide. 4th International Symposium on Freshwater from the Sea, Delyannis A., and Delyannis E., eds., **3**: 437-451.

Brame S., 1979: Mineralisation near the northeast margin of the Nelson batholith, southeast British Columbia. Unpublished M.Sc. thesis, The University of Alberta, 146 p.

Brown D.A., and Logan J.M., 1989: Geology and mineral evaluation of Kokanee Glacier Provincial Park southeastern British Columbia (82F11, 14). British Columbia Ministry of Energy, Mines and Petroleum Resources, Paper 1989-5, 47 p.

Brown P.E., 1989: FLINCOR: A microcomputer program for the reduction and investigation of fluid inclusion data. American Mineralogist, **74**: 1390-1393.

Brown P.E., and Lamb W.M., 1989: P-V-T properties of fluids in the system H2O-CO2-NaCl: New graphical presentations and implications for fluid inclusion studies. Geochimica et Cosmochimica Acta, **53**: 1209-1221.

Burruss R.C., 1981: Analysis of phase equilibria in C-O-H-S fluid inclusions. in Hollister L.S., and Crawford M.L., eds., Short Course in Fluid Inclusions: Applications to Petrology, Mineralogical Association of Canada: 39-74.

Cairnes C.E., 1934: Slocan mining camp, British Columbia. Geological Survey of Canada, Memoir 173, 137 p.

Cairnes C.E., 1935: Description of properties, Slocan mining camp, British Columbia. Geological Survey of Canada, Memoir 184, 274 p.

Carothers W.W., Adami L.H., and Rosenbauer R.J., 1988: Experimental oxygen isotope fractionation between siderite-water and phosphoric acid liberated CO2-siderite. Geochimica et Cosmochimica Acta, **52**: 2445-2450.

Carr S.D., 1985: Ductile shearing and brittle faulting in Valhalla gneiss complex, southeastern British Columbia. Current research, Part A, Geological Survey of Canada, Paper 85-1A: 89-96.

Carr S.D., Parrish R.R., and Brown R.L., 1987: Eocene structural development of the Valhalla Complex, southeastern British Columbia. Tectonics, **6**: 175-196.

Changkakoti A., Gray J., Krstic D., Cumming G.L., and Morton R.D., 1988: Determination of radiogenic isotopes (Rb/Sr, Sm/Nd and Pb/Pb) in fluid inclusion waters: An example from the BlueBell Pb-Zn deposit, British Columbia, Canada. Geochimica et Cosmochimica Acta, **52**: 961-967.

Clayton R.N., and Mayeda T.K., 1963: The use of bromine pentafluoride in the extraction of oxygen from oxides and silicates for isotopic analysis. Geochimica et Cosmochimica Acta, **26**: 43-52.

Clayton R.N., O'Neil J.R., and Mayeda T.K., 1972: Oxygen isotope exchange between quartz and water. Journal of Geophysical Research, v. 77: 3057-3067.

Constantopoulos J., and Larsen P.B., 1991: Oxygen and hydrogen isotope geochemistry of the Star-Morning mine, Coeur d'Alene mining district, Idaho. Geology, **19**: 131-134.

Cook F.A., Green A.G., Simony P.S., Price R.A., Parrish R.R., Milkereit B., Gordy P.L., Brown R.L., Coflin K.C., and Patenaude C., 1988: Lithoprobe seismic reflection structure of the southeastern Canadian Cordillera: Initial results. Tectonics, **7**: 157-180.

Cox J., 1979: The geology of the northwestern margin of the Nelson Batholith, British Columbia.

Unpublished M.Sc. thesis, University of Alberta.

Criss R.E., and Fleck R.J., 1990: Oxygen isotope map of the giant metamorphic-hydrothermal system around the northern part of the Idaho batholith, U.S.A. Applied Geochemistry, **5**: 641-655.

Criss R.E., and Hofmeister A.M., 1991: Application of fluid dynamics principles in tilted permeable media to terrestrial hydrothermal systems. Geophysical Research Letters, **18**: 199-202.

Criss R.E., and Taylor H.P.Jr., 1986: Meteoric-hydrothermal systems. In Valley J.W., Taylor H.P.Jr., and O'Neil J.R., eds., Stable isotopes in high temperature geological processes, Mineralogical Society of America, Reviews in Mineralogy **16**: 373-424.

Dahlgrün F., 1950: Die zinale verbreitung der gangformaltionen des Brocken-plutons im Harz, Erzmetall, **3**: 150-153.

Dalziel I.W., and Brown R.L., 1989: Tectonic denudation of the Darwin metamorphic core complex in the Andes of Tierra del Fuego, southernmost Chile: Implications for Cordilleran orogenesis. Geology, **17**: 699-703.

Davies H.L., and Warren R.G., 1988: Origin of eclogite-bearing, domed, layered metamorphic complexes ("core complexes") in the d'Entrecasteaux Islands, Papua New Guinea. Tectonics, **7**: 1-21.

Davis J.C., 1986: Statistics and data analysis in geology. Second edition, John Wiley, 646 p.

Dewey J.F., 1988: Extensional collapse of orogens. Tectonics, **7**: 1123-1139.

Drummond S.E., and Ohmoto H., 1985: Chemical evolution and mineral deposition in boiling hydrothermal systems. Economic Geology, **80**: 126-147.

Eaton D.W.S., and Cook F.A., 1990: Crustal structure of the Valhalla complex, British Columbia, from Lithoprobe seismic-reflection and potential-field data. Canadian Journal of Earth Sciences, **27**: 1048-1060.

Echtler H., and Malavieille J., 1990: Extensional tectonics, basement uplift and Stephano-Permian collapse basin in a late Variscan metamorphic core complex (Montagne Noire, southern Massif Central). Tectonophysics, **177**: 125-138.

Eckstrand O.R., ed., 1984: Canadian mineral deposit types: A geological synopsis. Geological Survey of Canada, Economic Geology Report 36, 86 p.

Einaudi M.T., and Burt D.M., 1982: Introduction-Terminology, classification, and composition of skarn deposits. Economic Geology, **77**: 745-754.

Emmons W.H., 1924: Primary downward changes in ore deposits. Transactions American Institute Mining and Metallurgical Engineers, **70**: 964-992.

Farrar E., Yamamura B.K., and Clark A.H., 1990: $^{40}Ar/^{39}Ar$ ages of magmatism and tungsten-polymetallic mineralization, Palca 11, Choquene district, southeastern Peru. Economic Geology, **85**: 1669-1676.

Fyles J.T., 1967: Geology of the Ainsworth-Kaslo area, British Columbia. British Columbia Ministry of Energy, Mines and Petroleum Resources, Bulletin 53, 125 p.

Fyles J.T., Harakal J.E., and White W.H., 1973: The age of sulfide mineralization at Rossland, British Columbia. Economic Geology, **68**: 23-35.

Fryklund V.C., 1964: Ore deposits of the Coeur d'Alene district, Shoshone County, Idaho. U.S. Geological Survey Professional Paper 445, 139 p.

Gabrielse H., and Yorath C.J., 1989: DNAG #4. The Cordilleran orogen in Canada. Geoscience

Canada, **16**: 67-84.

Gerstenberger H., 1989: Autometasomatic Rb enrichments in highly evolved granites causing lowered Rb-Sr isochron intercepts. Earth and Planetary Science Letters, **93**: 65-75.

Ghosh D.K., 1986: Geochemistry of the Nelson-Rossland area, southeastern British Columbia. Unpublished Ph.D. thesis, University of Alberta, Edmonton.

Godwin C.I., and Sinclair A.J., 1982: Average lead isotope growth curve for shale-hosted zinc-lead deposits, Canadian Cordillera. Economic Geology, **77**: 675-690.

Godwin C.I., Gabites J.E., and Andrew A., 1988: Leadtable: a galena lead isotope data base for the Canadian Cordillera. British Columbia Ministry of Energy, Mines and Petroleum Resources, Paper 1988-4, 188 p.

Golyshev S.I., Padalko N.L., and Pechekin S.A., 1981: Fractionation of stable oxygen and carbon isotopes in carbonate systems. Geochemistry International, **18**: 85-99.

Gough I.D., 1986: Mantle upflow tectonics in the Canadian Cordillera. Journal of Geophysical Research, **91**: 1909-1919.

Graybeal F.T., Smith D.M.Jr., and Vikre P.G., 1986: The geology of silver deposits. In Wolf K.H., ed., Handbook of strata-bound and stratiform ore deposits, **14**: 1-184.

Gregory R.T., and Criss R.E., 1986: Isotopic exchange in open and closed systems. in Valley J.W., Taylor H.P., Jr., and O'Neil J.R., eds., Stable isotopes in high temperature geological processes, Reviews in Mineralogy v. 16, Mineralogical Society of America: 91-127.

Guilbert J.M., and Park C.F.Jr., 1986: The geology of ore deposits. Freeman, 985 p.

Hannak W.W., 1981: Genesis of the Rammelsberg ore deposit near Goslar/Upper Harz, Federal Republic of Germany. In Wolf K.H., ed., Handbook of strata-bound and stratiform ore deposits, **9**: 551-642.

Harris R.H., Lange I.M., and Krouse H.R., 1981: Major element and sulfur isotopic variations in the Lower Chester vein, Sunshine mine, Idaho. Economic Geology, **76**: 706-715.

Harrison J.E., 1972: Precambrian Belt basin of northwestern United States: Its geometry, sedimentation, and copper occurrences. Geological Society of America Bulletin, **86**: 1215-1240.

Hart S.R., 1988: Heterogeneous mantle domains: signatures, genesis and mixing chronologies. Earth and Planetary Science Letters, **90**: 273-296.

Hedley M.S., 1945: Geology of the Whitewater and Lucky Jim mine areas, Slocan District, British Columbia. British Columbia Ministry of Energy, Mines and Petroleum Resources, Bulletin 22, 54 p.

Hedley M.S., 1952: Geology and ore deposits of the Sandon area, Slocan mining camp, British Columbia. British Columbia Ministry of Energy, Mines and Petroleum Resources, Bulletin 29. 130 p.

Höy, T., 1980: Geology of the Riondel area, Central Kootenay Arc, southeastern British Columbia. British Columbia Ministry of Energy, Mines and Petroleum Resources, Bulletin 73, 89 p.

Hunt P.A., and Roddick J.C., 1988: A compilation of K-Ar ages. Report 18. in Radiogenic age and isotopic studies: Report 2, Geological Survey of Canada, Paper 88-2: 127-153.

Irvine W.T., 1957: The Bluebell mine, British Columbia. in Structural Geology of Canadian Ore Deposits, Canadian Institute Mining Metallurgy, **2**: 95-104.

Jones A.G., Kurtz R.D., Oldenburg D.W., Boerner D.E., and Ellis R., 1988: Magnetotelluric observations along the Lithoprobe southeastern Canadian Cordilleran transect. Geophysical Research Letters, **15**: 677-680.

Jones M.B., Schmuck R.A., and Field C.W., 1973: K-Ar dates from the Valley Copper and Lornex deposits, Guichon Creek batholith, Highland Valley district, British Columbia. Isochron West, **7**: 17-20.

Kanasewich E.R., 1962: Quantitative interpretations of anomalous lead isotope abundances, Unpublished Ph.D. thesis, University of British Columbia.

Kerrich R., and Rehrig W., 1987: Fluid motion associated with Tertiary mylonitization and detachment faulting: $^{18}O/^{16}O$ evidence from the Picacho metamorphic core complex, Arizona. Geology, **15**, p. 58-62.

Kerrich R., 1988: Detachment zones of Cordilleran metamorphic core complexes: thermal fluid and metasomatic regimes. Geologische Rundschau, **77**, p. 157-182.

Klepacki D.W., 1985: Stratigraphy and structural geology of the Goat Range area, southeastern British Columbia, Unpublished Ph.D. thesis, Massachusetts Institute of Technology.

Kutina J., 1963: The distinguishing of the monoascendent and polyascendent origin of associated minerals in the study of the zoning of the Příbram ore veins. Symposium. Problems of Postmagmatic Ore Deposition, Prague, **1**: 200-206.

Laznicka P., 1985: Empirical metallogeny. Developments in Economic Geology, **19**, 1758 p.

Leach D.L., Landis G.P., and Hofstra A.H., 1988: Metamorphic origin of the Coeur d'Alene base- and precious-metal veins in the Belt basin, Idaho and Montana. Geology, **16**: 122-125.

LeCouteur P.C., 1973: A study of lead isotopes from mineral deposits in southeastern British Columbia and in the Anvil Range, Yukon Territory. Unpublished Ph.D. thesis, University of British Columbia.

Lindgren W., 1933: Mineral deposits. McGraw-Hill, 930 p.

Lister G.S., Davis G.A., 1989: The origin of metamorphic core complexes and detachment faults formed during Tertiary continental extension in the northern Colorado River region, U.S.A. Journal of Structural Geology, **11**: 65-94.

Little H.W., 1960: Nelson map-area, west half, British Columbia (82 F W 1/2). Geological Survey of Canada, Memoir 308, 205 p.

Logan J.M., 1986: Geochemical constraints on the genesis of Ag-Pb and Zn deposits, Sandon, British Columbia. Unpublished M.Sc. thesis, The Univeristy of British Columbia, 178 p.

Logan J.M., 1988: Mineral occurrences and lead isotope data for Kokanee Glacier Provincial Park and surrounding area. British Columbia Ministry of Energy, Mines and Petroleum Resources, Open File 1988-11D.

Logan J.M., Gabites J.E., and Brown D.A., 1988: Galena lead isotope characteristics of mineralization in Kokanee Glacier Provincial Park, southeastern British Columbia. British Columbia Ministry of Energy, Mines and Petroleum Resources, Geological Fieldwork, Paper 1988-1: 535-541.

Lynch J.V.G., 1989a: Hydrothermal zoning in the Keno Hill Ag-Pb-Zn vein system, Yukon: A study in structural geology, mineralogy, fluid inclusions, and stable isotope geochemistry. Unpublished Ph.D. thesis, The University of Alberta, 190 p.

Lynch J.V.G., 1989b: Large-scale hydrothermal zoning reflected in the tetrahedrite-freibergite

solid solution, Keno Hill Ag-Pb-Zn district, Yukon. Canadian Mineralogist, **27**: 383-400.

Lynch J.V.G., Longstaffe F.J., and Nesbitt B.E., 1990: Stable isotopic and fluid inclusion indications of large-scale hydrothermal paleoflow, boiling, and fluid mixing in the Keno Hill Ag-Pb-Zn district, Yukon Territory, Canada. Geochimica et Cosmochimica Acta, **54**: 1045-1059.

Macdonald A.S., 1974: The Salmo lead-zinc deposits: A study of their deformation and metamorphic features. Unpublished Ph.D. thesis, The University of British Columbia, 225 p.

Magaritz M, and Taylor H.P., 1986: Oxygen 18/oxygen 16 and D/H studies of plutonic granitic and metamorphic rocks across the Cordillera batholiths of southern British Columbia. Journal of Geophysical Research, **91**: 2193-2217.

Majorowicz J.A., and Gough D.I., 1991: Crustal structures from MT soundings in the Canadian Cordillera. Earth and Planetary Science Letters, **102**: 444-454.

Malavieille J., Guihot P., Costa S., Lardeaux J.M., and Gardien V., 1990: Collapse of the thickened Variscan crust in the French Massif Central: Mont Pilat extensional shear zone and St. Etienne Late Carboniferous basin. Tectonophysics, **177**: 139-149.

Mathews W.H., 1983: Early Tertiary resetting of potassium-argon dates in the Kootenay Arc, southeastern British Columbia. Canadian Journal of Earth Sciences, **20**: 867-872.

Matte Ph., Maluski H., Rajlich P., and Franke W., 1990: Terrane boundaries in the Bohemian Massif: Result of large-scale Variscan shearing. Tectonophysics, **177**: 151-170.

McCrea J.M., 1950: The isotope chemistry of carbonates and a paleotemperature scale. Journal Chemistry Physics, **18**:849-857.

Megaw P.K., Ruiz J., and Titley S.R., 1988: High-temperature, carbonate-hosted Ag-Pb-Zn(Cu) deposits of northern Mexico. Economic Geology, **83**: 1856-1885.

Mertz D.F., Lippolt H.J., and Schnorrer-Kohler G., 1989: Early Cretaceous mineralizing activity in the St. Andreasberg ore district(Southwest Harz, Federal Republic of Germany). Mineralium Deposita, **24**: 9-13.

Möller P., Morteani G., Hoeffs J., and Parekh P.P., 1979: The origin of the ore-bearing solution in the Pb-Zn veins of the western Harz, Germany, as deduced from rare-earth element and isotope distributions in calcite. Chemical Geology, **26**: 197-215.

Möller P., Morteani G., and Dulski P., 1984: The origin of the calcites from Pb-Zn veins in the Harz Mountains, Federal Republic of Germany. Chemical Geology, **45**: 91-112.

Mortimer N., van der Heyden P., Armstrong R.L., and Harakal J., 1990: U-Pb and K-Ar dates related to the timing of magmatism and deformation in the Cache Creek terrane and Quesnellia, southern British Columbia. Canadian Journal of Earth Sciences, **27**: 117-123.

Mutschler F.E., Wright E.G., Ludington S., and Abbott J.T., 1981: Granite molybdenite systems. Economic Geology, **76**: 874-897.

Nielsen H., 1968: Schwefel-isotopenverhaltnisse aus St. Andreasberg und anderen Erzvorkommen des Harzes. Neues Jahrbuch Mineralogie. Abhandlungen, **109**: 289-321.

Nguyen K.K., Sinclair A.J., and Libby W.G., 1968: Age of the northern part of the Nelson batholith. Canadian Journal of Earth Sciences, **5**: 955-957.

Ohmoto H., 1968: The Bluebell mine, British Columbia, Canada: Part I; Mineralogy, paragenesis, fluid inclusions, and the isotopes of lead, carbon, oxygen, and hydrogen. Unpublished Ph.D. thesis, Princeton University.

Ohmoto H., 1971: Fluid inclusions and isotope study of the lead-zinc deposits at the Bluebell Mine, British Columbia, Canada. Soc. Mining Geol. Japan, Special Issue **2**: 93-99.

Ohmoto H., Lasaga A.C., 1982: Kinetics of reactions between aqueous sulfates and sulfides in hydrothermal systems. Geochimica et Cosmochimica Acta, **46**: 1727-1745.

Ohmoto H., and Rye R.O., 1970: The Bluebell Mine, British Columbia. I. Mineralogy, paragenesis, fluid inclusions, and the isotopes of hydrogen, oxygen, and carbon. Economic Geology, **65**: 417-437.

O'Neil J.R., and Taylor H.P., Jr., 1967: The oxygen isotope and cation exchange chemistry of feldspars. American Mineralogist, **52**: 1414-1437.

Orr J.F.W., 1971: Mineralogy and computer-oriented study of mineral deposits in Slocan City camp, Nelson Mining Division, British Columbia. Unpublished M.Sc. thesis, The University of British Columbia, 143 pages.

Park C.F.Jr., 1955: The zonal theory of ore deposits. Economic Geology, 50th Anniversary Volume: 226-248.

Parrish R.R., 1984: Slocan Lake Fault: A low angle fault zone bounding the Valhalla Gneiss Complex, Nelson map area, southern British Columbia. Geological Survey of Canada, Current Research, Part A, Paper 84-1A: 323-330.

Parrish R.R., Carr S.D., and Parkinson D.L., 1988: Eocene extensional tectonics and geochronology of the southern Omineca Belt, British Columbia and Washington. Tectonics, **7**: 181-212.

Posepny F., 1902: The genesis of ore-deposits. The American Institute of Mining Engineers, Second Edition, 806 p.

Parry W.T.. 1986: Estimation of X_{CO2}, P, and fluid inclusion volume from fluid inclusion temperature measurements in the system NaCl-CO2-H2O. Economic Geology, **81**: 1009-1013.

Platt J.P., and Vissers R.L.M., 1989: Extensional collapse of thickened continental lithosphere: A working hypothesis for the Alboran Sea and Gibraltar arc. Geology, **17**: 540-543.

Potter R.W., 1977. Pressure corrections for fluid-inclusion homogenization temperatures based on the volumetric properties of the system NaCl-H_2O. Journal of Research, U.S. Geological Survey, **5**: 603-607.

Potter R.W., Clynne M.A., and Brown D.L., 1978: Freezing point depression of aqueous sodium chloride solutions. Economic Geology. **73**: 284-285.

Rajlich P., 1987: Variszische duktile tektonik im Bohmische massif. Geologische Rundschau, **76**: 755-786.

Reid M.R., Hart S.R., Padovani E.R., and Wandless G.A., 1989: Contribution of metapelitic sediments to the composition, heat production, and seismic velocity of the lower crust of southern New Mexico, U.S.A. Earth and Planetary Science Letters, **95**: 367-381.

Reynolds P.H., and Sinclair A.J., 1971: Rock and ore-lead isotopes from the Nelson Batholith and the Kootenay Arc, British Columbia, Canada. Economic Geology, **66**: 259-266.

Reynolds S.J., and Lister G.S., 1987: Structural aspect of fluid-rock interactions in detachment zones. Geology, **15**: 362-366.

Richards J.R., Fletcher I.R., and Blockley J.G., 1981: Pilbara galenas: Precise isotopic assay of the oldest Australian leads, model ages and growth curve implications. Mineralium Deposita, **16**: 7-30.

Roddick J.C., 1983: High precision intercalibration of ^{40}Ar-^{39}Ar standards. Geochimica et Cosmochimica Acta, **47**:887-898.

Roddick J.C., 1990: $^{40}Ar/^{39}Ar$ evidence for the age of the New Quebec Crater, Northern Quebec. in Radiogenic age and isotopic studies: Report 3, Geological Survey of Canada, Paper 89-2: 7-16.

Roddy M S., Reynolds S.J., Smith B.M., and Ruiz J., 1988: K-metasomatism and detachment-related mineralization, Harcuvar Mountains, Arizona. Geological Society of America Bulletin, **100**: 1627-1639.

Roedder E., 1984: Fluid inclusions. In Ribbe P.H., ed., Reviews in Mineralogy, Mineralogical Society of America, **12**, 646 p.

Roscoe S.M., 1948: A silver-lead-zinc deposit in the Slocan district, British Columbia. Unpublished M.Sc. thesis, Queen's University, 72 p.

Routhier P., 1963: Les gisements métallifères. Géologie et principes de recherches. Masson, 1282 p.

Routhier P., 1980: Où sont les métaux de l'avenir? Mémoire du B.R.G.M. 105, 410 p.

Rudnick R.L., and Goldstein S.L., 1990: The Pb isotopic compositions of lower crustal xenoliths and the evolution of lower crustal Pb. Earth and Planetary Science Letters, **98**: 192-207.

Russell R.D., and Farquhar R.M., 1960: Lead isotopes in geology. Interscience Publishers Inc.

Sasaki A., Arikawa Y., and Folinsbee R.E., 1979: Kiba reagent method of sulfur extraction applied to isotope work. Bulletin Geological Survey Japan, **30**: 241-245.

Sawkins F.J., 1990: Metal deposits in relation to plate tectonics. Springer- Verlag, Second Edition, 461 p.

Scaillet S., Féraud G., Lagabrielle Y., Ballève M., and Ruffet G., 1990: $^{40}Ar/^{39}Ar$ laser-probe dating by step heating and spot fusion of phengites from the Dora Maira nappe of the western Alps, Italy. Geology, **18**: 741-744.

Schalck D.K., 1989: The geology and alteration of the Gem stocks, Shoshone County, Idaho. In Chamberlain V.E., Breckenridge R.M., Bonnichsen B., eds., Guidebook to the geology of northern and western Idaho and surrounding area, Idaho Geological Survey Bulletin 28: 125-135.

Schoell M., 1970: K/Ar and Rb/Sr age determination on minerals and total rocks of the Harz-Mountains/Germany. Eclogae Geol. Helvetica, **63**: 299.

Schwartz M.O., 1989: Determining phase volumes of mixed CO2-H2O inclusions using microthermometric measurements. Mineralum Deposita, **24**: 43-47.

Selverstone J., 1988: Evidence for east-west crustal extension in the eastern Alps: implications for the unroofing history of the Tauern window. Tectonics, **7**: 87-105.

Sheppard S.M.F., and Schwarcz H.P., 1970: Fractionation of carbon and oxygen isotopes and magnesium between coexisting metamorphic calcite and dolomite. Contributions to Mineralogy and Petrology, **26**: 161-198.

Sinclair A.J., 1964: A lead isotope study of mineral deposits in the Kootenay Arc, Unpublished Ph.D. thesis, University of British Columbia.

Sinclair A.J., Tessari O.J., and Harakal J.E., 1980: Age of Ag-Pb-Zn mineralization, Keno Hill-Galena Hill area, Yukon Territory. Canadian Journal of Earth Sciences, **17**: 1100-1103.

Smith B.M., Reynolds S.J., Day H.W., and Bodnar R.J., 1991: Deep-seated fluid involvement in

ductile-brittle deformation and mineralization, South Mountains metamorphic core complex, Arizona. Geological Society of America Bulletin, **103**: 559-569.

Spencer J.E., and Welty J.W., 1986: Possible controls of base- and precious-metal mineralization associated with Tertiary detachment faults in the lower Colorado River trough, Arizona and California. Geology, **14**: 195-198.

Sperling H., and Nielsen H., 1973: Schwefel-isotopenuntersuchungen an der Blei-Zink-Erzlagerstatte Grund (Westharz, Bundesrepublik Deutschland). Mineralium Deposita, **8**: 64-72.

Spurr J.E., 1912: Theory of ore deposition. Economic Geology, **7**: 485-492.

Steiger R.H., and Jäger E., 1977: Subcommission on geochronology: convention on the use of decay constants in geo- and cosmochronology. Earth and Planetary Science Letters, **36**: 359-362.

Strussi J.-M., 1989: Granitoid chemistry and associated mineralisation in the French Variscan. Economic Geology, **84**: 1363-1381.

Suzuoki T., and Epstein S., 1976: Hydrogen isotope fractionation between OH-bearing minerals and water. Geochimica et Cosmochimica Acta, **40**: 1229-1240.

Taylor H.P., Jr., 1979: Oxygen and hydrogen isotope relationships in hydrothermal mineral deposits. in Barnes H.L., ed., Geochemistry of hydrothermal ore deposits, Second Edition, John Wiley: 236-277.

Tischendorf G., 1989: Some conceptual aspects of the relationships between plutonism, volcanism, and metallogenesis in the continental crust. Z. geol. Wiss., **17**: 553-557.

Tischendorf G., and Schwab G., 1989: Metallogenesis of the transition period between Hercynian orogenesis and subsequent platform stage in Central Europe. Z. geol. Wiss., **17**: 815-842.

Tischendorf G., and Förster H.-J., 1990: Acid magmatism and related metallogenesis in the Erzgebirge. Geological Journal, **25**: 443-454.

Uglow W.L., 1917: Gneissic galena ore from the Slocan district, British Columbia. Economic Geology, **12**: 643-662.

Varsek J.L., and Cook F.A., 1991: Seismic reflection geometry of a folded and detached accretionary complex: Kootenay arc, British Columbia. Geology, **19**: 159-162.

van Breemen O., Aftalion M., Bowes D.R., Dudek A., Mísař Z., Povondra P., and Vrána S., 1982: Geochronological studies of the Bohemian massif, Czechoslovakia, and their significance in the evolution of Central Europe. Transactions of the Royal Society of Edinburgh: Earth Sciences, **73**: 89-108.

Vinx R., 1982: The Harzburg gabbro, north Germany-a synorogenic layered mafic intrusion. Neues Jb. Miner. Abh., **144**: 1-28.

Wallace C.A., Lidke D.J., and Schmidt R.G., 1990: Faults of the central part of the Lewis and Clark line and fragmentation of the Late Cretaceous foreland basin in west-central Montana. Geological Society of America Bulletin, **102**: 1021-1037.

Walther H.W., 1986: Federal Republic of Germany. In Dunning F.W., and Evans A.M., eds., Mineral deposits of Europe, **3**: 175-301.

Wanless R.K., Stevens R.D., Lachance G.R., and Delabio R.N., 1973: Age determinations and geological studies. K-Ar isotopic ages, Report 11, Geological Survey of Canada Paper 73-2.

Watson K.W., 1986: Silver-lead-zinc deposits of the Keno Hill-Galena Hill area, Central Yukon.

In Yukon Geology, Vol. 1: Exploration and Geological Services Division, Yukon, Indian and Northern Affairs Canada: 83-88.

Westra G., and Keith S.B., 1981: Classification and genesis of stockwork molybdenum deposits. Economic Geology,**76**: 844-873.

Wijbrans J.R., and McDougall I., 1986: $^{40}Ar/^{39}Ar$ dating of white micas from an Alpine high-pressure metamorphic belt on Naxos (Greece): the resetting of the argon isotopic system. Contributions to Mineralogy and Petrology, **93**: 187-194.

Yates R.G., and Engels J.C., 1968: Potassium-argon ages of some igneous rocks in northern Stevens County, Washington. U.S. Geological Survey Professional Paper 600-D: D242-D247.

Yates M.G., and Ripley E.M., 1985: Fluid inclusion and isotopic studies of the Galena mine, Coeur d'Alene district, Idaho. Geological Society of America, Abstracts with Programs, **17**: 756.

Žák K., and Dobeš P., 1991: Stable isotopes and fluid inclusions in hydrothermal deposits: Příbram ore region. Rozpr. Čs. Akad. Věd, **101**: in press.

Zartman R.E., and Stacey J.S., 1971: Lead isotopes and mineralization ages in Belt Supergroup rocks, northwestern Montana and northern Idaho. Economic Geology, **66**: 849-860.

Zartman R.E., and Doe B.R., 1981: Plumbotectonics - The model. Tectonophysics, **75**: 135-162.